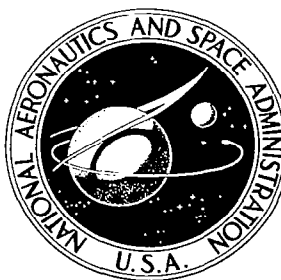


NASA CONTRACTOR REPORT

NASA CR-628



NASA CR



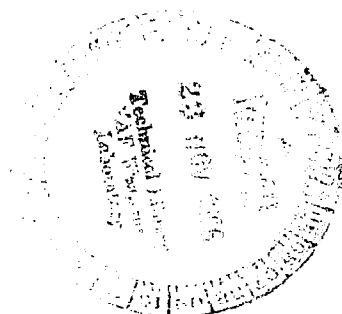
LOAN COPY: RETURN TO
AFWL (WLIL-2)
KIRTLAND AFB, N MEX

THE VESTIBULAR SYSTEM AND HUMAN DYNAMIC SPACE ORIENTATION

by Jacob L. Meiry

Prepared by
MASSACHUSETTS INSTITUTE OF TECHNOLOGY
Cambridge, Mass.

for



NATIONAL AERONAUTICS AND SPACE ADMINISTRATION • WASHINGTON, D. C. • OCTOBER 1966



THE VESTIBULAR SYSTEM AND HUMAN
DYNAMIC SPACE ORIENTATION

By Jacob L. Meiry

Distribution of this report is provided in the interest of information exchange. Responsibility for the contents resides in the author or organization that prepared it.

Prepared under Grant No. NsG-577 by
MASSACHUSETTS INSTITUTE OF TECHNOLOGY
Cambridge, Mass.

for

NATIONAL AERONAUTICS AND SPACE ADMINISTRATION

For sale by the Clearinghouse for Federal Scientific and Technical Information
Springfield, Virginia 22151 - Price \$3.75

THE VESTIBULAR SYSTEM AND HUMAN
DYNAMIC SPACE ORIENTATION

by

Jacob L. Meiry

Submitted to the Department of Aeronautics and Astronautics, Massachusetts Institute of Technology, on May 15, 1965, in partial fulfillment of the requirements for the degree of Doctor of Science.

ABSTRACT

The motion sensors of the vestibular system are studied to determine their role in human dynamic space orientation and manual vehicle control. The investigation yielded control models for the sensors, descriptions of the subsystems for eye stabilization, and demonstrations of the effects of motion cues on closed loop manual control.

Experiments on the abilities of subjects to perceive a variety of linear motions provided data on the dynamic characteristics of the otoliths, the linear motion sensors. Angular acceleration threshold measurements supplemented knowledge of the semicircular canals, the angular motion sensors. Mathematical models are presented to describe the known control characteristics of the vestibular sensors, relating subjective perception of motion to objective motion of a vehicle.

The vestibular system, the neck rotation proprioceptors and the visual system form part of the control system which maintains the eye stationary relative to a target or a reference. The contribution of each of these systems was identified through experiments involving head and body rotations about a vertical axis. Compensatory eye movements in response to neck rotation were demonstrated and their dynamic characteristics described by a lag-lead model. The eye motions attributable to neck rotations and vestibular stimulation obey superposition when both systems are active.

Human operator compensatory tracking is investigated in simple vehicle orientation control systems with stable

and unstable controlled elements. Control of vehicle orientation to a reference is simulated in three modes: visual, motion and combined. Motion cues sensed by the vestibular system and through tactile sensation enable the operator to generate more lead compensation than in fixed base simulation with only visual input. The tracking performance of the human in an unstable control system near the limits of controllability is shown to depend heavily upon the rate information provided by the vestibular sensors.

ACKNOWLEDGEMENTS

The author gratefully acknowledges the guidance and support from his thesis advisors, Professor Y. T. Li, Professor L. R. Young and Professor H. P. Whitaker. Professor Li, the Director of the Man-Vehicle Control Laboratory, and Professor Young were closely associated with the research in all phases.

The author also expresses his appreciation to Professor W. R. Markey, who served initially as thesis advisor, and to Dr. A. D. Weiss, Massachusetts General Hospital, for his invaluable medical advice and for many stimulating discussions.

He is grateful to Mr. John Barley, who provided technical support; he wishes to thank all the volunteers serving as subjects; Miss Mary Moore for typing the manuscript and Miss Ruth Aldrich and Mrs. Polly Hurst for their help in preparing the draft.

Acknowledgement is also made to the M.I.T. Computation Center for the time allowed on its IBM 709⁴ Computer, done as Problem M3538.

Finally the author wishes to dedicate this thesis to his parents for their constant encouragement.

This research was supported in part by a grant from NASA, Nsg-577.

TABLE OF CONTENTS

<u>Chapter No.</u>		<u>Page No.</u>
CHAPTER I	INTRODUCTION	1
1.1	Scope of the Research	2
1.2	Application of the Research	7
CHAPTER II	THE VESTIBULAR SYSTEM	12
2.1	Physiology and Anatomy	13
2.2	Orientation-Reference Coordinates	19
2.3	Control Variables	21
2.4	Identification Processes	22
CHAPTER III	THE SEMICIRCULAR CANALS	25
3.1	Input Vector and Sensitive Axis	25
3.2	A Physical Model for the Semicircular Canals	26
3.3	Rotation about the Vertical (Y_h) Axis	28
3.4	Habituation	40
3.5	Rotation about a Horizontal Axis	44
3.6	A Mathematical Model for the Semicircular Canals	48
CHAPTER IV	THE OTOLITHS - LINEAR ACCELERATION SENSORS	54
4.1	The Utricle and the Saccule	55
4.2	The Utricle - Sensor Characteristics	56
4.3	Habituation	76
4.4	Mathematical model for the Utricle	77

<u>Chapter No.</u>		<u>Page No.</u>
CHAPTER V	THE EYE - A DEPENDENT SENSOR	81
5.1	Control of Lateral Eye Movements	81
5.2	Compensatory Eye Movements - Vestibular Stimulation	85
5.3	Compensatory Eye Movements - Neck Proprioceptors	96
5.4	Compensatory Eye Movements - Vestibular and Neck Proprioceptors Stimulation	107
5.5	Stabilization of Eye Position in Space	112
CHAPTER VI	SIMPLE MANUAL CONTROL SYSTEMS WITH MOTION INPUTS	117
6.1	The Vestibular System as an Input Channel in Manual Control Systems	119
6.2	A Manual Control System with Pure Horizontal Rotation	123
6.3	Manual Control System with Linear Motion	128
6.4	Control of Motion with Respect to the Gravity Vector	129
6.5	Summary	133
CHAPTER VII	VISUAL AND VESTIBULAR CONTROL OF AN UNSTABLE SYSTEM	135
7.1	Control of an Unstable System	136
7.2	An On-Off Model for the Human Operator	141
7.3	Discussion	153
CHAPTER VIII	CONCLUSIONS	156
8.1	The Vestibular System	157
8.2	The Eye Movement Control System	158
8.3	Control of Vehicle Orientation	161

<u>Chapter No.</u>		<u>Page No.</u>
Appendix A	Any-Two-Degrees of Angular Freedom Motion Simulator	163
Appendix B	Linear Motion Simulator	167
Appendix C	Anatomy of the Neck - Rotation	170
Appendix D	Measurement of Describing Functions for the Human Operator	172
BIBLIOGRAPHY		178

LIST OF ILLUSTRATIONS

<u>Figure No.</u>		<u>Page No.</u>
1.1	Block diagram for control of vehicle orientation	3
1.2	General block diagram of the man-vehicle control problem (ref. 153)	5
1.3	The man-vehicle control system studied in this thesis	6
2.1	The membranous inner ear (ref. 7)	14
2.2	Schematic drawing of a cross section of an otolith and its macula (ref. 77)	16
2.3	Schematic drawing of a cross section through an ampula and crista (ref. 77)	16
2.4	The head planes and the head axis system	20
3.1	Schematic diagram of the semicircular canal (ref. 157)	27
3.2	Duration of sensation as a function of the velocity step input (ref. 157)	32
3.3	Subjective angular velocity after a 40°/sec velocity step (ref. 157)	35
3.4	Latency times for perception of angular acceleration about the vertical axis (Y_h)	39
3.5	Latency times for perception of angular acceleration about the vertical axis (Y_h)	41
3.6	Latency times for perception of angular accelerations about the roll axis (X_h)	47
3.7	Semicircular canal block diagram - short period of stimulation	49
3.8	Bode plot of semicircular canals model. Rotation about the vertical axis (Y_h)	51

Figure No.Page No.

4.1	The subjective inclination (β_y) plotted as a function of the shear acceleration in the plane of the utricle (ref. 151)	60
4.2	Profile of peak sinusoidal input accelerations	64
4.3	Subjective perception of motion reversal - phase versus frequency	65
4.4	Bode plot of otoliths model	68
4.5	Latency times for perception of horizontal linear acceleration, supine	71
4.6	Latency times for perception of horizontal linear acceleration, upright	71
4.7	Illustration of motions sensed by seated subject (ref. 155)	74
4.8	Otoliths block diagram	78
5.1	Block diagram of the eye movement control system	83
5.2	Profile of input sinusoid amplitudes	89
5.3	Vestibular nystagmus and "cumulative" eye position, $f = 0.5$ cps	90
5.4	Bode plot of vestibular compensatory eye movements (slow phase)	92
5.5	Vestibular nystagmus with environmental fixation point, $f = 0.5$ cps	95
5.6	Vestibular compensatory eye movements with Earth-fixed fixation point, $f = 1.0$ cps	97
5.7	Bode plot of compensatory eye movements (vestibular stimulation with Earth fixation point)	98
5.8	Compensatory eye movements by neck receptors, $f = 0.6$ cps	100
5.9	Bode plot of compensatory eye movements by neck proprioception	102

<u>Figure No.</u>		<u>Page No.</u>
5.10	Eye movements, neck proprioception and environmental fixation point, $f = 0.8$ cps	105
5.11	Eye movements - neck proprioception with Earth fixation point, $f = 0.2$ cps	106
5.12	Bode plot of compensatory eye movements (vestibular and neck proprioception)	109
5.13	Bode plot of eye movements (vestibular, proprioception and Earth-fixed fixation point)	111
Table 5.1	Space stabilization of eye	113
5.14	Model for multi-input horizontal eye movement control system	115
6.1	Block diagram of simple compensatory manual control system (ref. 129)	118
6.2	Velocity control with visual or motion mode	121
6.3	Describing function of the human operator in visual and combined mode. Horizontal rotation	127
6.4	Describing function of the human operator in motion mode. Rotation with respect to the gravity vector	134
7.1	Control of inverted pendulum with visual or motion feedback	137
7.2	Time-record-control of inverted pendulum showing bang-bang use of linear controller	140
7.3	Proposed on-off control model for human operator in "difficult" control task	143
7.4	Experimental trajectory and switching lines	144
7.5	Calculated phase portrait and switching lines	147
7.6	Switching line slope for control of inverted pendulum	150
7.7	RMS error for control of inverted pendulum	152

<u>Figure No.</u>		<u>Page No.</u>
8.1	Block diagram of the vestibular system	159
Table 8.1	The vestibular system	160
A.1	The NE-2 motion simulator in the yaw-roll mode	165
A.2	The display scope and the control stick used with the NE-2 Motion Simulator	166
B.1	The Linear Motion Simulator on its track	168
B.2	The interior of the Linear Motion Simulator	169

CHAPTER I

INTRODUCTION

Daily human activity includes complex orientation, postural control and movement coordination. All these tasks depend upon his perception of motion. The vestibular system is recognized as the prime motion sensing center in the human. Its sensing capabilities are probably most compatible with every-day movements of man relative to his surroundings. However, man-made vehicles have extended the operating environment of man, and thereby delegated new responsibilities to human's sensory system.

This thesis studies primarily the vestibular sensory system. Augmented by tactile and visual information, the perception of motion by the vestibular sensors is used in man's orientation in three-dimensional space. In a manual control system, all these sensors provide input information for the motion control commands of the operator.

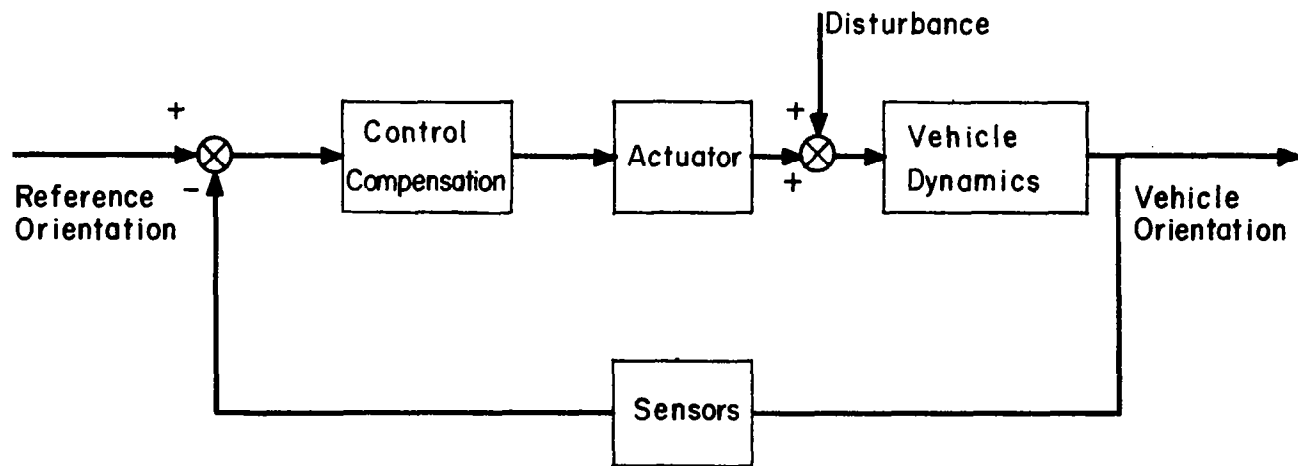
Feedback control theory and its methodology are used to describe the characteristics of the sensors in conjunction with vehicle control. Mathematical models are presented for the dynamic response of the vestibular sensors. Analogies between these sensors and electro-mechanical instruments designed for similar functions are

drawn. The control activities of the human operator in representative manual control systems with and without motion inputs are studied. The characteristics are summarized by a new nonlinear model as well as the conventional describing functions. The resultant control models will be of value to control engineers concerned with the performance of manual control loops. The models for the vestibular sensors demonstrate functional relationships which can lead to further physiological research. Both engineers and physiologists will gain insight into the capabilities of an important biological system, and its use by the human in tasks of orientation control.

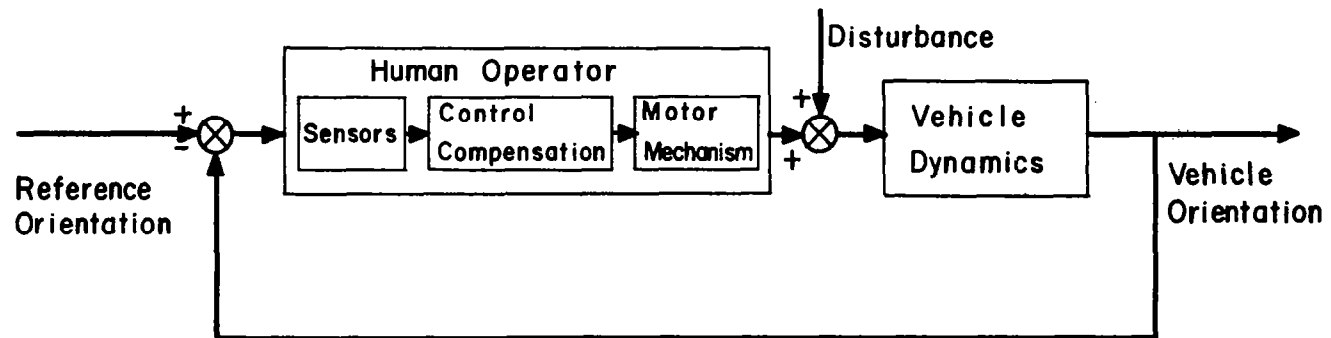
1.1 SCOPE OF THE RESEARCH

Control of orientation depends upon the ability to determine, quantitatively, changes of orientation with respect to a given kinematically defined reference orientation. As in navigation and control, orientation is defined as the attitude and position of a body-fixed coordinate system, measured relative to a given earth-fixed frame.

The feedback loop for any orientation control, automatic or manual, can be represented by the functional block diagram in Fig. 1.1a. For an electromechanical servo system, the functional blocks are identifiable, their input-output relations are measurable, and the whole system is amenable to rigorous mathematical evaluation. When the



a. General Control of Vehicle Orientation



b. Human Operator Control of Vehicle Orientation

Fig. 1.1 Block Diagram for Control of Vehicle Orientation

task of orientation control is given to a human operator, the system block diagram is modified to that of Fig.1.1b. Application of servoanalysis to such manual control systems has two major goals: 1) mathematical models of each of the "components" (sensors, compensation, etc.) may be identified; 2) overall human operator transfer functions may be obtained and applied to manual control system analysis.

In general, orientation control by a human operator is a multi-input control system as shown in Fig. 1.2.¹⁵³ Human control characteristics in fixed base simulation, with visual input and manual output have been studied extensively for a wide variety of controlled elements.^{50, 89, 129, 148} The research in this thesis is concerned with another important path undertaken through this loop. Sensory information is processed through the mechanism of the vestibular system, supplemented by tactile sensation and visual reference. At the motor end, the operator uses manual control. The central nervous system(CNS) is the controller for the control system. Time variant characteristics of the operator, such as adaptation and learning are not included in this study. This subsystem of the general orientation control problem is given in Fig. 1.3.

The pattern of research follows the techniques that would be used in analysis of a comparable automatic control

¹⁵³ Superscripts refer to numbered items in the Bibliography.

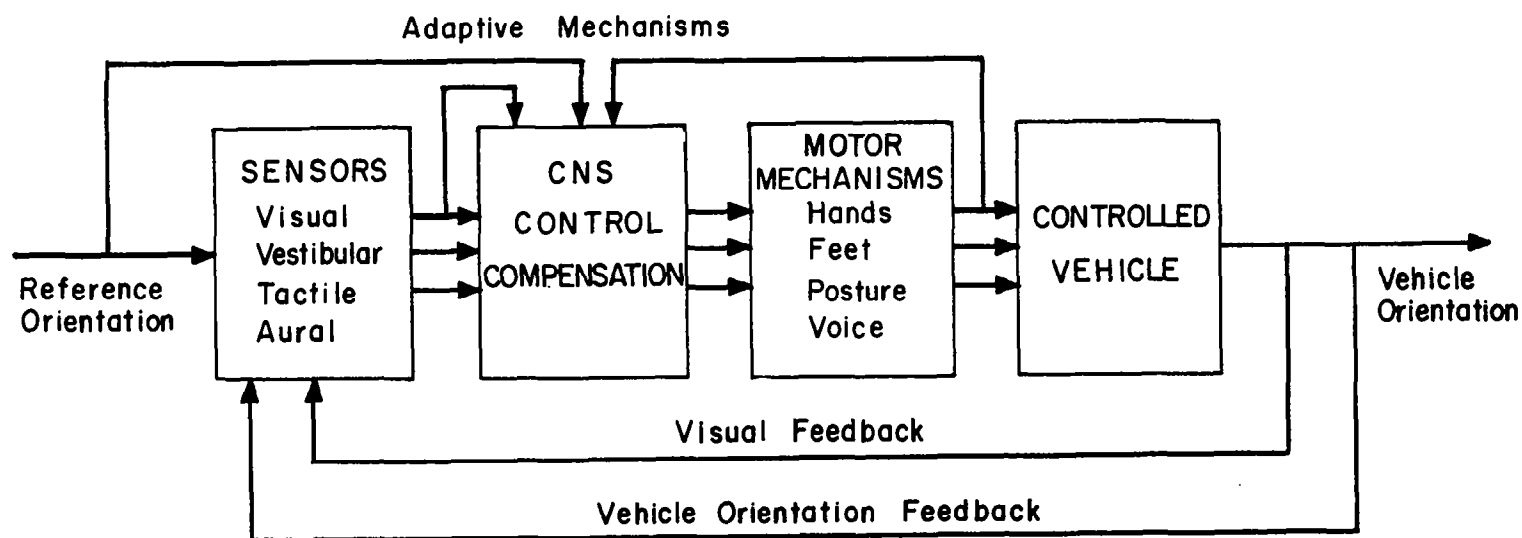


Fig. 1.2 General Block Diagram of the Man-Vehicle Control Problem (Ref. 153).

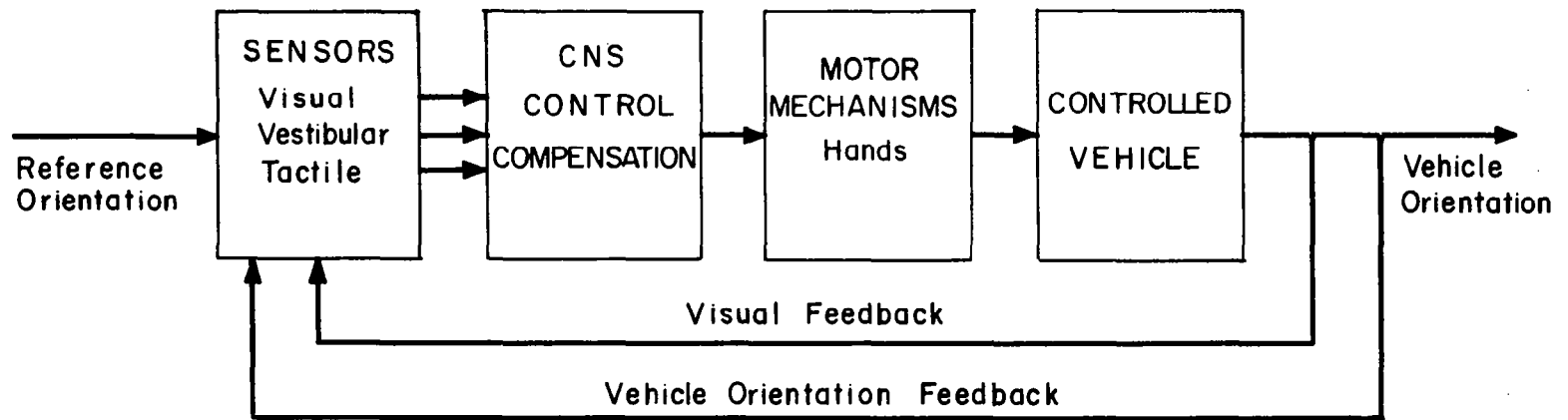


Fig. 1.3 The Man-Vehicle Control System Studied in This Thesis

system. The dynamic characteristics of the vestibular system are studied for their inherent interest and also as a "component" of the operator. Compensating eye movements in the presence of head and body motions are discussed from a space stabilization point of view. The capabilities of the human operator are reviewed on the basis of the information he receives from his various sensors. Manual control of orientation, when the vehicle is driven in modes of motion specific to a given sensor or combination of sensors, is analyzed in terms of operator describing functions. Finally, the compensation capabilities of the human operator in controlling the orientation of an unstable system are investigated in pure visual, pure vestibular, and combined modes. Results are presented in terms of an on-off model for the operator and analyzed in the phase plane.

1.2 APPLICATION OF THE RESEARCH

1.2.1 Physiology and Biology

Subjective orientation is a result of the processing of numerous inputs coming from separate sensors. In physiology, motion is sensed by receptors informing the brain about localized sensations; in feedback theory this is considered as a system with multiple sensors feeding a controller. The goal of the research in the two fields are complementary. The control engineer is interested in the overall performance of the sensors, the physiologist in the description of the associated body mechanisms.

Engineering characteristics of the vestibular system, the neck proprioceptors or the body pressure receptors described in terms of a model, do not guarantee a physiological correspondence. The mathematical model describes the sensors' response in a compact mathematical notation and is easy to simulate and analyze. There is no reason to expect that a lag-lead network corresponds to the actual biological mechanism. However, the underlying physiological processes associated with a model could be investigated. The physiologist, guided by the functional relationship of the mathematical model, could postulate and search for the physiological counterparts of the engineering analog.

1.2.2 Aerospace Medicine and Psychology

Is the human fit to accomplish space missions? Is a given individual conditioned to the expected motion parameters of the mission? These questions are of great importance in this era of rapid technological achievements. The common denominator of this medical and psychological interest and responsibility is the ability of the human to judge his spatial orientation.

Spatial disorientation or vertigo may be crucial for survival and successful completion of a mission. Poor motor coordination and prolonged reaction time are manifestations of inability to deal effectively with the environment. The psychological symptoms accompanying vertigo are equally serious.

The mathematical model of the vestibular system is basic for evaluating the expected subjective orientation of the human. Expected vehicle motions from a mission profile may be applied to the vestibular system model to predict potential difficulties. On the basis of the vestibular model, a medical criterion for personnel selection may be developed along with a minimum standard for medical fitness of flying personnel.

The psychological training of the human should not be underestimated. Pilots have been trained to fly by instruments and to ignore conscious sensations of body orientation. Ice skaters and ballet dancers learn to suppress certain vestibular or visual information. Appropriate psychological conditioning must consider the environment where the human will be functioning. This environment imposes dynamic conditions which the operator compares to a set of previous experiences. The observations or illusions which arise under these conditions are a function of his previous exposure to similar input accelerations. The mathematical model of the vestibular system is valid for the normal environmental conditions for man on earth. Training for operation in different environments should be considered as modifications with respect to this built-in "reference".

1.2.3 Control Engineering and Human Engineering

The control engineer attempts to associate a mathematical description with each physical element of a control

system. This description represents a relation between the input variable to the component and its output regardless of the type of physical parameters involved (acceleration, current, torque, etc.). A body of test methods has been developed for identification of these input-output transfer functions. Similarly, methods of analysis are available to evaluate the stability and performance of a control system on the basis of the characteristics of its individual components. In a preliminary design of an automatic control system, the control engineer can analyze a whole series of systems, select components with characteristics meeting his criteria and make design decisions on the basis of mathematical analysis.

The human has sensors, can act as a controller and can compensate, and has the strength to execute control decisions. Each or all of these human capabilities can be utilized in a control system. However, the analysis of manual control systems, even in the preliminary design stage, is still generally done by simulation. This approach is necessary, since our current knowledge of the engineering characteristics of man is quite limited. Simulation is certainly a necessity in the final design stages of manned systems. However, a degree of flexibility in design of manned systems comparable to that found in automatic system design may be achieved with the formulation of models which adequately represent control characteristics of the human.

The experimental data presented in this thesis is summarized in simple mathematical models of the vestibular motion sensors, a model of the eye control system in the presence of rotational motion, and describing functions for the human operator in manual control systems with motion inputs.

This research work represents a further step in the description of overall human control characteristics and those of his sensors. As such, it can be used to estimate the ability of the human to obtain orientation information with his various sensors and subsequently to utilize it for vehicle orientation control.

Human engineering is concerned with the accomodation of the human operator in an environment which will allow him to perform his task most efficiently. Relevant parts of this research concern the effects of head motion on the human's ability to fixate an instrument or to perceive vehicle motion. The models of the vestibular sensors and the eye movement control system can be used as guides for vehicle interior design, appropriate to the control tasks assigned to the human operator.

CHAPTER II

THE VESTIBULAR SYSTEM

The non-auditory section of the human inner ear is the recognized center of motion sensors. This center, the vestibular system, is one of the sensory systems which provides information of body orientation and balance. Since the ability of the human to orient himself and preserve equilibrium with the surrounding environment is a basic prerequisite for normal existence, a sizable research literature is devoted to the various aspects associated with the function of the vestibular system. The medical researchers study the balance mechanisms of mammals and attempt to correlate their findings with the role and the function of the vestibular system in humans. The dynamic characteristics of the vestibular sensors and pertinent data on thresholds of perceptions of motion with corresponding response times is another field of concentrated research effort.

The present chapter will review the background material on the vestibular system. Chapter III will analyze the semicircular canals, the human angular accelerometers, with their characteristics as determined by previous work and from experiments by the author. The otoliths, the linear motion

sensor of the vestibular system, is the subject of Chapter IV, where experimental results obtained here along with a critical examination of the otolith sensing capabilities are summarized in a mathematical model. These three chapters present the physiological and the engineering description of the human motion sensors as known at the present time.

2.1 PHYSIOLOGY AND ANATOMY^{76,77,7}

The inner ear is divided into two parts: 1) the cochlea serving auditory function, and 2) a non-auditory portion, the vestibular system. This structure, also called the labyrinth, lodges the sensors associated with maintenance of balance and orientation in three-dimensional space. One distinguishes between the bony labyrinth and the membranous labyrinth. The bony labyrinth is a cavity tunnelled in the temporal bone of the skull. Its structure forms three ducts, the semicircular canals, and the vestibule. This elaborate canal system contains in its cavities the membranous labyrinth suspended in perilymph. The suspension system of the membranous labyrinth does not allow it to move relative to the skull. Thus the accelerations acting on the membranous labyrinth are those applied to the head. The bony semicircular canals lodge the three semicircular canals, while the vestibule contains the utricle and the saccule (Fig. 2.1).⁷ The membranous labyrinth contains fluid called endolymph.

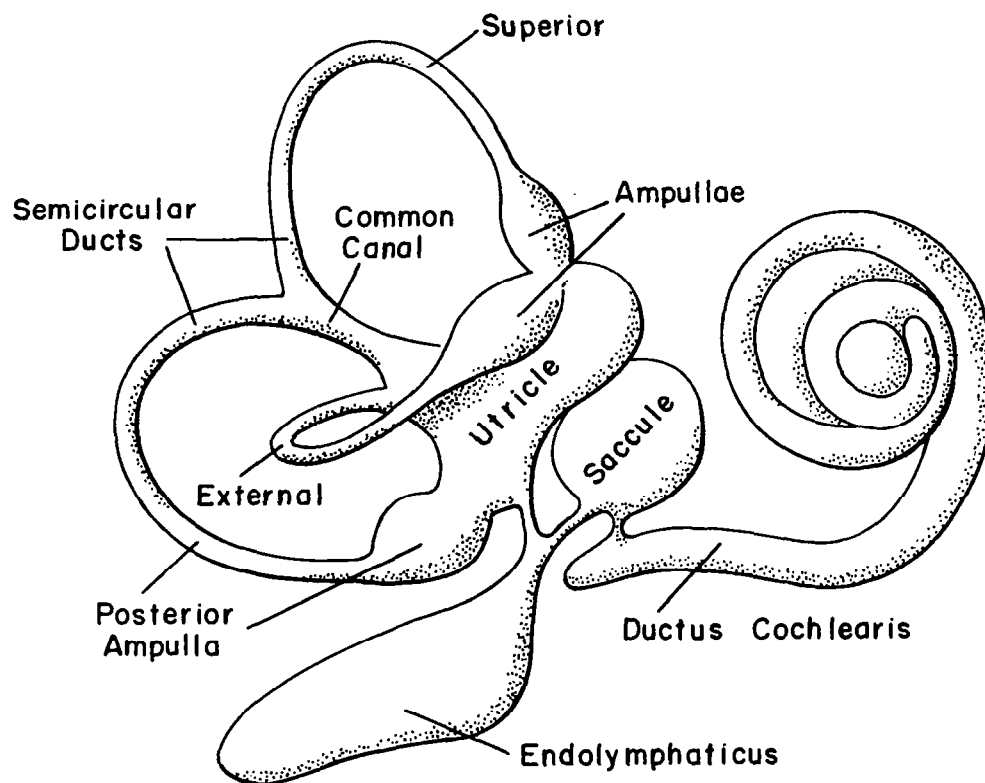


Fig. 2.1 The Membranous Inner Ear (Ref. 7)

The utricle is the large, oblong sac occupying the vestibule. Its lower part forms a pouch where it thickens over an area of about 6mm^2 ($2\text{mm} \times 3\text{mm}$), and is known as the macula. The otolith, a gelatinous substance with calcium carbonate grains in it, and of specific density of around 2.95, is supported over the macula by strands allowing a limited sliding travel of about 0.1mm . The macula is the receptor end of this otolithic organ, providing the bed for the utricular branch of the vestibular nerve. It also has sensory hairs imbedded in it, which at their other end penetrate the otolith. Fig. 2.2 is a cross section of the utricle showing the macula and the otolith together with their supporting and sensory cells.⁷⁷ Note that the macula and otolith are not exactly planar; a small portion of the sensor makes an angle of 120° with the mean plane of the macula. Nevertheless, the plane associated with the utricle is a plane which, for an erect head, is elevated between 26° to 30° above the horizontal plane. The two utricles (one from each inner ear) are located in the same plane.

The utricle is a multi-dimensional linear accelerometer with the otolith being the moving mass. The plane, associated with the sensor, is relevant in determining the input accelerations to it.

The saccule is an organ with histological structure identical to that of the utricle. The plane of the saccular macula is perpendicular to that of the utricle.

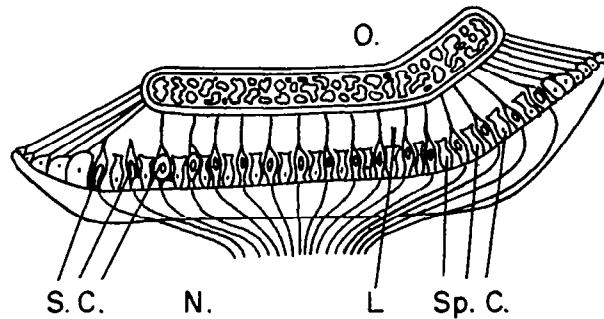


Fig. 2.2 Schematic Drawing of a Cross Section of an Otolith and its Macula. O. is the Otolith, Suspended by Strands which Run from the Margins to the Macula, Consisting of Supporting Cells (Sp.c) and Sensory Cells S.C. Between the Otolith and the Macula There is a Thin Layer (L) to Allow the Otolith to Slide Over the Macula. N. is the Nerve (Ref. 77)

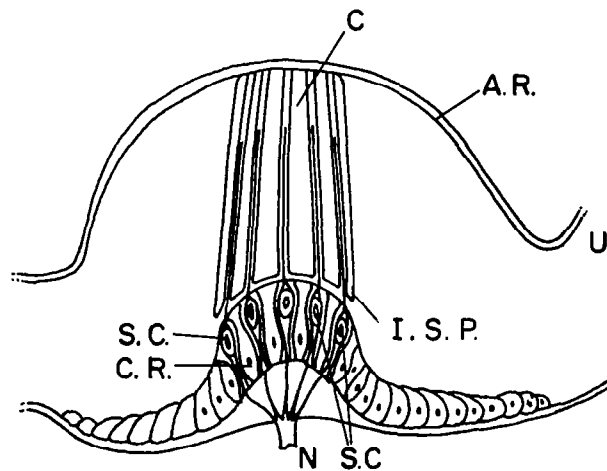


Fig. 2.3 Schematic Drawing of a Cross Section Through an Ampulla and Crista. A.R., Ampulla Roof. C.R., Crista, Consisting of S.C. (Sensory Cells), Supporting Cells and N. (Nerve Fibres). Between Cupula and Crista There is the I.S.P. (Interspecific Space) U., Utricle (Ref. 77)

The three semicircular canals are above and behind the vestibule. Their structure is planar, lying in planes which are roughly orthogonal to each other. The horizontal (lateral) canal is in a plane elevated about 25° to 30° from the horizontal plane. The other two canals, the posterior and the superior vertical, are in approximately vertical planes (see Fig. 2.1). Note that the horizontal canals of the two ears lie in the same plane, while the superior canal of the left ear is coplanar with the posterior one of the right ear and vice versa.

The three semicircular canals have very nearly the same structure and dimensions. Each canal starts at the utricle, forms approximately $2/3$ of a circle with outer diameter of 4 to 6mm, dilates at the ampulla, contracts again and terminates at the other end of the utricle. The canals have five orifices to the utricular sac, since the posterior and the superior canals have a common duct along the intersection line of their planes. The ampulla is nearly sealed by the ampullary crista and the cupula. The crista contains supporting hairs and sensory cells which project into the cupula, a dome-like gelatinous mass (Fig. 2.3)⁷⁷ The cupula is of equal density to the endolymph which fills the narrow (0.3mm in diameter) semicircular canals. In contrast to the structure of the utricle and the saccule, there is no interspace between the crista and the cupula, although sliding movement of the cupula is feasible.

The semicircular canals are heavily damped, angular accelerometers. Their arrangement in three perpendicular planes provides a way to sense components of angular acceleration along three axes which are amenable to easy vectorial manipulation.

The vestibular nerve sends a branch to each crista of the canals and the utricular macula, while two branches are imbedded in the saccule. The transmission of information from the vestibular sensors to the central nervous system is by frequency modulation. When unstimulated, the sensors show nerve action potentials of about 8 to 10 pulses per second. For the semicircular canals, the firing rate will increase or decrease according to the direction of the input angular acceleration and in proportion to its strength. Similar responses may be recorded for the utricular macula but without clear directional response.

The physiology and topology of the labyrinth throw some light upon its sensory characteristics. The fact that the semicircular canals have their mean planes very nearly perpendicular allows three dimensional sensing of angular accelerations. Since the canals open into the utricle, interaction between canals is plausible by virtue of endolymph flow. Moreover, the posterior and the superior canals share a common duct. Thus they are stimulated to a different degree, perhaps, but simultaneously. The dynamic characteristics of the canals depend upon the specific density of the cupula and the endolymph, and would alter

if the cupula does not seal the ampulla while deflected.

To summarize, the anatomy of the labyrinth displays two different groups of sensors. Their structure is distinctly different, as are their sensory functions.

2.2 ORIENTATION-REFERENCE COORDINATES

The location and the mean planes of the vestibular sensors, as well as their attitude in the head is known. Thus the geometric coordinates of the vestibular system are unique in any given head axis system. Since there is no relative motion between the head and the labyrinth sensors, head movements can be referred to as inputs of the vestibular system. Consequently, a head fixed, axes frame, which considers the symmetry of the labyrinths, is a convenient coordinate system to define in it the accelerations acting on the skull.

Two perpendicular planes are defined for the head, the frontal plane and the sagittal plane. The latter divides the head into two symmetrical halves and contains the sagittal X_h (fore and aft) axis and the vertical Y_h axis. The intersection of the frontal and the sagittal planes form the vertical axis such that it runs colinear to the gravity vector. If the origin of the head coordinate system is located between the labyrinths, the sagittal axis, for an erect head, will run horizontal, and the vertical axis is along the neck (Fig. 2.4). The lateral axis, Z_h , completes the right handed coordinate system. Note that

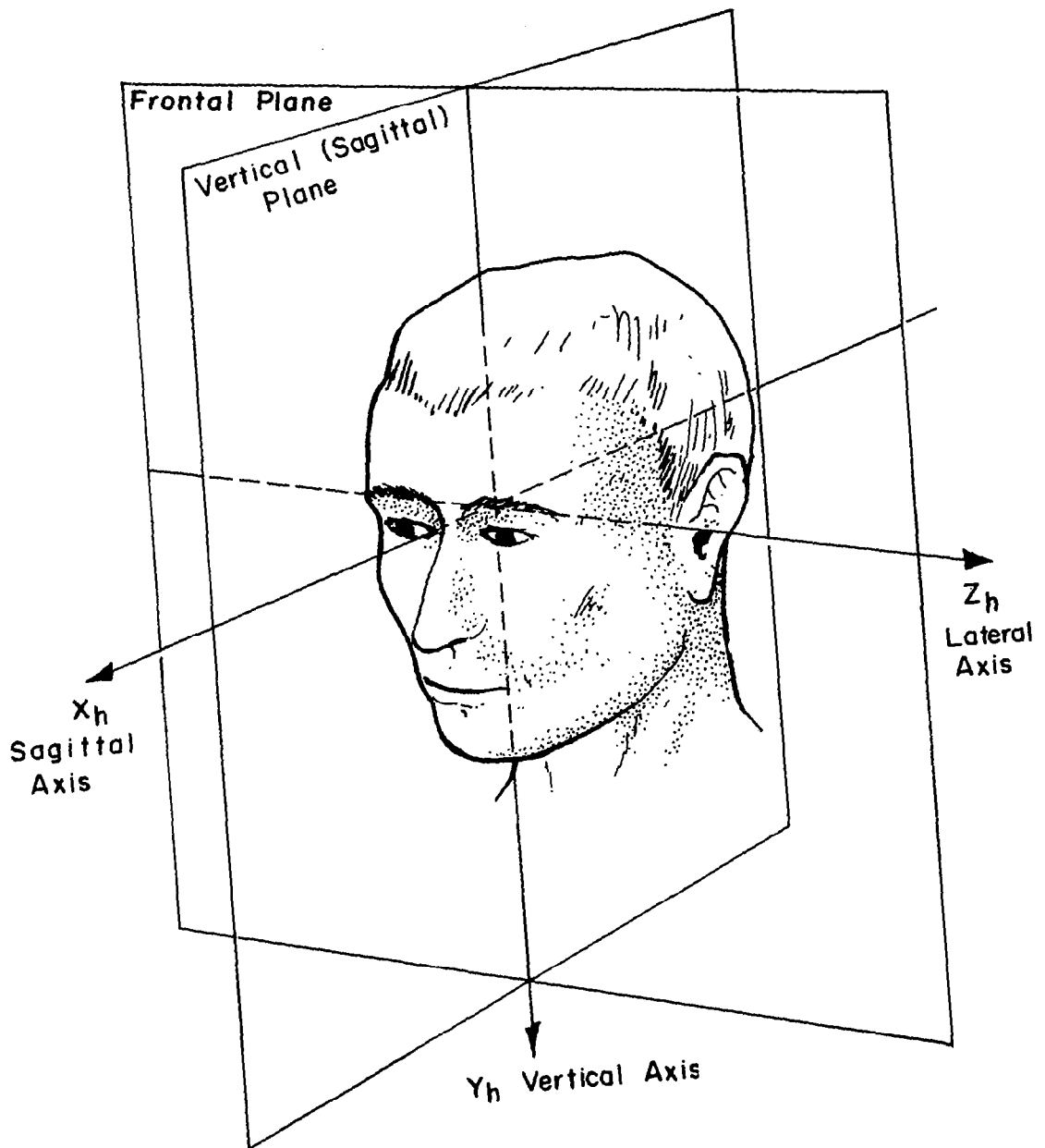


Fig. 2.4 The Head Planes and the Head Axis System

the frame defined here is related to the functional planes of the sensors by a single transformation through an alignment matrix $[\xi]$.

Orientation of the body is defined with respect to a given system of coordinates - the reference system. Dynamic orientation is then the ability to determine the relative motion between the head axes system and the reference coordinates. The natural selection of the reference frame (X_e, Y_e, Z_e) is to have it coincide with the head axes for normal unaccelerated body posture. These earth-fixed axes do not rotate or translate.

The issue of normal posture refers to the relative position of the head with respect to the trunk. Absence of bending or torsion of the neck is a normal configuration of head and body interconnection. In this context, suspension of the body upside-down, with the head free, is still an acceptable posture.

2.3 CONTROL VARIABLES

The vestibular sensors are sensitive to accelerations, thus the input variable to the vestibular system is a vector having direction and magnitude. The output quantity, however, is not a vector in the strict sense. Information from the semicircular canals and the otoliths is sent to the central nervous system and thereafter an awareness of the sensation of motion is perceived. This perceived output variable preserves the indication of direction like a

vector. However, sense of magnitude is applicable only on a comparative basis, where motions are faster or slower without an absolute scale. It is unusual to assign a perceived variable as an output of a control system, particularly when it only resembles the input. Nevertheless, perceived orientation is the most important sensation the human experiences in response to an input acceleration and will be considered here as the output of the vestibular system. There are also some objective measurements of activity of the vestibular sensors, the most known ones being observations of compensatory eye movements. However, those are derived variables with some transfer characteristics related to the output of the vestibular sensors.

In conclusion, the vestibular system should be examined as a sensory complex of accelerometers with certain dynamic characteristics which establish the input-output relations between accelerations applied in the head axes frame and perceived orientation as indicated by the human.

2.4 IDENTIFICATION PROCESSES

In humans, identification of sensing capabilities of the vestibular system is associated closely with experiments of psychophysical nature. Validity and usefulness of experimental work of this kind depends on the correlation one can draw between the precise, and usually well defined, input conditions and the human response.

Control engineering theory offers a number of identification techniques where only yes and no types of responses will suffice. For a step or an impulse input, indication of onset of perception or termination of it contains the pertinent data on the characteristics of the sensor. Standard frequency response for a linear system required only phase lag or lead data to identify the time constants of the system.

Stimulation of the vestibular system is a source of various illusions which the human interprets as a subjective orientation. For identification purposes, these illusions are an excellent tool to obtain the time course of a sensation or a steady state value (gain and sensitivity) of a transfer function. The objective measurements of vestibular activity, such as measurement of eye movements, is probably the most effective and reliable method of response identification. As noted before, compensatory eye movements indicate stimulation of the semicircular canals. However, the relation between these movements and the dynamics of the canals has to be determined by comparison with psychophysical experiments.

Finally, identification techniques suitable for manual control systems could be applied to the vestibular sensors. If the experimental subject (human operator for these conditions) is placed in an orientation control loop with the function of a sensor and a controller assigned to him, the system response can be analyzed in terms of control

characteristics of equivalent "black boxes". The block corresponding to the human operator will indicate the intrinsic dynamics of his sensors and the effects of data processing by the central nervous system.

CHAPTER III

THE SEMICIRCULAR CANALS

The semicircular canals are the rotational sensors of the vestibular system. When stimulated, they participate in the control of the postural reflexes of the body and initiate compensatory eye movements in order to preserve the body balance and reference with respect to the environment. Consciously, the human is aware of the rotations his head undergoes. The information on orientation the human can obtain from his semicircular canals can be analyzed by control engineering methods and summarized in a mathematical model describing the dynamic characteristics of the three semicircular canals.

3.1 INPUT VECTOR AND SENSITIVE AXIS

Rotation of the head has been identified as the motion which stimulates the semicircular canals. Another observation indicates that the canals cease to show activity during prolonged periods of rotation with constant angular velocity. The conclusion is that the semicircular canals are sensitive to angular accelerations, which are applied about an axis normal to the plane of the canal. Since there are three semicircular canals in each ear, input accelerations

are sensed along three mutually orthogonal axes and probably summed vectorially in the central nervous system.

When the canals are stimulated, the human is consciously aware of a rotational motion, a perceived sensation of rotation. Furthermore, the time course of the perceived sensation will depend upon the dynamic behavior of the canals, which can be simulated by a simple mechanical model.

3.2 A PHYSICAL MODEL FOR THE SEMICIRCULAR CANALS

The theory of operation of the semicircular canals was first set by Steinhausen and is based on the concept of a heavy damped torsion pendulum for the cupular mechanism.¹⁵⁴ In this model, the fluid ring of the canals corresponds to the moment of inertia of the pendulum and the spring restoring torque is provided by the elasticity of the cupula. The heavy damping is attributed to the viscous torques arising from the flow of the endolymph through the capillary canals (Fig. 3.1).¹⁵⁷ This theory is based on the assumption that over a certain range of angles the cupula deflects while still sealing the ampulla. The assumption of a pendulum model indicates that the cupulo-endolymph system will obey a second order linear differential equation first formulated by van Egmond, Groen and Jongkees.¹⁵⁷ As shown in Fig. 3.1, the cupula deflection is assumed equal to the angle of rotation of the endolymph. This assumption approximates the canals to a tube with a constant, cross sectional area. The angular deviation of the cupula with respect

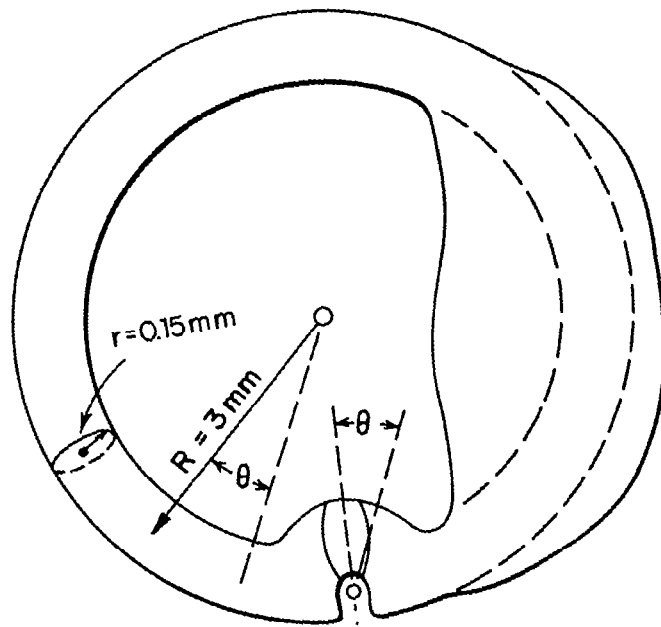


Fig. 3.1 Schematic Diagram of the Semicircular Canal (Ref. 157)

to the skull is given by:

$$I\ddot{\theta} + B\dot{\theta} + K\theta = I\alpha \quad (3.1)$$

where I = moment of inertia of the endolymph,

B = viscous damping torque, at unit angular velocity (rad/sec) of the endolymph with respect to the skull,

K = stiffness, torque per unit angular deflection of the cupula,

θ = angular deviation of the cupula with respect to the skull (rad),

$\dot{\theta}$ = angular velocity of the cupula with respect to the skull (rad/sec),

$\ddot{\theta}$ = angular acceleration of the cupula with respect to the skull (rad/sec²), and

α = input angular acceleration along the sensitive axis of the canal (rad/sec²).

Equation (3.1) represents the time response of the cupula, in any given semicircular canal, as a function of the input stimulation. The response is seen to depend upon two parameters: $\frac{B}{I}$ and $\frac{K}{I}$.

3.3 ROTATION ABOUT THE VERTICAL (Y_h) AXIS

The reference frame of orientation and the head axes were assumed to coincide for a non-moving, erect head (see Sec. 2.2). For these initial conditions, rotation of the head about the earth-fixed vertical axis (Y_e) stimulates the

semicircular canals sensitive to accelerations about the Y_h axis. The tangential and centrifugal accelerations associated with this rotation are below the threshold of perception of the otoliths. If angular accelerations are applied about the Y_e (and Y_h) axis, the parameters of the canals can be determined without interference effects from the linear acceleration sensitive otoliths.

The second order characteristic equation for the canals (Eq. 3.1) has two roots, ω_1 and ω_2 :

$$\omega_1 \text{ and } 2 = \frac{\frac{B}{I} \pm \sqrt{\left(\frac{B}{I}\right)^2 - 4\frac{K}{I}}}{2} \quad (3.2)$$

However, since the viscous torque is very high compared to the elastic one, an assumption has been made that $\frac{K}{B} \ll \frac{B}{I}$ yielding two real roots:

$$\begin{aligned} \omega_1 &\cong -\frac{K}{B} \\ \omega_2 &\cong -\frac{B}{I} \end{aligned} \quad (3.3)$$

The transfer function of the canals, from angular acceleration about the head vertical axis (α_{Y_h}) to cupula position (θ) is given by:

$$\frac{\theta(s)}{\alpha_{Y_h}(s)} = \frac{1}{(s + \omega_1)(s + \omega_2)} \quad (3.4)$$

where s = the Laplace transform operator.

The time constants of the cupular model $\frac{B}{K}$ and $\frac{I}{B}$ are widely separated, thus imposing a certain difficulty on their experimental evaluation. Van Egmond et al. established the values of those time constants within 10 to 20 per cent allowance for experimental errors.¹⁵⁷ Their assumption is that the perceived sensation of angular velocity is related to the cupula deflection. According to this assumption, measurements taken on parameters of perceived sensations correspond to the parameters of the cupular model.

The duration of a transient response of the cupula to a velocity step, plotted against the magnitude of the step input is called by van Egmond "subjective cupulogram". Indeed, measurement of duration of perception as reported by a subject is one reliable method to determine the value of $\frac{B}{K}$. The core of the method relies on the instantaneous stop of a platform moving with constant angular velocity and subsequently recording the time of sensation reported by the subject. Mathematically, for a step of γ°/sec , the time response of the cupula, initially at rest will be:

$$\theta(t) = \gamma \frac{I}{B} \left(e^{-\frac{K}{B}t} - e^{-\frac{B}{I}t} \right) \quad (3.5)$$

Physically, due to the angular momentum imparted to the endolymph and the viscous torque, the cupula is deflected to a certain maximum angle following which it slowly returns to zero under the influence of its own elastic torque opposed by viscosity. The sensation the subject reports

during the process, is of rotation in the direction of the input step with slowly decreasing velocity. In agreement with the assumption that $\frac{K}{B} \ll \frac{B}{I}$, the return phase of the cupula will exhibit simple exponential decay:

$$\theta(t) = \gamma \frac{I}{B} e^{-\frac{K}{B}t} \quad (3.6)$$

since the term $e^{-\frac{B}{I}t}$ of equation (3.5) is $e^{-\frac{B}{I}t} \ll 1$.

The sensation of rotation the subject perceived, will stop, the moment the cupula reaches a deflection θ_{\min} (theta minimum) which corresponds to the deflection for threshold of perception. Then, the approximate time for this event will be:

$$t = \frac{B}{K} \log \left(\frac{\frac{I}{B} \gamma}{\theta_{\min}} \right) \quad (3.7)$$

or

$$t = \frac{B}{K} \log \frac{I}{B \theta_{\min}} + \frac{B}{K} \log \gamma \quad (3.8)$$

A series of time measurements for angular velocity step responses plotted on semi-logarithmic scale will yield the time constant $\frac{B}{K} = 10$ sec (see Fig. 3.2).¹⁵⁷

Besides testing for transient response, the cupular model for the semicircular canals can also be studied in the transformed frequency domain. The increasing phase shift of subjective sensation of angular velocity with respect to the input acceleration is an indication reflecting the time constants of the model. Consider an input sinusoidal rotation with frequency $\omega_0 = \sqrt{\frac{K}{I}}$, the undamped

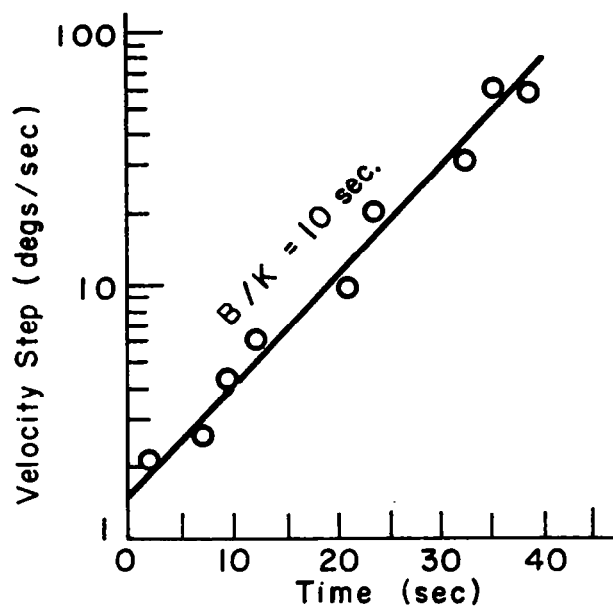


Fig. 3.2 Duration of Sensation as a Function of the Velocity Step Input (Ref. 157)

natural frequency of the cupular model. For this input the angular deflection of the supula lags the input acceleration by 90° . Thus, the cupula is in phase with the input angular velocity, which is zero at the peaks of the rotation. At these instances, the subjective feeling will be that of rest. Experimenting with a torsion swing, van Egmond found that:

$$\omega_0 = 1.0 \text{ rad/sec} \quad (3.9)$$

With this result, the second time constant, $\frac{I}{B}$, of the cupular model is evaluated as:

$$\frac{I}{B} = \frac{1}{\omega_0} \frac{K}{B} = 0.1 \text{ sec} \quad (3.10)$$

With the proper values of time constants, the transfer function for the semicircular canals as given in Eq. (3.4) corresponds to:

$$\frac{\theta(s)}{\alpha_{Y_h}(s)} = \frac{1}{(10s + 1)(0.1s + 1)} \quad (3.11)$$

Eq. (3.11) indicates that the steady state angle of the cupula, subjected to stimulation of constant angular acceleration is $\theta(t=\infty) = \alpha_{Y_h}$. The assumption can be verified by using the velocity step response test in conjunction with subjective estimation of total angular travel. When van Egmond instructed his subjects to report completion of

full revolutions, the experimenter could determine the average subjective velocity for the subject. Indeed, the indication confirmed decay with a time constant of $\frac{B}{K} = 10$ sec. However, when the velocity was extrapolated to its initial value, it agreed absolutely with the applied step of angular velocity (see Fig. 3.3).¹⁵⁷ This finding brings to the modification of the cupular transfer function when associated with subjective perception of angular velocity such as:

$$\frac{\text{Subjective angular velocity (s)}}{a_{y_h}(s)} = \frac{10}{(10s+1)(0.1s+1)} \quad (3.12)$$

Note that the parameters of the cupular model and the associated transfer function as presented in Eq. (3.12) were tested for subjective perception. This is in agreement with the definition of a transfer function for the vestibular sensors where the output variable is perceived sensation.

The time constants of the cupular model for input accelerations about the vertical head axis, especially the long one, can be measured by objective methods based on the compensatory eye movements elicited during periods of stimulation of the canals. Chapter V will discuss the relations between the semicircular canals and the eye motor system. Another identification method, dealing with an illusion of vestibular origin is examined in Sec. 3.4.

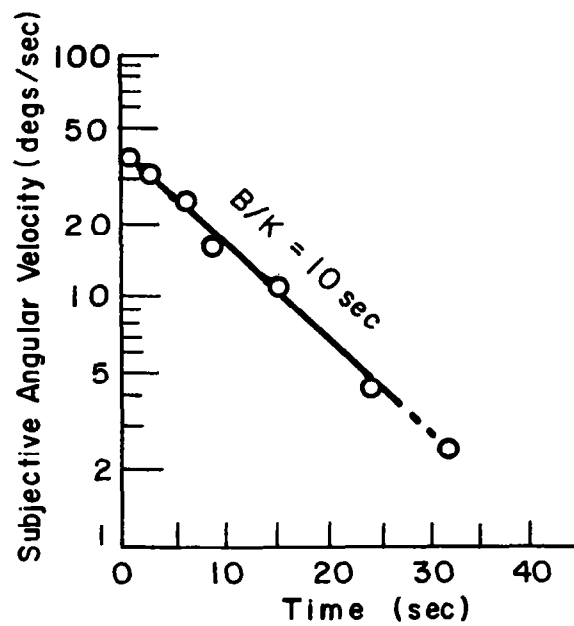


Fig. 3.3 Subjective Angular Velocity after a 40°/sec Velocity Step (Ref. 157)

Pure theoretical attempts to estimate the parameters of the semicircular canals are based on approximating them to circular tubes with viscous flow in it. The results show a time constant of $\frac{B}{K} = 27$ sec., which is much higher than measured experimental values.

3.3.1 Threshold of Perception

Studies of human perception of angular acceleration indicate the phenomenon of threshold. At the threshold, or below it, the existence of a constant input acceleration for prolonged time will not be noticed. Physically, the threshold is associated with the minimal deflection of the cupula which will lead to a conscious sensation of rotation. The time from the onset of the input until it is perceived, the latency time, will be a function of the magnitude of the input vector, and the dynamics of the sensor.

A technique utilizing the step response in acceleration of the semicircular canals is widely accepted as a subjective measurement of threshold.³² The method applies a known constant angular acceleration to the subject and his latency time is recorded. The step response of the semicircular canals to an input acceleration about the vertical axis Y_h is:

$$\begin{aligned}\theta(t) &= \alpha_{Y_h} + \frac{\alpha_{Y_h}}{10-0.1} \left(0.1e^{-10t} - 10e^{-0.1t} \right) \\ &\cong \alpha_{Y_h} \left(1 - e^{-0.1t} \right)\end{aligned}\quad (3.13)$$

where α_{Y_h} = input angular acceleration, $^{\circ}/\text{sec}^2$. Consequently, if θ_{\min} is the deviation of the cupula at the threshold,

$$\theta_{\min} = 0.1\alpha_{Y_h} \tau \left(1 - \frac{0.1\tau}{2} + \frac{0.01\tau^2}{6} - \dots \right) \quad (3.14)$$

with τ = latency time, sec.

The product $\alpha_{Y_h} \tau$ is called by van Egmond et al. the "Muelder product", and their observations showed it approximately constant and equal to 1.5 to 2.0 $^{\circ}/\text{sec}$ over the range 1 to 5 $^{\circ}/\text{sec}^2$. If the "Muelder product" is constant, it implies that the product of latency time and input acceleration will remain constant for a certain range of input accelerations.

However, the applicability of the "Muelder product" is limited to regions where the additional terms of the series in Eq. (3.14) do not exceed say 10 per cent, or $\tau \leq 2.5$ sec. The controversy about the validity of the product for accelerations about the threshold when latency times are longer than 2.5 sec is indeed well founded as Eq. (3.14) shows.⁴⁷

The validity of the "Muelder product" over the range of accelerations from 0.1 $^{\circ}/\text{sec}^2$ to 10 $^{\circ}/\text{sec}^2$ was tested by the author. The step response technique for measuring threshold of perception was used to measure latency time. The subjects, seated in a hooded cab of a moving base simulator (see Appendix A), were administered constant

angular accelerations about the earth-fixed vertical axis (Y_e) with random order in direction and magnitude, six readings at any given acceleration. Headrest and support for the back of the subject kept his head erect under the axis of rotation and with no strain to the neck muscles. Perceived rotation was measured by a "forced choice" method: the subject had to manipulate a control stick indicating the direction of movement, as well as the onset of his subjective detection of rotation. The experimental sequence provided 30 seconds of rest between consecutive runs. Three subjects were used for these experiments.

Fig. 3.4 presents the experimental results averaged over the three subjects, along with the expected latency time computed from Eq. (3.14). The expected latency time curve was computed relative to the experimental value at $\alpha_{Y_h} = 1.0^\circ/\text{sec}^2$. A perfect agreement between latency times predicted from Eq.(3.14) and measured values is found over the region of angular accelerations from 0.3 to $5^\circ/\text{sec}^2$. Near the threshold (about $0.14^\circ/\text{sec}^2$ determined on 75 per cent correct identification of input direction), the departure from theoretical results is probably due to scatter in the data caused just by the fact that measurements are taken near the limit of detection. Similarly, when latency times approach the response time of the human, the experimental data shows longer latencies than predicted. Results obtained for pilots by Clark and Stewart³² using identical techniques are also presented in Fig.3.4. There is no significant difference between results measured with those subjects (pilots) and the subjects, with no flying experience, used here. The mean

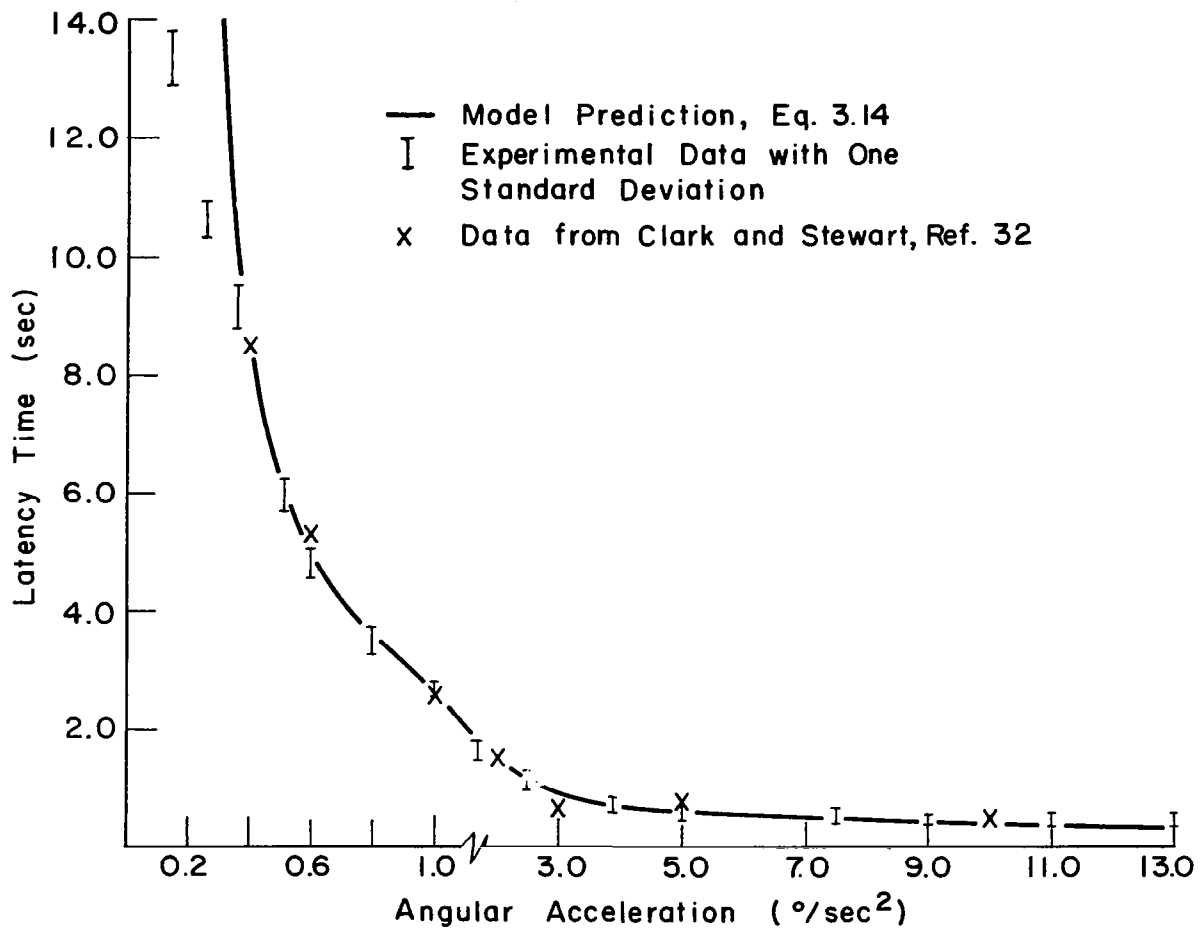


Fig. 3.4 Latency Times for Perception of Angular Acceleration about The Vertical Axis (Y_h)

Note: Scale Change of Angular Acceleration

latency times measured here are also presented in Fig. 3.5. Plotted on a log-log scale, the "Muelder product" is a line with slope of - 1. Examination of Fig. 3.5 indicates the region of validity for this product. As noted before, the product $\alpha_{y_h} \tau = \text{constant}$ is not a valid approximation while the input angular accelerations are smaller than $1.0^\circ/\text{sec}^2$. Additional terms from Eq. (3.14) improve the correspondence between measured and expected latency times.

On the basis of this series of experiments, the following conclusions are justified:

- 1) The threshold for perception of angular acceleration around a vertical axis will vary subjectively between 0.1 and $0.2^\circ/\text{sec}^2$ with a mean of about $0.14^\circ/\text{sec}^2$.

- 2) Latency times for detection of small accelerations can be predicted accurately from the model for the semicircular canals.

- 3) For its range of validity ($\tau \leq 2.5 \text{ sec}$) the "Muelder product" holds with somewhat higher value ($2.6^\circ/\text{sec}$) than usually reported.

3.4 HABITUATION

Objective measurements of the semicircular canals' activity by recording compensatory eye movements (see Sec. 5.2) and subjective cupulograms indicate changes in response due to frequent stimulation. The phenomenon is called habituation, pointing to a variation of parameters according to the recent history of stimulation for the

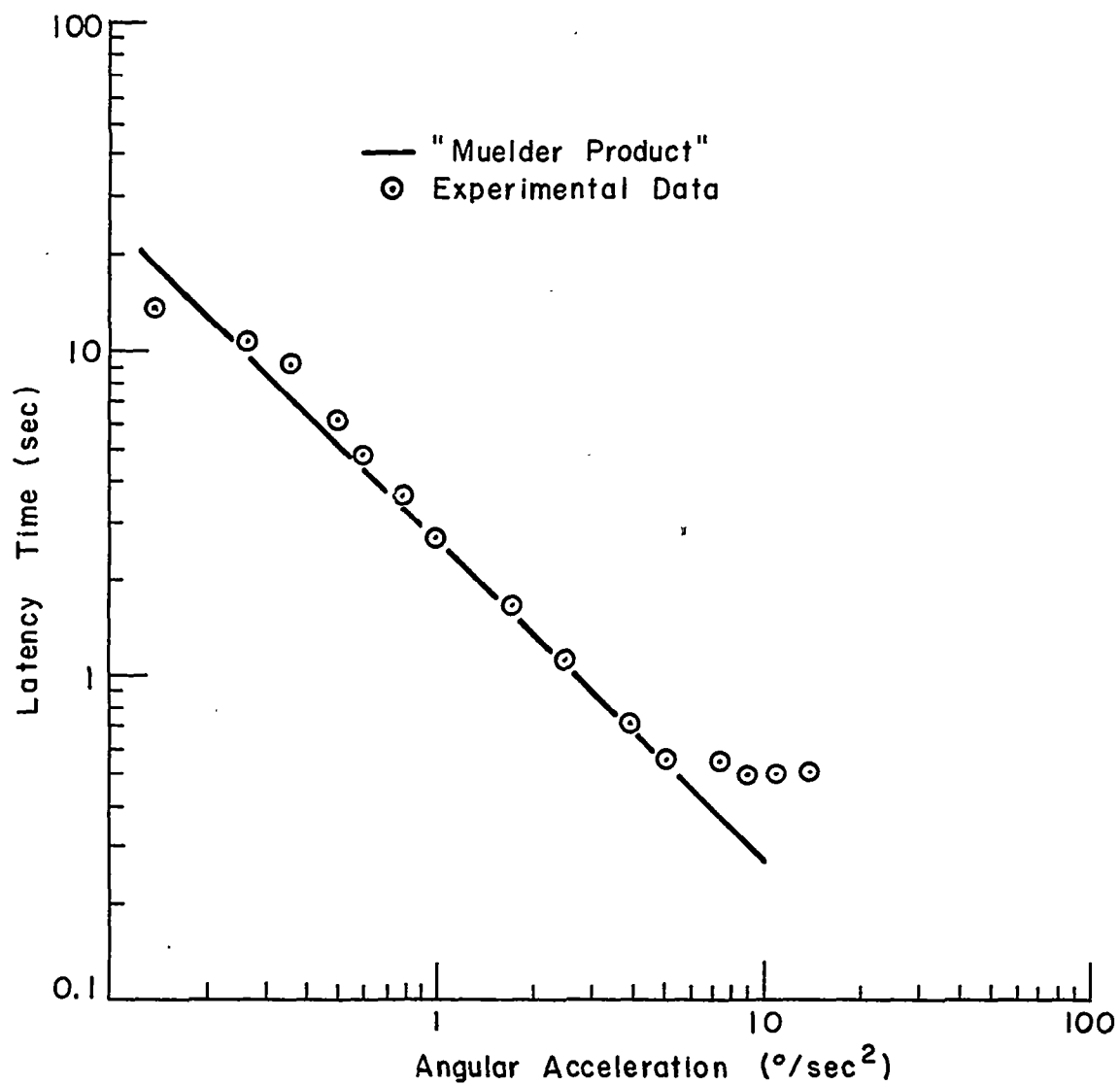


Fig. 3.5 Latency Times for Perception of Angular Acceleration About the Vertical Axis (Y_h)

canals. Indeed, the question is raised whether certain characteristics of the sensors measured at any given time are not heavily influenced by the experimental methods used to obtain these results.

Differences are reported between subjective cupulograms and cupulograms for objective, compensatory eye movements. Moreover, the habituation effect becomes pronounced, for a given technique, while the experimental pattern is repeated several times. For the vestibular system, the output vector has been defined here as subjective perception of angular velocity. Similarly, the focus should be on time variations found for the parameters of the semicircular canals measured by subjective indication. Values for $\frac{B}{K}$ obtained by the repetitive technique of subjective cupulometry show $\frac{B}{K} = 8$ to 10 sec.⁷⁷ Those observations will pertain as long as the semicircular canals are not exposed to continuous stimulation lasting for several hours, at which time a gradual decrease of the time constant is found.⁷⁷ However, a period of rest restores the cupulogram to its original value, regardless of the level reached prior to it. This evidence is sufficient to conclude that the physical model of the semicircular canals and the experimental values attached to its parameters, represents the expected, average response of a human living in an environment which does not impose stimulation beyond "normal". In this context, normal stimulation can be defined as exposure to rotations necessitated by

everyday life. The response of the canals is probably adapted to living conditions on earth, similar to the way habituation takes place when those conditions are changed.

Objective cupulograms measuring the velocity of the slow phase of vestibular nystagmus (see Sec. 5) find $\frac{B}{K}=16$ sec. Those responses will hold for stimulation periods well beyond the time when effects are noticed on subjective measurements. However, for professionals with constant exposure to angular accelerations, like figure skaters and pilots, the objective cupulograms show the habituation phenomenon along with the accompanying recovery from it.

The habituation to stimulation is in general attributed to the central nervous system.^{77,52} This notion on habituation is supported by the fact that compensatory eye movements, being of a somewhat reflex nature, do not adapt easily. Indeed, for very sensitive subjects, objective and subjective cupulograms agree numerically, indicating adapted response for most of the subjects, randomly selected.⁷⁷ Still, neither the mechanism of habituation nor the periods of time involved are known.

Experiments on cats stimulated repeatedly with sinusoidal rotation of one given frequency show marked habituation of compensatory eye movements to this particular frequency while effects taper off for the adjacent spectrum of frequencies.⁴¹ These findings support the notion that habituation is central, since it is hard to attribute mechanical fatigue of the canals to a certain frequency

only. However, as stated before, besides identifying the phenomenon, no control description can be attached to it yet.

In an effort to overcome the effect of habituation on the long time constant of the semicircular canals, Cawthorne et al. used the oculogyral illusion to indicate the time response of the cupula in response to an impulse of angular acceleration.¹⁸ During the oculogyral illusion, a light which is stationary with respect to the subject, will appear to him as moving with him in the direction of motion of the subject. The illusion has been explained to be due to the compensatory eye movements, thus acceleration to the left produces eye rotation to the right and an accompanying motion of the visual target opposite to it. The velocity of the oculogyral illusion in response to an impulse of acceleration, as obtained by Cawthorne, shows a time constant, $\frac{B}{K} = 24$ sec. However, at present it is not completely clear whether the oculogyral illusion originates solely in the vestibular system. Therefore, parameters measured by this method are still questioned.

3.5 ROTATION ABOUT A HORIZONTAL AXIS

Investigators have assumed that the torsion pendulum model for the cupula deflection is valid for rotation about any head axis. However, experimental efforts to validate this assumption and to determine the time constants of the model (see Eq. (3.3)) were undertaken almost exclusively

for rotation around the vertical head axis (Y_h). The deterrent is, of course, the difficulty to produce rotation about a horizontal axis (pitch or roll) without stimulating the linear motion sensors of the vestibular system.

In the literature, two experiments are reported to measure the long time constant, $\frac{B}{K}$, in perception of rotation about the sagittal and the lateral axes of the head.^{102,108} Neither of these experiments preserved the normal head-neck posture as discussed in Chapter II; thus results are possibly affected by proprioception. The angular accelerations were applied about the earth-fixed vertical axis with the head tilted to reach the proper head axis. Jones et al. recorded by subjective cupulometry for roll (X_h) $\frac{B}{K} = 6.1$ sec and for pitch (Z_h) $\frac{B}{K} = 5.3$ sec. From eye movement evaluation of response to a single velocity step input, the corresponding values are $\frac{B}{K} = 6.6$ sec and $\frac{B}{K} = 4.0$ sec respectively.¹⁰²

With a similar technique of stimulation, Ledoux used the data on the topography of the vestibular system to stimulate each coplanar pair of canals by accelerations about an axis perpendicular to its mean plane. Objective cupulometry in planes parallel to the planes of the canals did not show variations of characteristics among the three pairs of semicircular canals.¹⁰⁸

No data on the short time constant $\frac{I}{B}$ and the sensitivity of the canals stimulated in pitch and roll is available. Nevertheless, it is plausible to assume them as equal to those for rotation in yaw.

3.5.1 Threshold of Perception (Experiment by the Author)

Using the technique of applying steps of angular accelerations and recording the latency time until rotation is perceived, the threshold of sensation for rotation around the head sagittal axis (roll) was determined. The measured latency times for perception of small accelerations were used to obtain the long time constant, $\frac{B}{K}$, of the canals sensitive to angular accelerations about this axis.

The experimental method and procedure were identical to those described in Sec. 3.3.1. The point to note is that the simulator cab was rotated about the earth-fixed vertical axis (Y_e). The subject seated, was accommodated to rest his head, face down, on a head rest under the axis of rotation of the simulator. By bending the body at the waist rather than the neck, the "normal" posture of head-neck, or a position within a few degrees from it was preserved throughout the experiment.

Under these circumstances, the vestibular linear motion sensors were not stimulated during the experiment except for the steady change of orientation of the head with respect to gravity. The tangential and centrifugal accelerations here are below the threshold of these sensors.

The experimental results are presented in Fig. 3.6. Threshold of perception is found approximately at $0.5^\circ/\text{sec}^2$ angular acceleration and a rather sharp separation between sensation and lack of it is noted. The mean latency times,

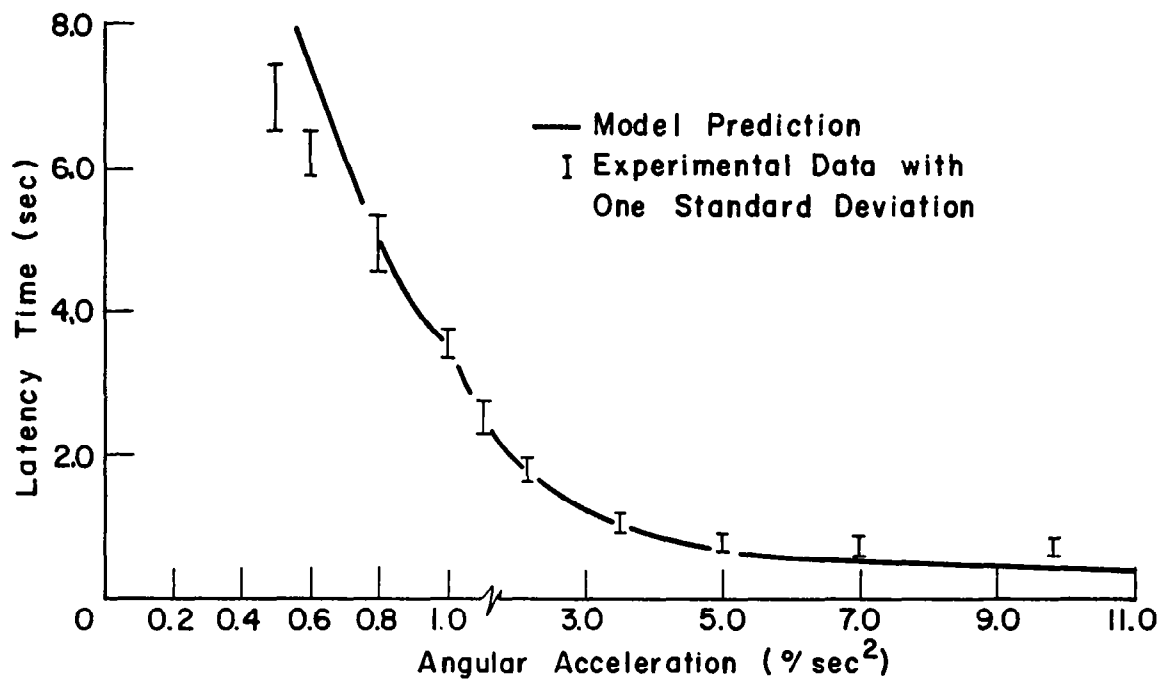


Fig. 3.6 Latency Times for Perception of Angular Accelerations about The Roll Axis (X_h)

Note : Scale Change of Angular Acceleration

averaged over the three subjects were used to estimate the long time constant of the semicircular canals in this configuration. Making the assumption that the short time constant is 0.1 sec and fitting an equation of the form of Eq. (3.14) to the data yields $\frac{B}{K} = 7$ sec. Latency times measured in these experiments were compared with results from responses for rotation around the vertical head axis (Y_h) and the difference between the mean values were found highly significant ($P < 0.005$) for accelerations lower than $5.0^\circ/\text{sec}^2$. Assuming the short time constant of the sensors as 0.1 sec and an agreement between the subjective and the input velocity over the range of 0.14 rad/sec to 10 rad/sec will yield the following transfer function:

$$\frac{\text{Subjective angular velocity (s)}}{\alpha_{X_h}(s)} = \frac{7}{(7s+1)(0.1s+1)}$$

3.6 A MATHEMATICAL MODEL FOR THE SEMICIRCULAR CANALS

The experimental data presented in this chapter reflects certain characteristics of the semicircular canals which can support a state of knowledge mathematical model for this portion of the vestibular system.⁸ The block diagram in Fig. 3.7 shows the dynamic characteristics of the canal system and the physiological organs to which they are attributed. Angular accelerations measured in the earth-fixed frame (α_e) are resolved into components in the head axis system by the orientation matrix $[A]$,

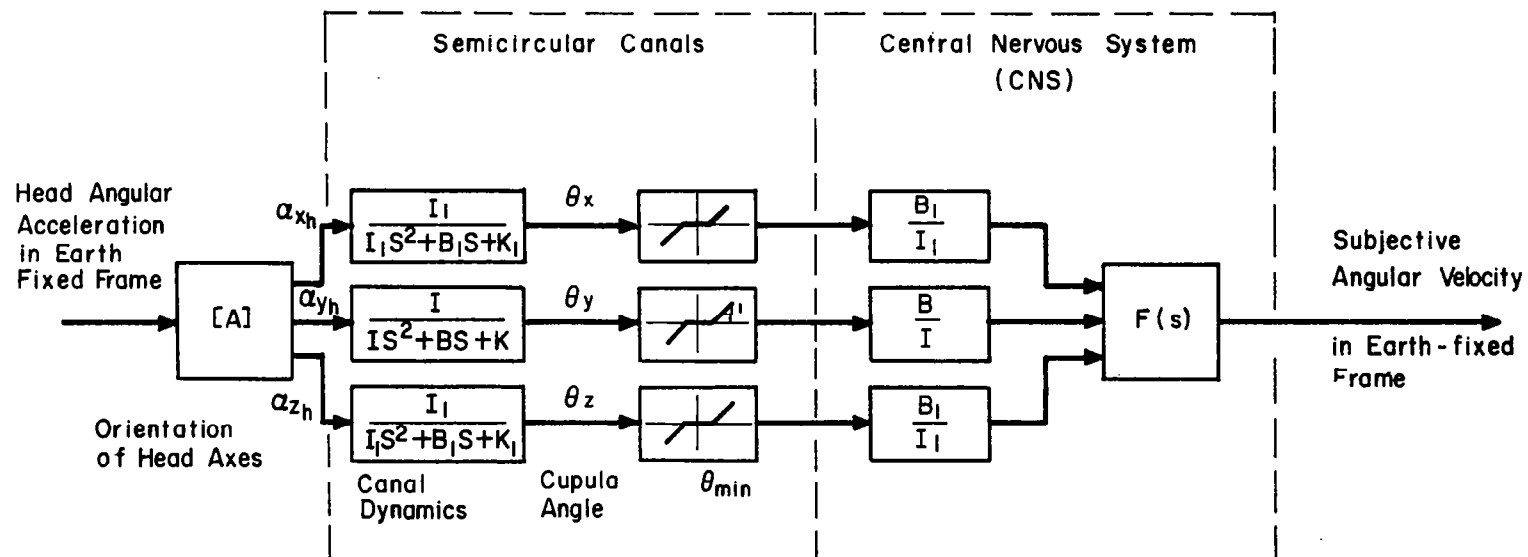


Fig. 3.7 Semicircular Canal Block Diagram - Short Period of Stimulation

which is dependent upon the orientation of the skull. In the semicircular canals, stimulated by the input acceleration, the cupula deviates from its null position in agreement with the highly damped second order model. When the cupula deviation exceeds the threshold level, this information is picked up by the central nervous system to be interpreted consciously as subjective angular velocity. Note that this model is not representing characteristics of any given canal, neither is it associated with stimulation of physiological synergic (acting together) pairs, but outlining perception of accelerations in the head axis system as defined in Chapter II. As presented here, the dynamics of the canals associated with perception of angular accelerations about the X_h and Z_h axes (roll and pitch) are assumed to be equal. The central nervous system, CNS, is shown here as a block $F(s)$ to underline the fact that certain unknown transfer characteristics are associated with it. As discussed in Sec. 3.4, habituation is a control process attributed to CNS. When the semicircular canals are not affected by excessive stimulation, the perceived sensation of rotation is assumed to depend entirely upon the canal dynamics thus rendering $F(s) = 1$.

What is the physical vector that corresponds to the subjective perception of angular velocity? This question is concerned with the mental evaluation of information provided by the semicircular canals. Fig. 3.8 is the frequency response of the canals. (Bode plot) for rotation

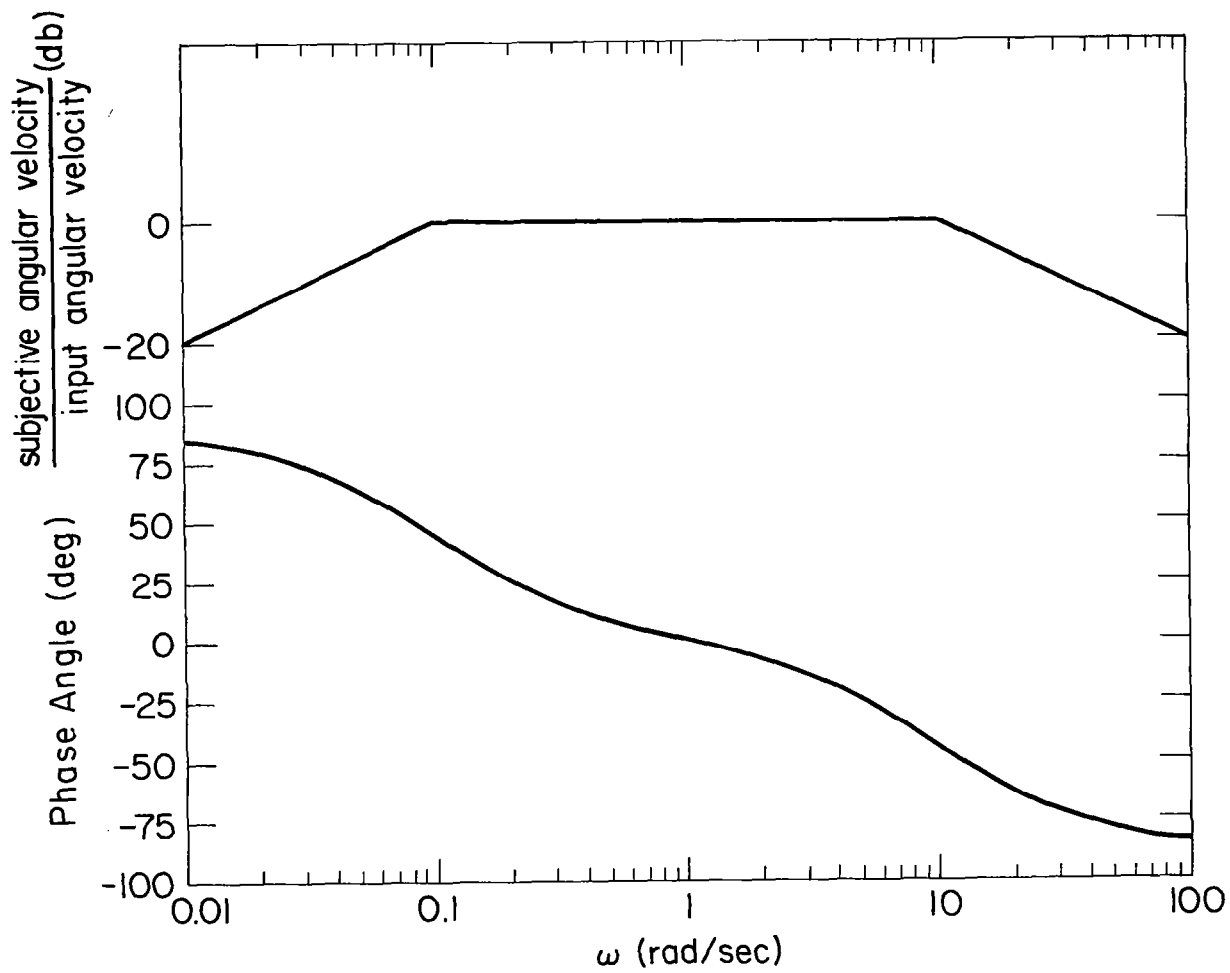


Fig. 3.8 Bode Plot of Semicircular Canals Model. Rotation about the Vertical Axis (Y_h)

about the vertical head axis (Y_h) with the input vector being the angular velocity of rotation and the output is the subjective perception of angular velocity assumed proportional to the cupula deflection. Note that over a wide range of frequencies, namely 0.1 to 10 rad/sec, the subjective sensation is that of the angular velocity of the motion. Similar observations hold for perception of angular velocities about the horizontal axes although with a slightly condensed frequency range, thus rendering the semicircular canals as angular velocity meters over most of the frequency spectrum of head movements during everyday activity. Moreover, while a rotation with constant angular velocity will go unperceived by the canals, a constant angular acceleration motion will be sensed over a certain period of time in a manner that perception will coincide with the instantaneous angular velocity of the rotation. Eq. (3.13) shows that cupula deviation will be proportional very closely to the instantaneous angular velocity ($\alpha_h t$) for the first 6 to 8 seconds after applying the input acceleration. Whether the CNS is capable to add vectorially signals arriving from the canals when the input acceleration is about an intermediate axis of the canals is still an open question. Qualitative measurements of compensatory eye movements indicate a positive answer; however, subjective perception might differ in this aspect.

The validity of the control model and the use of it has to be viewed in light of the limitations one has to

impose due to insufficient experimental support:

1) Dynamic Range. Eq. (3.1) shows that for a step input the steady state deviation of the cupula is equal numerically to the input angular acceleration. However, the morphological structure of the semicircular canals and the basic assumption on the cupula sealing the ampulla in its deviated position will probably limit the range of cupular travel within $\pm 30^\circ$. Thus a dynamic range of about 100 to 150 for accelerations about the Y_h axis (from $0.2^\circ/\text{sec}^2$ to $30^\circ/\text{sec}^2$) and somewhat smaller range for accelerations about the X_h and the Z_h axes are reasonable to expect from these sensors while remaining within their linear characteristics.

2) Habituation. The phenomenon has considerable effect on subjective perception of rotation. Also, perceived estimates of angular velocity, but not compensatory eye movements, have been found to decline, contrary to the model prediction, when an input acceleration persisted for periods longer than 30 sec.⁸⁶ Thus the model is valid for short lasting rotations (about 10 sec) and limited to moderate periods of stimulation which do not cause substantial habituation.

Within the outlined reservations, the control engineering model for the semicircular canals and its associated parameters is a complete set of specifications on those sensors.

CHAPTER IV

THE OTOLITHS - LINEAR ACCELERATION SENSORS

The perception of the orientation of the head (and the body) in space, relative to the force fields of the environment, is universally considered to be the function of the otolithic organs. Accordingly, the presence of specific forces acting on the body in its coordinate system is the input to the subjective feeling of orientation provided by these sensors. On a higher level, the otoliths regulate the postural reflexes of the body and the counterrolling compensatory eye movements which preserve the appropriate equilibrium in a given spatial attitude. In all, the otolithic organs are a center of detection and control of the voluntary changes of posture along with monitoring orientation during passive maneuvers of the head and the body as a whole.

However, in spite of the vital importance of the sensor, little was known about its dynamic characteristics and expected response to specific stimulation. The following discussion will attempt to unify the information scattered in the literature with experimental results

obtained by the author into a concise control engineering model of the utricle otoliths.

4.1 THE UTRICLE AND THE SACCULE

The anatomical structure of the labyrinth in a human reveals two pairs of otolithic organs, the utricle and the saccule (see Fig. 2.1). The structure is characterized by a non-moving part, the macula, and the sliding otoliths. It is the movement of the heavy otolith over the macula which gives rise to the perceived sensation of tilt or motion.

The specific function of each of the two otolithic organs in motion sensing has been the subject of extensive research effort. In mammals, physiological studies of reflexes and recording of firing rate from the utricle branch of the vestibular nerve demonstrate activity for stimulation with linear accelerations.¹ No similar nerve response to accelerations has been measured from the saccule. A specific study aimed to investigate its activity concludes with the statement that the saccule is probably associated with auditory sensation of vibrations.¹²⁶ However, some authors still do not exclude the saccule as a motion sensor.¹³⁰ In general, incorporation of the saccule as an orientation sensor has been required due to the inadequate knowledge of the stimulation process of the utricle. On the basis of the existing experimental evidence,

the utricle should be recognized as the only otolithic sensor stimulated by linear accelerations.

4.2 THE UTRICLE - SENSOR CHARACTERISTICS

The effort to describe the sensor characteristics of the utricle concentrated on studies of comparative physiology in mammals, and orientation experiments with humans. In animals, in particular, cats, recordings of nerve firing identified the input vector causing stimulation of the otolith (the term "otolith" will be used here for the "utricle otolith") as tilt away from the vertical.^{1,40}

In a fish, electronic microscopy showed an arrangement of sensory hairs with preferred axis of stimulation forming a semicircle.¹⁶³ This finding might indicate that input vector resolution is possible according to the location of the sensory hair (or hairs) from which nerve firing was received. One can compare this structure of the utricle to a sensor covered with a lattice of strain gages where the input magnitude is obtained by measuring the gage with the maximum output. The spatial location of the strain gage will determine the direction of the input acceleration.

Since subjective perception of inclination with respect to the gravity vector persists as long as this orientation is maintained, the otoliths were designated as static receptors. The implication is, of course, that the utricle is stimulated by changes of the head attitude, thus providing a sense of angular position, while this indication is

only transient for the semicircular canals.

The distinction between the gravity field and accelerations in any coordinate system is impossible to make. One can argue here that the utricle is a specific force receptor, where specific force is the vectorial difference of the gravity vector and other intermittent accelerations. Following this broad definition, linear acceleration per se, without restriction on its source, is considered the input variable for the otolithic sensor. Accordingly, exposure to centrifugal or linear acceleration as well as coriolis forces will be interpreted by the human as re-orientation with respect to the gravity vector, provided other sensors or sensory systems do not supplement the perceived sensation.

The theory of operation for the utricle and its otolith conceals the key to evaluation of several related characteristics of the sensor. Is the otolith an omnidirectional vector sensor informing on magnitude and direction, or just a directional transducer?

Topologically, for an erect head, the utricles are located on a plane which is elevated about 30° above the horizontal plane. Although the macula and the otolith are not strictly planar, most investigators treat them as such.^{130,151} The theories put forth to explain the stimulation causing the otolith displacement range from pull or traction, (de Kleyn, 1921),⁴⁵ pressure (Quix, 1922)¹⁴⁵ or gliding movement (Breuer, 1891).¹³

While de Kleyn supported the notion of force perpendicular to the otolith as the stimulus, Quix explained it by the weight of the otolith, and Breuer implied that the sensor is responding to the direction of the shear force parallel to the macula plane but not to its magnitude. Recently, the shear principle has been rather universally accepted as the mode of operation for the utricle.

Sufficient experimental evidence exists to support the following two statements on the otolithic organs:

- 1) The utricle is a multi-directional sensor sensitive to specific force.
- 2) The utricle is stimulated by the shear acceleration in the plane of the otolith.

These statements imply that perception of the input variable is in vectorial form; not only the direction of the field force is perceived, but also its strength.

In humans, mostly attempts to evaluate static or steady state conditions of perception of orientation were undertaken. The perceptual phenomenon of tilting surroundings one experiences when subjected to variations of the resultant force in his head axes system has been designated as the oculogravic illusion.¹¹ The phenomenon is a very useful tool to measure subjective orientation (location of the vertical or the horizontal relative to the actual physical inclination). Another experimental procedure uses the human ability to locate the gravity vector when tilted in the frontal plane.

The objective measurements of otoliths output is recording of compensatory counterrolling eye movements.^{130,160} Dependence of those eye movements upon the magnitude of resultant acceleration has been demonstrated for increased gravitational and 1.0g gravity field.¹⁷³

Static measurements of the subjective horizon for varying elevation of the head axes system (discrete rotations around Z_e axis) render linear correlation of perception with the shear acceleration on the utricle (Fig. 4.1).¹⁵¹ For an erect head, the shear on the macula is along an axis elevated about 20° above the sagittal axis. Consequently the subjective horizon will correspond to the actual horizon for 0.4g backward shear acceleration on the otoliths. The measurements confirm the assumption that sensation is dependent upon the magnitude of the shear acceleration, since there is a linear relationship between shear and subjective perception. Experimentally this relationship is valid for $\pm 90^\circ$ of bending fore and aft. However, incomplete or rather erroneous spatial orientation is suggested by the slope of the line in Fig. 4.1. Nevertheless, the sensor is responding to acceleration changes in the sagittal plane in agreement with its assumed characteristics.

Tilt in the frontal plane is associated with perception of the vertical when only gravity is present or perception of the resultant vector for exposure to gravity and linear

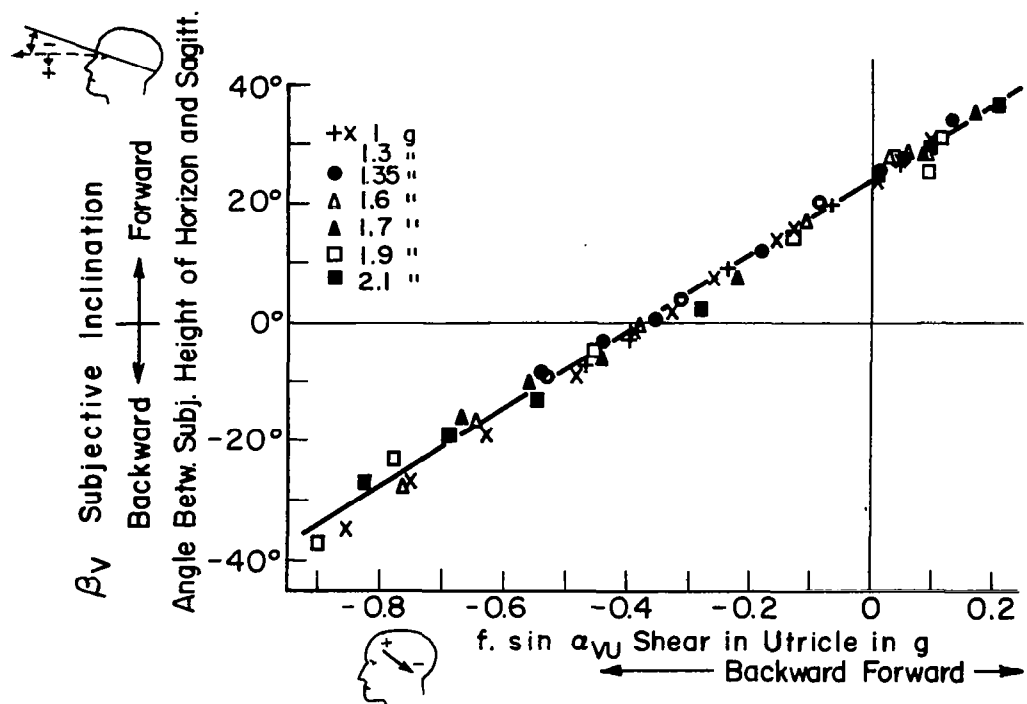


Fig. 4.1 The Subjective Inclination (β_V) Plotted as a Function of the Shear Acceleration in the Plane of the Utricle (Ref. 151)

accelerations. Psychophysical experiments show equal ability for reorientation without directional dependence.¹²³ The observation confirms the expected symmetry of perception in the frontal plane, a feature deduced on the basis of the structure of the utricle. Another comment which is valid for the lateral tilt is that the configuration produces shear acceleration components along two perpendicular directions. The resultant shear acceleration on the otoliths very closely obeys a $\cos^2\beta$ relation, where β is the angle of tilt. Counterrolling eye movements which rotate the eye in opposite direction to the body tilt show this relationship very closely.¹³⁰

At present, a summary stating that the utricle has sensing capabilities in all directions is well warranted.

4.2.1 Dynamic Response of the Otoliths

The important contribution of the utricle in space orientation is the continuous monitoring of body attitude relative to the environmental forces. However, the extent of orientation information originating at this sensor cannot be fully evaluated without a detailed knowledge of its dynamic characteristics. Intermediate sensations the human will perceive during transfers from one postural orientation to another, or during exposure to intermittent linear accelerations are a function of the sensor's dynamics.

Basically, the questions are what physical vector the otolithic organ senses when it is repeatedly stimulated with a certain time varying pattern of acceleration, and what is the frequency response of the otolith?

The theory of control engineering shows that, in a minimum phase linear system, input-output relations are defined, except for a gain constant, by either the phase difference between output and a sinusoidal input or by the ratio of their respective amplitudes. Therefore, the dynamic characteristics of a linear system are fully determined in the transformed frequency domain when its response is tested over a significant range of input frequencies.

The utricle has been identified as a sensor with linear characteristics when linear accelerations, within the range of $\pm 1.0g$ of shear acceleration on the otoliths, are applied in the sagittal plane (see Fig. 4.1). Consequently an experiment which compares the phase relationship between the subjective perception of velocity and the input velocity or acceleration is admissible for valid testing of the frequency response of the otoliths.

a) Method: A linear motion simulator with characteristics described in Appendix B was used for the experiment. The subject is seated upright with his sagittal axis horizontal and along the direction of motion. His head is supported on a head rest and his body strapped

firmly to the chair. The simulator is driven back and forth along the track with a single frequency, sinusoidal function. Perception of the subject is communicated by a displacement of a light, spring-restrained, stick. Following pre-experimental instructions, the subject indicates only the direction of motion he undergoes. Position of the simulator along the track and subject indication were continuously recorded on a paper recorder throughout the experiment. Three subjects with previous experience in psychophysical studies were used for this study.

b) Results: The frequency response of the utricle was examined over the range of 0.02 cps to 0.9 cps at discrete increments of 0.01 cps for the low frequencies and steps of 0.1 cps for the high frequency end. The profile of peak acceleration for the experiment is given in Fig. 4.2, the decline of it below 0.1 cps being due to the limited length of the track. Since the subjects were instructed to indicate the direction of their movement, their response during one cycle of back and forth oscillation, at any given frequency, resembled a square wave with a "dead zone" of no indication whenever the stimulus fell below the individual threshold of perception. The operator's response is, of course, his subjective perception of velocity. The phase angle this subjective velocity lags or leads the input velocity is presented in Fig. 4.3.

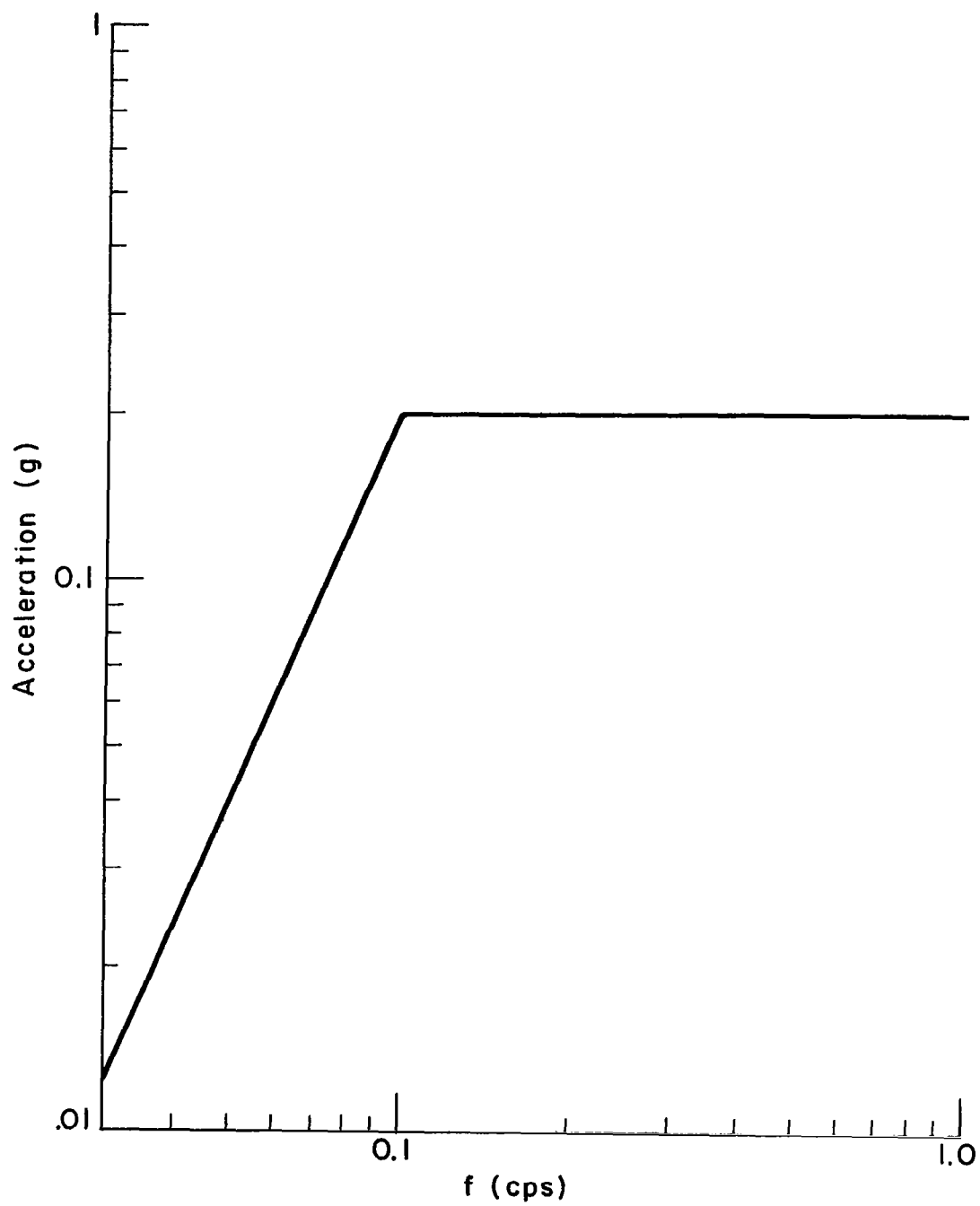


Fig 4.2 Profile of Peak Sinusoidal Input Accelerations

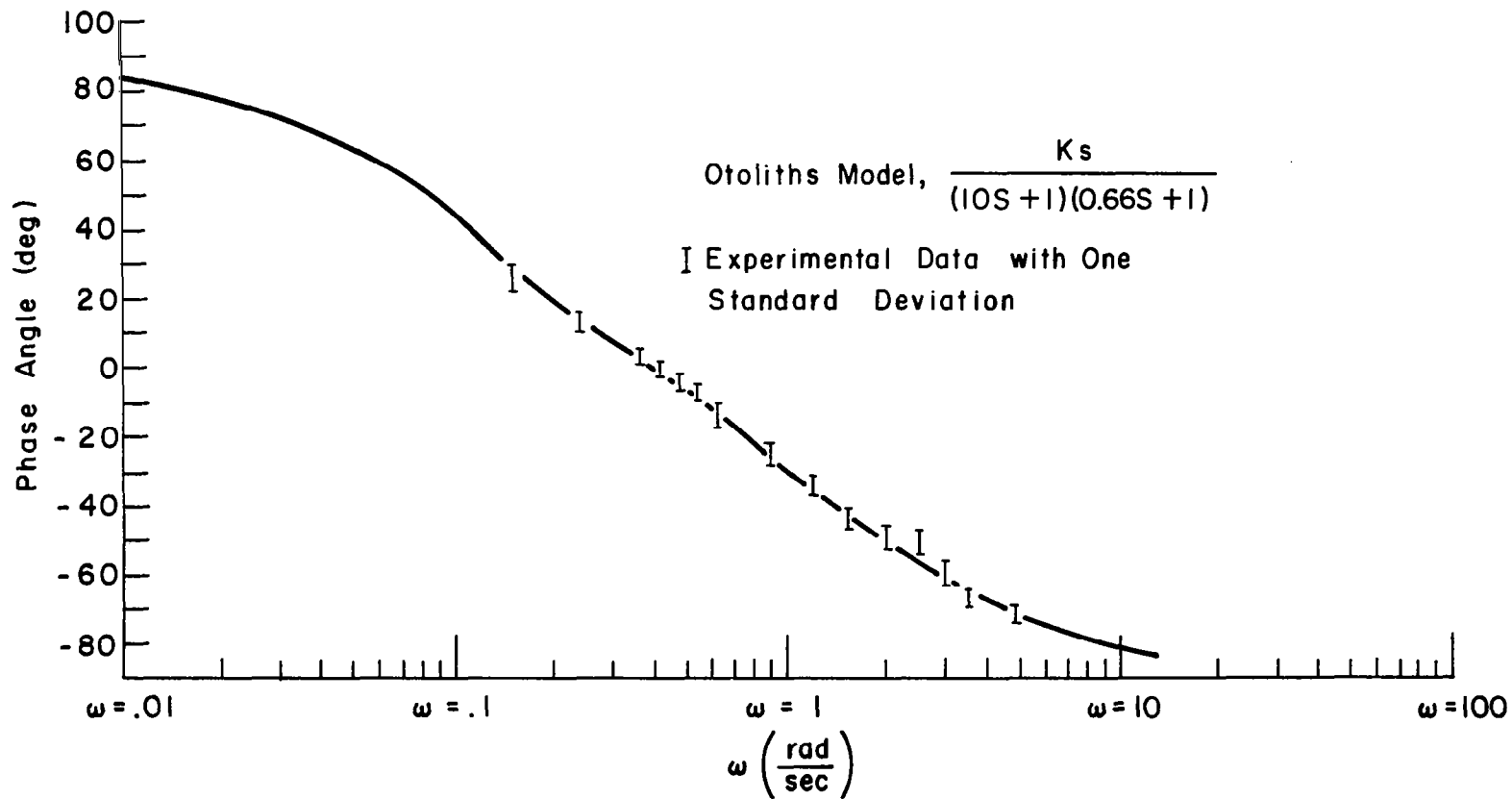


Fig. 4.3 Subjective Perception of Motion Reversal - Phase Versus Frequency

Inter-subject differences in phase angle data were not statistically significant ($P > 0.1$). Thus results from the three subjects were pooled with mean values at each frequency shown in Fig. 4.3. One standard deviation of phase angle at any given frequency did not exceed 2° . Examination of the phase angle for perception of subjective velocity reveals that at low frequencies, it leads the input velocity, at about 0.40 rad/sec it is in phase with it and beyond that frequency, human perception lags behind the input velocity. The response is typical of second order systems with time constants $T_1 = 10$ sec, $T_2 = 0.66$ sec. This theoretical curve fit with break frequencies at $\omega_1 = 0.1$ rad/sec and $\omega_2 = 1.5$ rad/sec is the solid curve in Fig. 4.3. The phase lag associated with the second order system is in good agreement with the experimental results. In view of this finding, an assumption is made here that the dynamic characteristics of the utricles are represented by a linear second order characteristic equation. The transfer function from input acceleration to subjective sensation of velocity will take the form of:

$$\frac{\text{subjective velocity (s)}}{a_{x_e} (s)} = \frac{K}{(10s+1)(0.66s+1)} \quad (4.1)$$

where a_{x_e} = linear acceleration along the horizontal

earth-fixed, X_e , axis. The frequency response of the otoliths from an input velocity along the X_e axis to subjective velocity is shown in Fig. 4.4. Note that the gain constant K has not been measured.

4.2.2 Threshold of Perception

Threshold of perception for the utricle is significant in terms of minimum deviation in orientation detectable by the sensor. If threshold is associated with minimum displacement of the otolith, the latency time to detect input acceleration of a certain magnitude will correspond to the duration of travel of the otolith from rest position to the threshold deflection. Consequently, the threshold of the utricle is defined as the minimum acceleration which the sensor will detect provided the stimulus persisted for a sufficiently long period. For the otolithic organ, measurements of threshold and latency times in the sagittal plane were undertaken.

a) Method: Again the linear motion simulator described in Appendix B was used for these series of **experiments**. The subject, with strapped body and supported head, was accommodated in two positions: 1) seated upright facing the direction of motion; 2) lying supine with his longitudinal body axis along the track. The simulator was given a step in acceleration maintained until the subject indicated perception of motion. Directions (backwards or

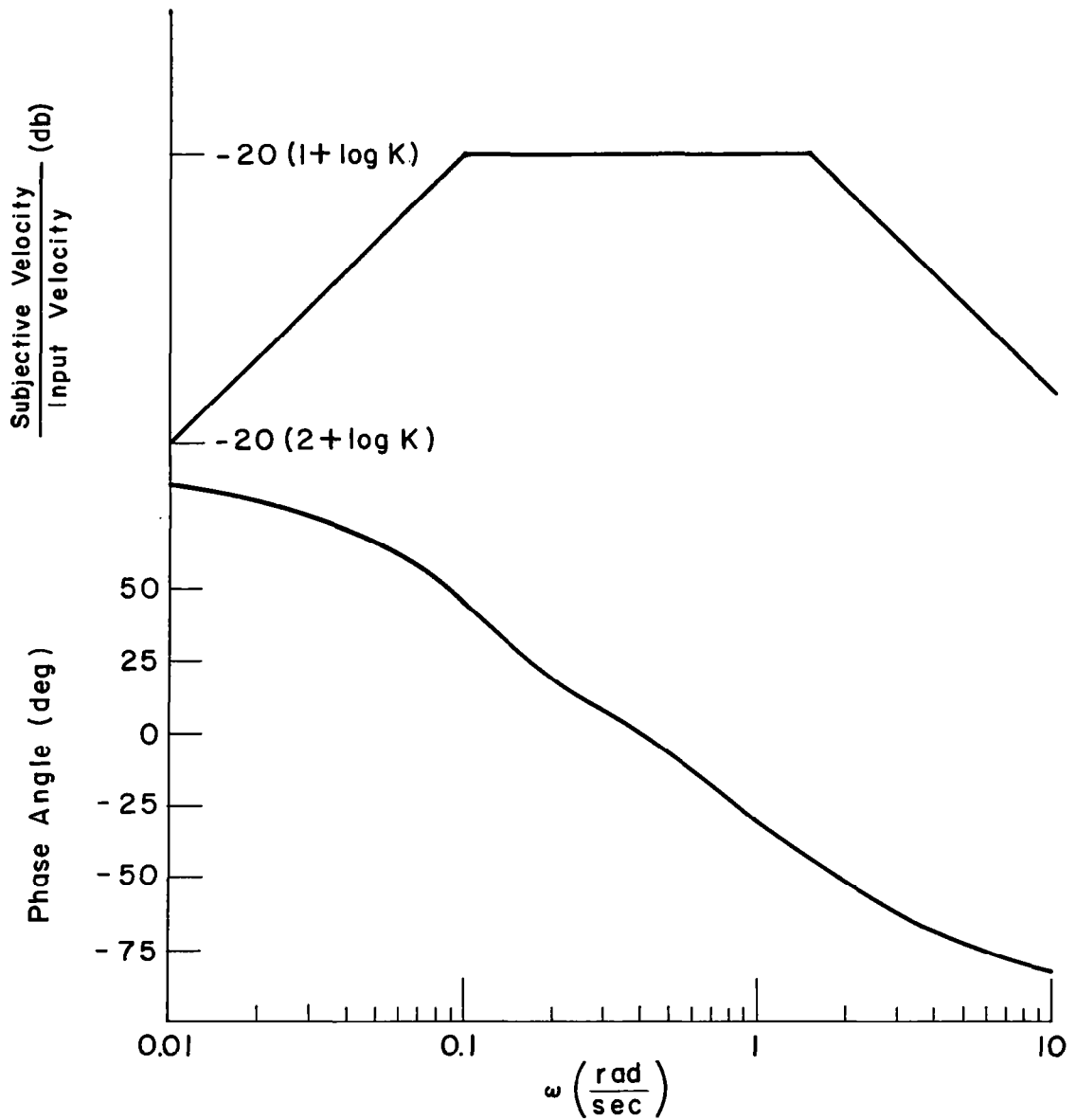


Fig. 4.4 Bode Plot of Otoliths Model

forwards) and magnitudes of acceleration were randomized with the only provision of demanding at least four responses for each input acceleration. Thirty seconds of rest or more were allowed between consecutive runs with the whole series lasting for less than one half hour. The measurements for the upright and the supine position were taken on two consecutive days, while the order changed among the three subjects used in the experiments.

b) Results: The response of the model for the otoliths to a step of acceleration is given by

$$\text{Subjective perception}(t) = a_{x_e} K (1 + 0.07e^{-1.5t} - 1.07e^{-0.1t}) \quad (4.2)$$

If we associate the physical vector of displacement of the otoliths with subjective perception, the threshold will correspond to some minimum travel d_{\min} such that:

$$d_{\min} = a_{x_e} K (1 + 0.07e^{-1.5\tau} - 1.07e^{-0.1\tau}) \quad (4.3)$$

with a unique relation between the latency times τ measured and the magnitude of the input acceleration, a_{x_e} .

Two immediate observations are apparent from Eq. (4.2):

1) the effect of the term $0.07e^{-1.5t}$, drops off almost completely after one second; 2) a very slow increase of the factor multiplying the input acceleration during the first second. One can expect then that a wide range of accelerations will be perceived with latency times of about one second.

Fig. 4.5 represents the mean latency times of the three subjects for the supine position as a function of input acceleration. The solid line is the theoretical curve from Eq. (4.3) referred to the experimental measurement at 0.01g. An excellent agreement between experimental results and theoretical prediction, over the whole range covered in the experiment, is noticed. It should be added that the standard deviation for any single time measurement did not exceed .2 seconds.

Fig. 4.6 shows the experimental latency times for the seated upright position. Note that according to the shear theory there is a difference of shear accelerations between the supine and the upright experimental positions. Since measurements of acceleration along the earth-fixed X_e axis were made, the shear acceleration on the otoliths (assumed 30° elevated above the sagittal axis) is:

$$0.866 \text{ ng}_e = a_o \text{ upright}$$

$$0.5 \text{ ng}_e = a_o \text{ supine} \quad (4.4)$$

where ng_e = input acceleration along X_e axis and
 a_o = shear acceleration on the otoliths.

Using these relations and the theoretical, expected latency times for the upright position were computed and are shown as the solid line on Fig. 4.6.

The thresholds of perception for the otoliths, based

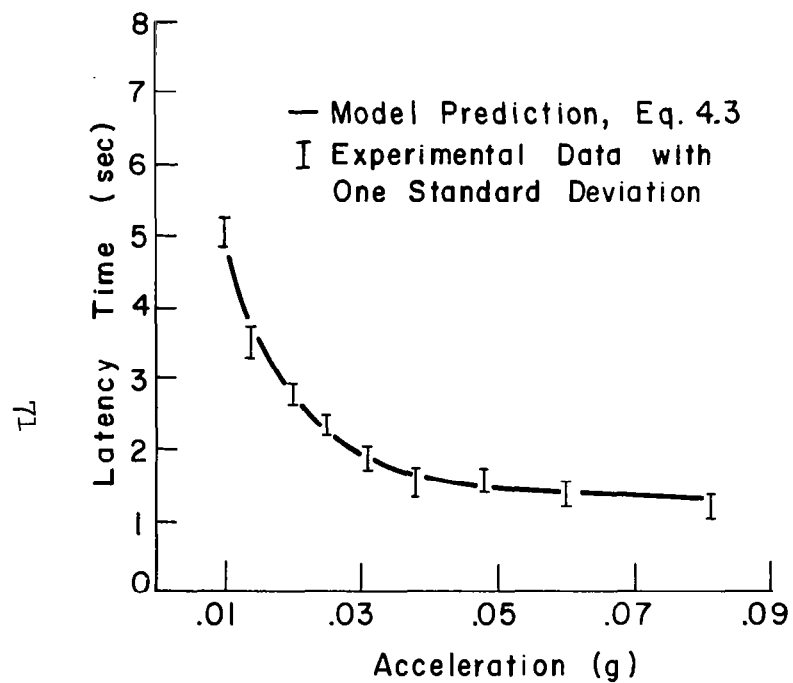


Fig. 4.5 Latency Times for Perception of Horizontal Linear Acceleration, Supine

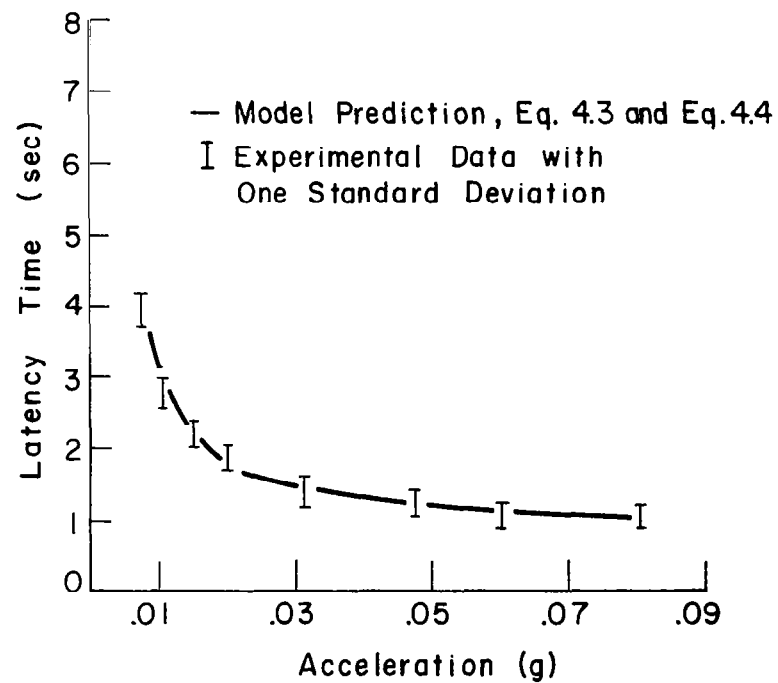


Fig. 4.6 Latency Times for Perception of Horizontal Linear Acceleration, Upright

on 75 per cent correct vector detection, are 0.01g for supine head and 0.006g for upright head.

4.2.3 Review of Supporting Publications

The experimental program undertaken by the author was sufficient to determine the dynamic characteristics of the otoliths, and the non-linearity associated with the threshold. The results are for perception of linear motion along the sagittal axis. Supporting evidence to these findings is found in behavioral experiments reported in the literature.

Researchers working on motion sickness find particular susceptibility to it with linear motion around the frequencies $1/4$ to $1/3$ cps.¹⁰⁹ For the high frequencies, the attenuation in dynamics of the otoliths indeed serve as a limiter on the input accelerations while for frequencies below $1/4$ cps; probably equipment limitations on maximum acceleration is the cause for absence of sickness.

The parallel swing produces linear acceleration stimuli, together with some angular acceleration which depends upon the length of the suspending wires. Thus, although the method is not absolutely free of interacting semicircular canals and otoliths stimulation, measurements with it might be of limited use.

The threshold of perception was measured with sinusoidal stimulation on a swing by Walsh.¹⁵⁹ For a supine subject, he reports threshold of 0.009g to 0.012g. However, an attempt to determine latency times on the swing did not

render results which are compatible with other measurements by the same author. Also his attempt to determine phase relations between the subject indication and the actual motion did not render compatible values with this study. This is probably due to the fact that peak accelerations on the swing were very close to the threshold.

The best observation of the function of the otoliths which also illustrates the scope of information the otoliths will provide in an altered environment was made with a submerged subject in a rotating tank full of water.¹⁵⁵ The subject seated, was rotated with the tank, head over heels about his Z_h axis at constant angular velocity. The force acting on the otoliths is gravity. Therefore, the shear acceleration on the otoliths, for this maneuver, is

$$a_o = g \sin \omega t \quad (4.5)$$

where ω - angular velocity of the tank. The perceived sensation is illustrated in Fig. 4.7 taken from Ref. 155. Subjectively, the motion is interpreted as riding a Ferris wheel with varying amplitudes. First, why the Ferris wheel sensation? On a Ferris wheel, which rotates with constant angular velocity, the shear acceleration on the otoliths is combined from gravity and the centrifugal acceleration. Assuming the rider keeps his head erect, (otoliths plane about 30° above the horizontal plane), the shear acceleration on the otoliths is:

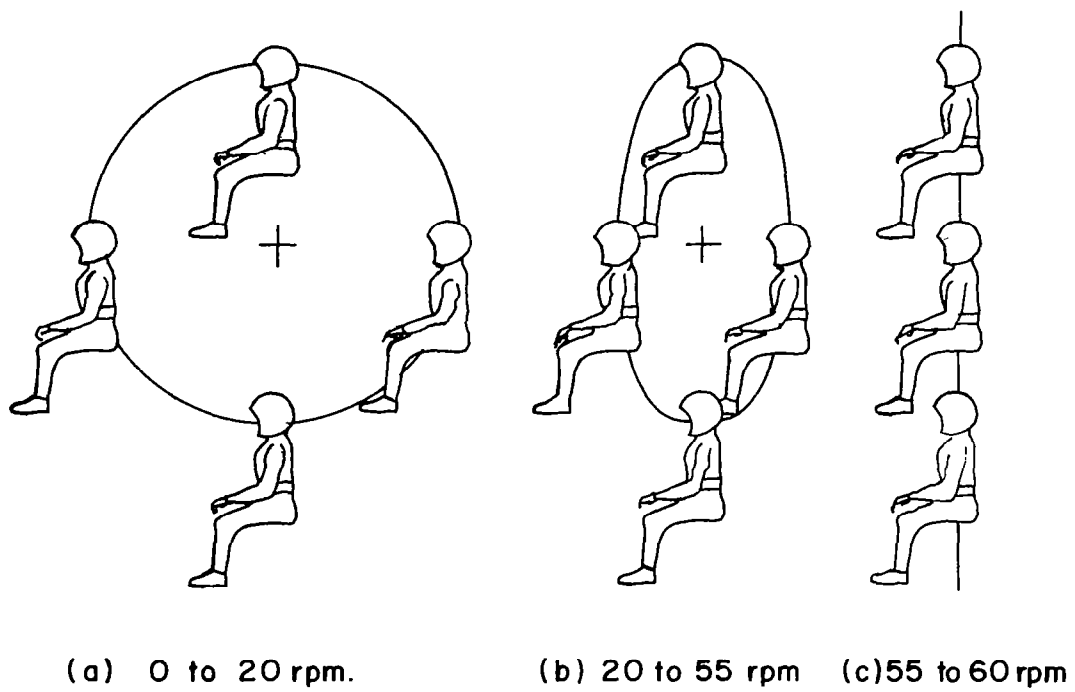


Fig. 4.7 Illustration of Motions Sensed by Seated Subject (Ref. 155)

$$a_o = (g + \omega_1^2 R \sin \omega_1 t) \sin \frac{\pi}{12} \quad (4.6)$$

where ω_1 = angular velocity of the Ferris wheel and

R = radius of the Ferris wheel.

Note that except for an additive constant acceleration ($1g$), the shear acceleration for the two cases have similar time patterns. Therefore, in absence of any other motion clues to the undergoing motion (tumbling head over heels), the subject will interpret it in terms of a commonly experienced, similar sensation - the Ferris wheel. It is important to stress the point here that the semicircular canals do not provide rotational information for both circumstances since the motion is with constant angular velocity.

The second observation is about the tendency to feel only plunging, up and down motion with increase in angular velocity. According to the Bode plot for the otoliths, sensation is attenuated with 40 db per decade beyond $1/4$ cps. Thus increasing portions of the rotation will pass unnoticed because the shear acceleration dropped below the threshold with the limiting case of only peaks being sensed. Since the maximum forces on the Ferris wheel are indeed at the top and the bottom of the loop, the interpretation forwarded by the subject is consistent with previous experience. Significantly enough, the departure from a circular pattern for the Ferris wheel occurs at 20 rpm ($1/3$ cps), close to the $1/4$ cps break frequency of the otoliths found here.

4.3 HABITUATION

The utricle is often referred to as a statolithic organ, indicating its sensitivity to static changes of orientation of the head with respect to the vertical. In this context, one would expect then little or no attenuation in perception due to frequent stimulation. Otherwise the monitoring capability of the sensor is to no avail. A comparative study of pilots and subjects with no flying experience indeed finds no significant difference between the groups in their ability to orient themselves.^{10,11} While long term habituation is excluded logically, it does not inhibit diminution of sensitivity to a new steady state level compatible with the input acceleration. In cats, a shifted otolith will show action potentials at a frequency proportional to the tilt and then the frequency during the following 30 seconds will settle down to a constant value which is about 60 per cent of the original.¹ Subjective experiments in humans found that readjustments to the gravity vector are significantly more accurate immediately after the tilt compared to readings after 60 seconds of stay in tilted position.¹²³ Moreover, the amount of adaptation in this experiment is of the order of 60 per cent of the initial angle of tilt. These findings are supported independently by additional experiments which show the effect of angular rate upon readjustment but almost no influence of the period of exposure to the tilt if longer than 30 sec.⁵⁷ A summary stating that a short term

adaptation of subjective perception takes place during 30 seconds is justified, but the data is not sufficient to put forward a control theory description of it.

4.4 MATHEMATICAL MODEL FOR THE OTOLITHS

The experimental results obtained by the author were from investigations of the otoliths' function in perceiving linear accelerations along the X_e axis. By correlating the data of the upright position with the supine one, it is evident that a unified presentation holds for any head orientation within the range of $\pm 90^\circ$ rotation of the head frame about the horizontal, earth-fixed axis Z_e . Observations by other researchers indicate the probability of similar response of the otoliths for lateral tilt. Thus one can speculate that the missing link in the control engineering description of the otoliths is the mechanism performing vectorial manipulations and not the dynamics of the sensors. Incidentally, this mechanism of directional resolution will have effect only on the sensitivity of the otoliths. The mathematical model of the otoliths is presented in Fig. 4.8. In this model, the specific force in earth-fixed coordinates is resolved to components in the plane of the utricle and perpendicular to it by the orientation matrix and the alignment matrix $[A \times \delta]$. The components along the plane of the otoliths constitute the shear acceleration on the otoliths. This acceleration stimulates the otoliths, which after exceeding the threshold, send

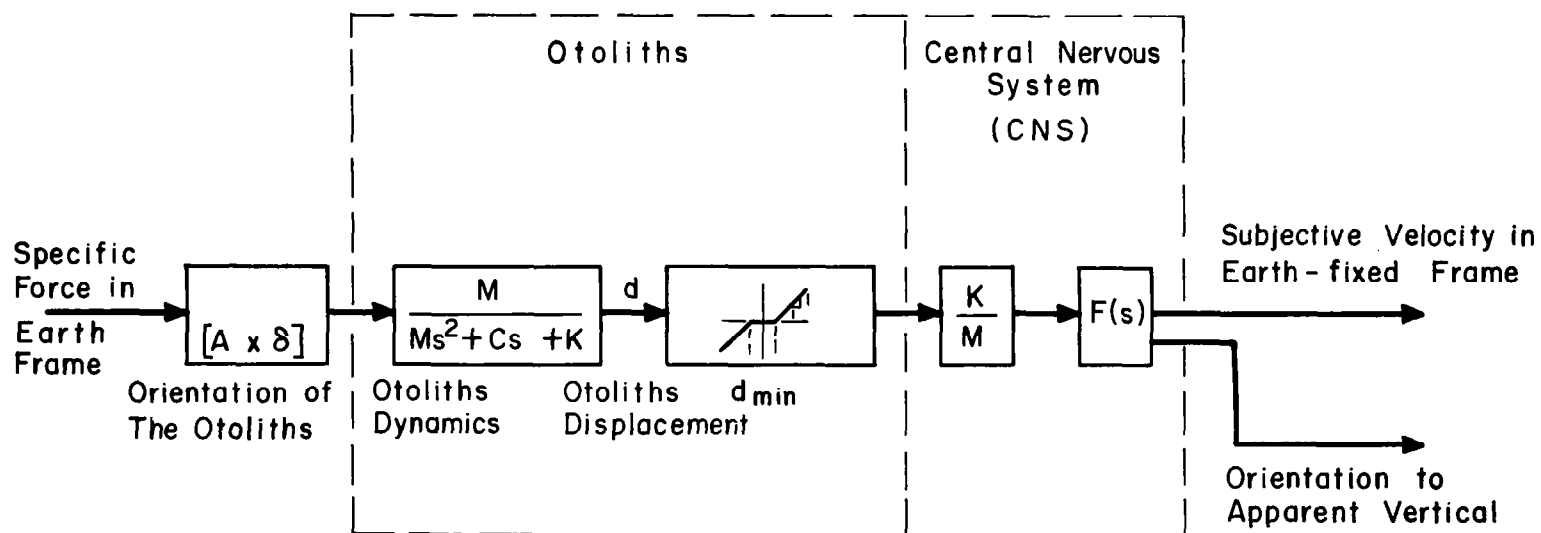


Fig. 4.8 Otoliths Block Diagram

information to the central nervous system, CNS, where it is interpreted as subjective perception. Some unknown transfer characteristics have to be assigned to the CNS (Sec. 4.2), thus $F(s)$.

The dynamic range of the sensor is not known precisely; however, it is at least 100 or more, since we are living in 1.0g environment and the threshold has been located as about 0.01g.

What is the subjective perception attributed to the utricle? Fig. 4.4, which is the frequency response of the sensor presents it as a velocity meter over the spectrum of frequencies corresponding to "normal" head movements. Similarly, the initial (1 to 4 sec) response of the otoliths stimulated by a constant linear acceleration will be proportional to the velocity of the maneuver. The model also indicates that the sensor cannot distinguish between gravity and other acceleration forces. Thus subjective perception of angle of elevation or tilt will be identical regardless of the way it was induced: 1) by a change of body orientation with respect to gravity; 2) by externally applied accelerations. Fig. 4.1 points out that subjective estimates of the angle of elevation are smaller than the actual elevation above the horizon (slope of the line 64%). Since this is steady state data, these readings are probably affected by habituation and reduced to about 60 per cent of the initial response. Therefore, for short exposures to tilt from the vertical and to elevation angles above the

horizon, the "instantaneous" slope will be about $100^{\circ}/g$, well correlated with the expected $90^{\circ}/g$, considering experimental scatter. When time limits are imposed on the duration of exposure to constant acceleration, the adaptation effect, $F(s)$, will not substantially affect the subjective orientation to the apparent vertical.

CHAPTER V

THE EYE - A DEPENDENT SENSOR

The eye perceives body orientation with respect to the environment. This information is of high resolution and is referred to objects observed in the immediate surroundings. In addition, the human can exercise voluntary control of eye movements in searching for a reference to which he relates his orientation. These capabilities of the visual system render the eye as an orientation sensor of prime importance to man. However, the ocular mechanism is by itself a multi-input servo control system with inputs fed to it by other orientation sensors, by the eye itself, and by the voluntary tracking intentions of humans. Therefore, the orientation cues the eye will provide depend upon the visual and motion conditions in the man-environment system, and the dynamic characteristics of the sensors involved in sensing spatial orientation.

5.1 CONTROL OF LATERAL EYE MOVEMENTS

The eye movement control system rotates the eye in order to maintain the image of an object of fixation upon the retina. A displacement of this image is caused by the motion of the visual target and by rotations of the head

on the body. The eye movement control system will respond to these motions with two different modes of eye movements: tracking and compensatory movements. Tracking eye movements follow the moving target in the visual field. Compensatory eye movements rotate the eye in a direction opposite to the rotation of the human body.

The eye has rotational freedom with respect to the skull and the skull as a whole may rotate with respect to the trunk with the neck as a pivot. Accordingly, the eyeball may be considered as mounted on two gimbals with limited freedom of motion with respect to the trunk.

Rotation of the whole gimbal system or relative rotation between the head and the trunk will cause compensatory eye movements. Angular accelerations stimulate the semicircular canals and rotation of the head upon the trunk excites receptors in the neck. Consequently three motion sensors are involved in the eye movement control system: the eye, the semicircular canals and the receptors in the neck.

The schematic diagram in Fig. 5.1 shows the multi-input feature of the eye movement control system. The semicircular canals and the relative rotation sensitive, neck receptors are the sensors which provide information about skull motion in space. Since any rotation of the head, if not compensated by an opposite eye movement, will result in image displacement on the retina, the motion information does not need any processing and is fed directly into the motor end of the eye control servomechanism to initiate

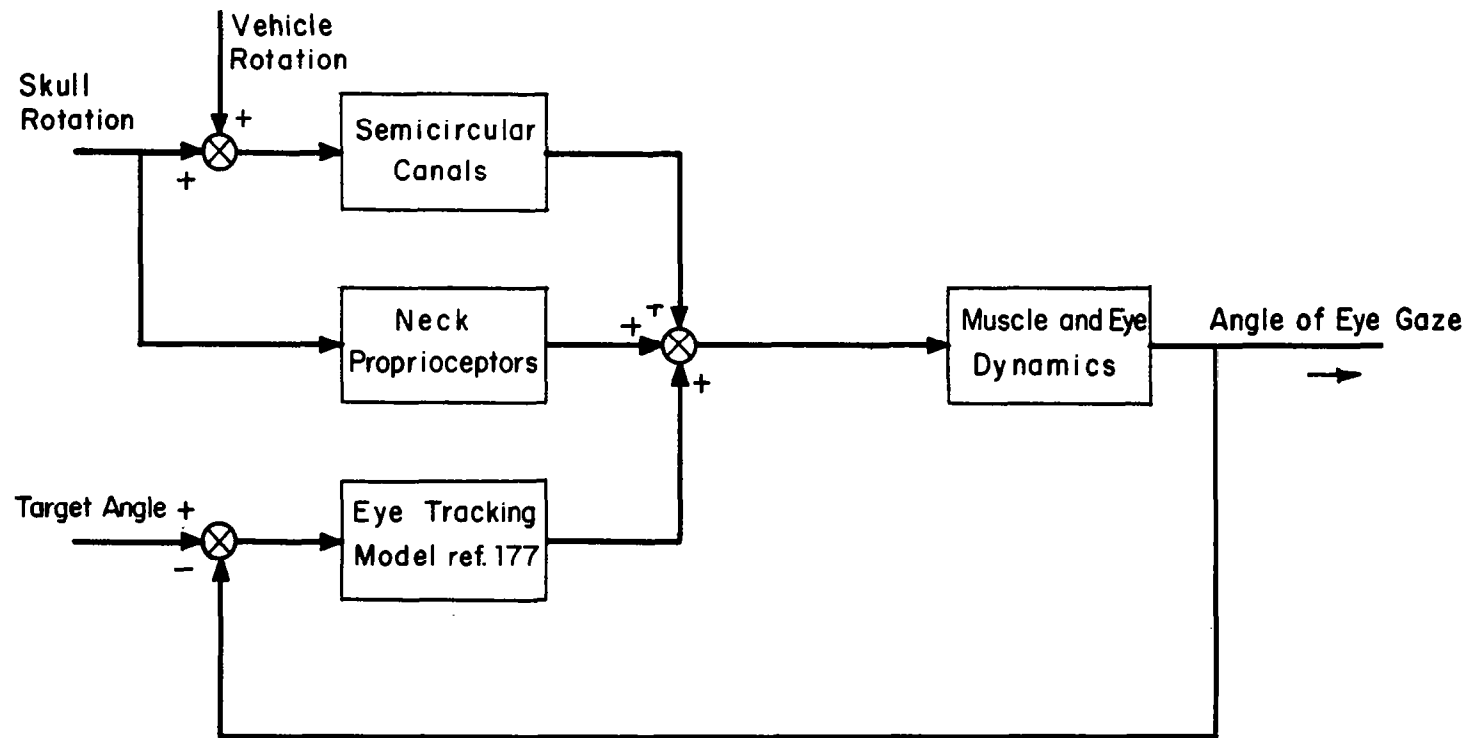


Fig. 5.1 Block Diagram of the Eye Movement Control System

immediate compensatory eye movements. The tracking movements branch of the control loop responds to an error between the actual image of a fixation point on the retina and its desired location.

The study of the eye movement control system presented in this chapter investigates the response of the system in the presence of relative rotation about the vertical axis between the human and the environment. Previously, this control system has been investigated for horizontal eye tracking movements.¹⁷⁷ Although compensatory eye movements attributed to the vestibular system are reported in the literature, a detailed frequency response measurement of them has not been presented.^{96,135}

The experimental work here is a frequency response study of the eye movement control system for horizontal eye movements. By investigating the separate control loops (except for the visual tracking branch) and their combination, a complete mathematical model of the system is obtained.

Rotation of the human body and head can be sensed by the semicircular canals, the neck receptors, or both. The eye movements corresponding to inputs from these sensors are presented as transfer functions from the input vector to the resultant eye motion. The system responses were also investigated when a visual fixation was made to an object both in a rotating and in an earth-fixed environment.

5.2 COMPENSATORY EYE MOVEMENTS - VESTIBULAR STIMULATION

The existence of compensatory eye movements accompanying periods of stimulation of the vestibular sensors has been documented extensively.^{38,77,83,86} As discussed in Chapter III, compensatory eye movements are considered as an objective measurement of the dynamic response of the semicircular canals. Rotations of the body around a vertical earth-fixed axis do not involve stimulation of the otoliths which exceeds the threshold level. The compensatory eye movements during such rotations and in general are considered to be controlled by the semicircular canals.

The phenomenon of compensatory eye movements maintained by stimulation of the vestibular sensors is known as vestibular nystagmus. This motion of the eye is characterized by a slow rotation opposite to the direction of rotation of the skull called the "slow phase" and fast return in phase with the rotation, the "fast phase". While the slow phase is clearly for image stabilization purposes, the sharp flick of the fast phase has been explained as a return to a new fixation point after a limit of travel off the center position of the eye was reached. However, the nearly uniform time intervals of the fast phase, and the randomness of the angular rotations prior to return suggest control of the central nervous system on it rather than caused by some saturation process.⁵⁹

5.2.1 The Cupular Model

The frequency response of the horizontal semicircular canals indicates dynamic characteristics of an angular velocity meter over a range of two decades of frequencies (see Fig. 3.8). Thus image stabilization on the retina of the eye during periods of head rotations is possible by control of the eye muscles through the vestibular system. Indeed, fibers from the vestibular nuclei of nerves ascend to reach the motor nuclei of the eye muscles.^{43,76} Provided the dynamics of the motor end of the eye are fast enough, the response of the eye to the input from the semicircular canals will resemble the response of the canals to the input rotations. In view of these considerations, the assumption about the velocity of the slow phase of the nystagmus being proportional to the cupula deflection in the canals credits the system design of nature with the best capabilities of image stabilization. According to this assumption, the expected frequency response of the compensatory eye movements, considering the slow phase motion only, can be evaluated as follows:

$$\frac{\theta(s)}{\varphi_{y_h}(s)} = \frac{s^2}{(s+\omega_1)(s+\omega_2)} \quad (5.1)$$

where Eq. (5.1) is the transfer function of the semicircular canals in response to an input angle, φ , of head

rotation. The velocity of the slow phase is assumed to be:

$$s p(s) = - A \theta(s) \quad (5.2)$$

with p as the cumulative eye position and the minus sign indicating eye movement opposite to the rotation of the skull. A is the sensitivity relating the eye angle, p , to the cupula angle, θ . Consequently,

$$\frac{p(s)}{\mathcal{L}_{Y_h}(s)} = - \frac{s A}{(s+\omega_1)(s+\omega_2)} \quad (5.3)$$

The term cumulative eye position is used to describe the total compensatory travel, relative to the skull, of the eye from a center position. The cumulative eye position is then the sum of all the segments of slow phase motion put end to end by eliminating the effects of several fixation points introduced through flicks of the fast phase.

An experiment to measure the transfer function of the eye movements attributed to stimulation of the semicircular canals (Eq. (5.3)) was performed by the author. The preferred technique of measurement calls for recording of eye movements of an open eye. In addition, experiments testing the cupular model for compensatory eye movements must keep the subject mentally alert throughout the test period.³⁸

a) Method: A moving base simulator driven sinusoidally about the earth vertical axis (Y_e) was used as the moving platform for these experimental series. The subject was

seated in the hooded cab, his head in the axis of rotation and kept in normal upright position by a biteboard, affixed to the moving cab so as to eliminate any neck movements during rotations. Eye movements relative to the skull were measured by a non-contact method based upon detection of the difference in reflected light from the sclera and the iris on both sides of one eye. A commercial model of an eye movements monitor with a linear range of $\pm 15^\circ$ and a resolution of 0.1° , mounted on glasses worn by the subject was used for the entire series of experiments described in this chapter. To comply with requirements of complete darkness in the cab (elimination of visual fixation point), the necessary illumination of the eye ball was achieved by an infrared light. Recording of the cab position and eye movements were taken continuously during the experiments. Three subjects participated in the experimental series discussed in this chapter.

b) Results and Discussion: The profile of frequencies and corresponding amplitudes of the input rotation are given in Fig. 5.2 This profile in effect kept the peak angular accelerations constant for high frequencies. Fig. 5.3 is a recording taken for $f = 0.5$ cps. The upper trace is the vestibular nystagmus measured relative to the skull, cumulative eye position is shown in the middle, and the lower trace is the input position of the cab. Note the clear sinusoidal shape exhibited by the cumulative eye position. With sufficient care exercised, this method of analysis

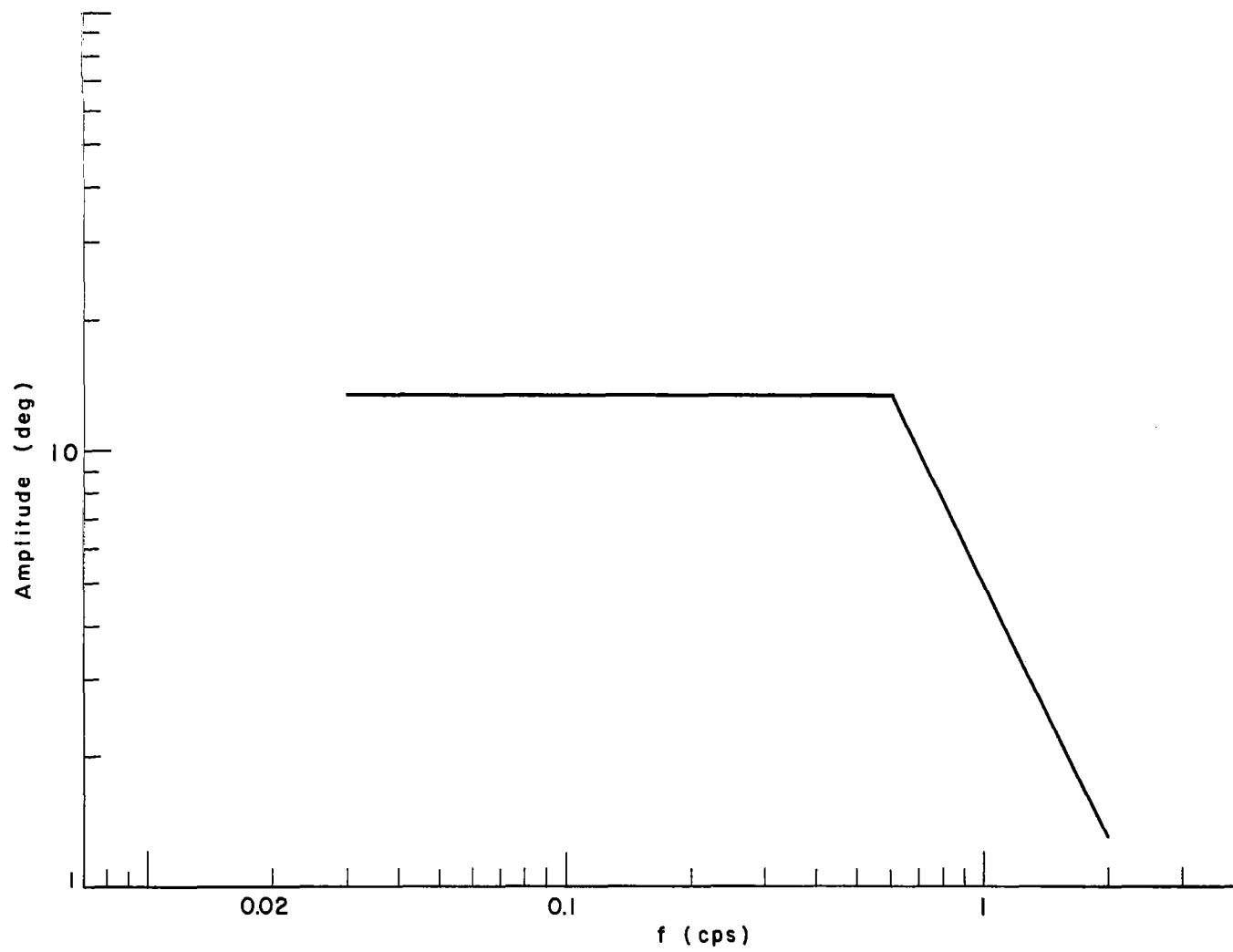


Fig. 5.2 Profile of Input Sinusoid Amplitudes

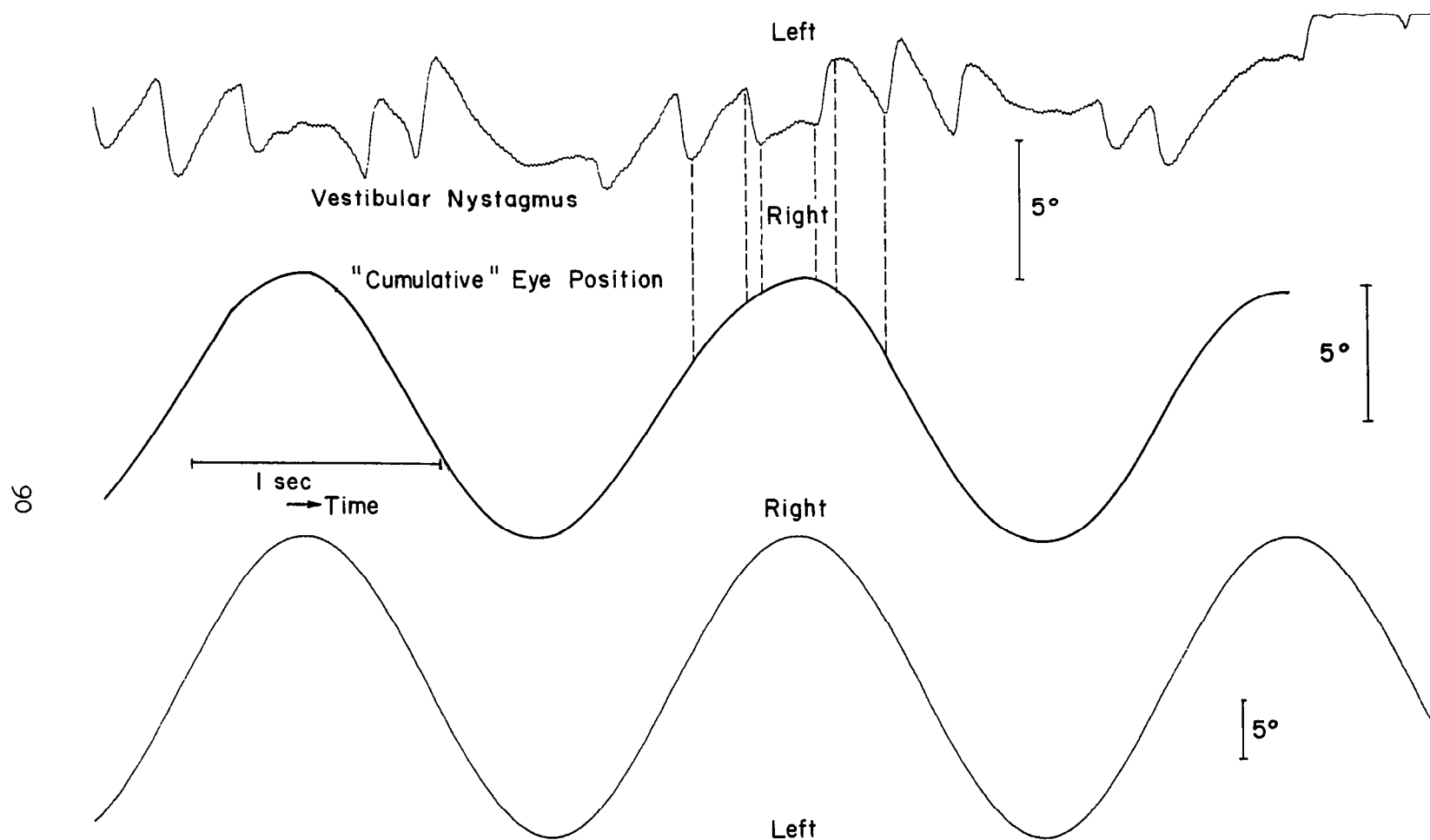


Fig. 5.3 Vestibular Nystagmus And "Cumulative" Eye Position, $f = 0.5$ cps
Note the Correspondence of Slow Phase Vestibular Nystagmus and "Cumulative" Eye Position.

rendered sinusoidal input-output relations for the whole spectrum of input frequencies (0.03 cps - 2.0 cps). Therefore, adequate information on the transfer function from input angular velocity to the compensatory eye velocity in terms of amplitude ratio and phase angle was obtained. This data is summarized in Fig. 5.4 which presents the experimental results along with a minimum phase transfer function fit to them. This relationship is given by:

$$\frac{\text{eye velocity (s)}}{\text{input angular velocity (s)}} = \frac{- 3.2 \text{ s}}{(8s+1)(0.04s+1)} \quad (5.4)$$

It is found that the break frequencies of the cupular model for objective measurement are displaced with respect to evaluation based on subjective perception (see Chapter III, Sec. 3.2). However, the important finding is concerned with the gain of the transfer function, or the ratio between the compensatory eye velocity and the skull velocity. This factor determines the extent of image stabilization upon the eye which can be achieved by the vestibular system, while angular accelerations are applied on the body as a whole. In contrast to a common presentation which assumes temporal (between two consecutive fast phase movements) preservation of a stationary picture by the eye, the compensation measured in these series of experiments is only fractional. Over a wide range of input frequencies (see Fig. 5.4) the eye compensatory velocity is about 40 per cent of the angular velocity of the skull with respect to

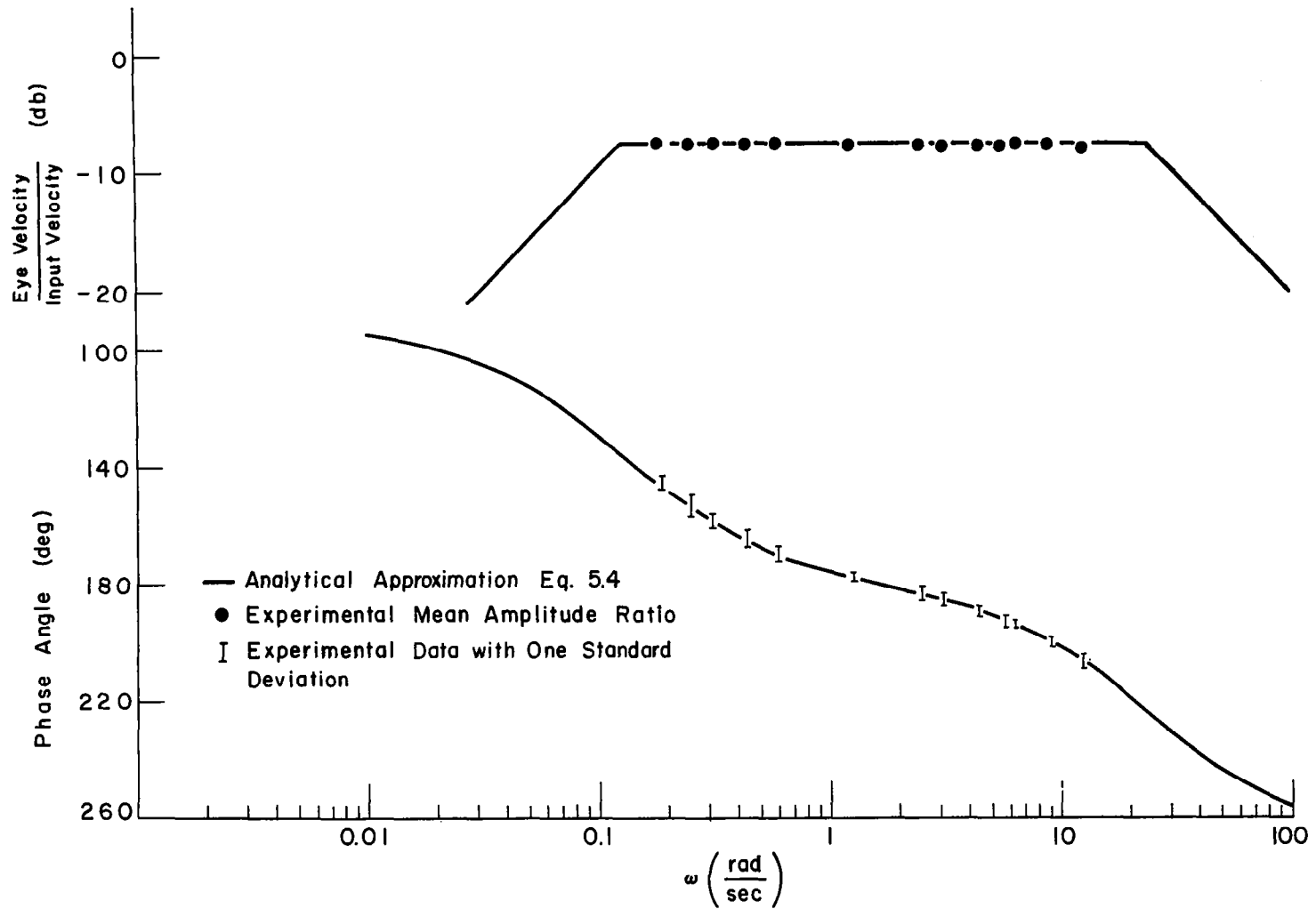


Fig. 5.4 Bode Plot of Vestibular Compensatory Eye Movements (Slow Phase)

the environment. Two other publications support this finding: the initial eye velocity responding to a step of angular velocity was found to be: (1) 43 per cent of the stimulus;¹⁰² (2) 45 per cent of the stimulus.¹⁰¹

The significance of the results presented here is far reaching. Since the angular velocity of the skull is not completely matched by the relative velocity of the eye with respect to the skull, the image upon the retina is not stationary but moves in the direction of rotation. Accordingly, one has to conclude that the vestibular system alone, or more specifically, the semicircular canals cannot achieve space stabilization of the eye when the skull, together with the body, undergoes passive rotations.

5.2.2 Environmental Fixation

The block diagram in Fig. 5.1 shows that the vestibular branch and the tracking path of the eye movement control system are activated when the subject is rotated and the eye has a visible fixation point. If the fixation point rotates with the subject, this is an environmental fixation. The situation corresponds to the common condition of travel in a maneuvering vehicle whose interior is fully illuminated and the view of the external world is obscured. The fixation point is stationary with respect to the traveller. However, its image upon the retina will move due to the compensatory eye movements initiated by the stimulated semicircular canals. The expected eye movements will

exhibit a saw tooth pattern, where the eye is deviated from its mean position by the vestibular branch and returned to it by visual tracking.

Experimentally, the proper environment was simulated by illuminating the inside of the cab of the moving base simulator. Otherwise, the experimental conditions were maintained as in Sec. 5.2.1 with the subjects instructed to maintain fixation upon a crossed marker mounted in the cab at eye level and four feet away.

Fig. 5.5 is a record taken at $f = 0.5$ cps. On the upper trace, one can distinguish the nystagmic beats changing from left to right every cycle. Note that by voluntary fixation the control system maintains the mean eye position fixed with respect to the skull. Consequently, the image of the rotating environment is kept approximately stationary on the retina. For the spectrum of frequencies examined in this series, the eye remained within $\pm 0.5^\circ$ of its mean position.

5.2.3 Earth-fixed Fixation Point

If an object in the non-moving surroundings is fixated upon, the control system of the eye will maintain its image on the retina, provided the limits of angular travel of the eye were not exceeded. Physically, the description applies to a human in a rotating vehicle and attempting to look at a given spot outside it. The vestibular compensatory eye movements and the tracking path of the control system are in

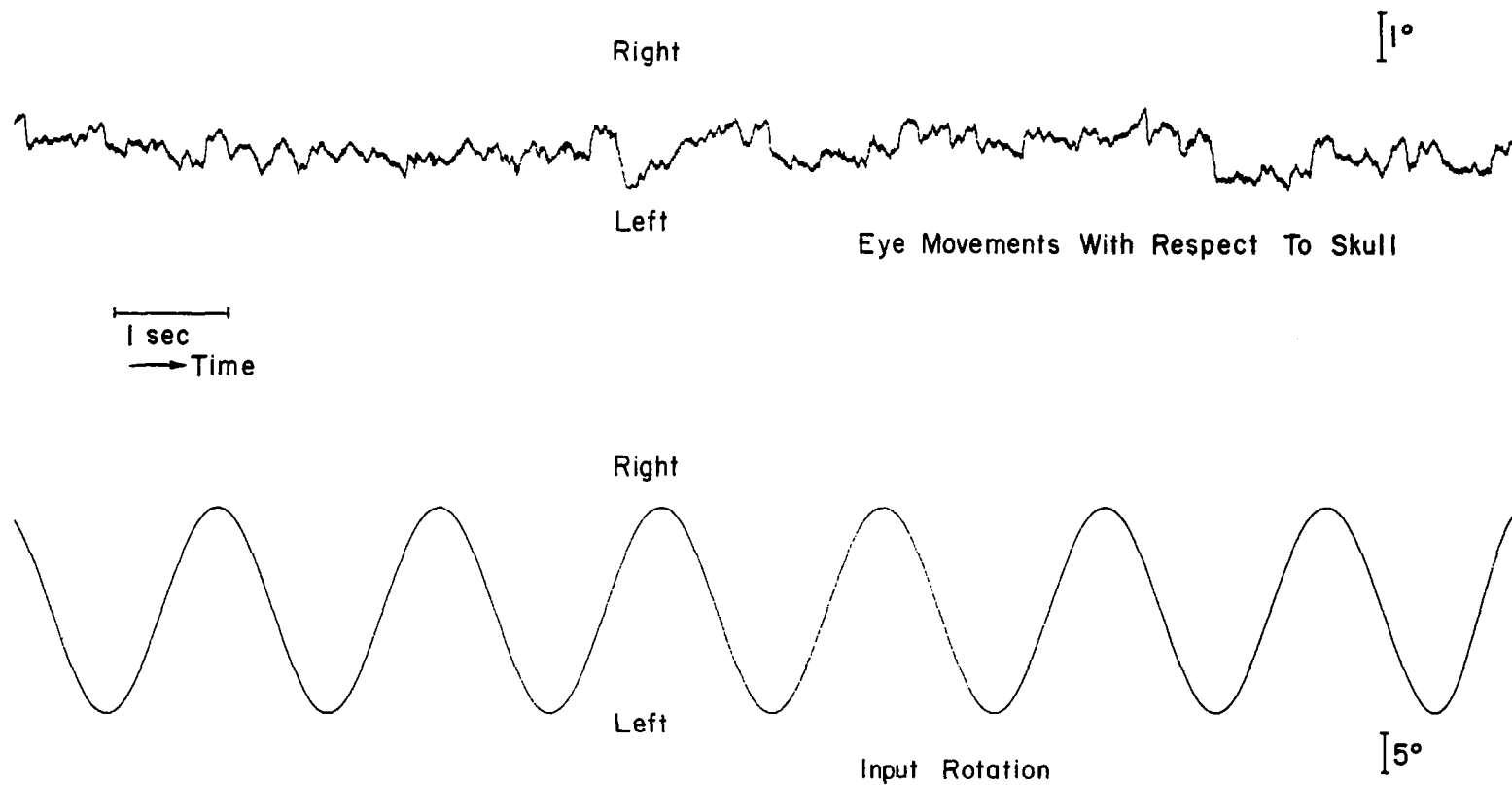


Fig. 5.5 Vestibular Nystagmus With Environmental Fixation Point, $f=0.5$ cps

phase for these conditions. Therefore they are combining to keep the fixation point image stationary.

Experimentally, by removing the hood from the cab of the moving base simulator and illuminating the surroundings, a duplication of the described conditions was achieved. A crossed marker was taped to the wall of the room 8 feet away from the subject and at his eye level. The subject was instructed to maintain fixation upon the marker throughout the experiment.

A record taken at $f = 1.0$ cps is shown in Fig. 5.6. Note the regularity of the eye position, tracing a perfect sinusoid, a feature observed for all the frequency range (0.03 cps - 2.0 cps) of the experiment. The frequency response of the eye movement control system with earth-fixed fixation point is presented in Fig. 5.7. Perfect compensation of amplitude is achieved over the range of two decades of frequencies approximately, with the phase lag, however, increasing rapidly beyond 0.5 cps. These results point out the capacity of the control mechanism to maintain a stationary reference for the visual system in presence of disturbances in the form of vehicle rotations. The observation holds as long as the limit of rotation of the eye has not been exceeded during the rotational maneuver.

5.3 COMPENSATORY EYE MOVEMENTS - NECK PROPRIOCEPTORS

The role of neck receptors as a source of compensatory eye movements has been suggested by physiologists in

Eye Movements With Respect To Skull

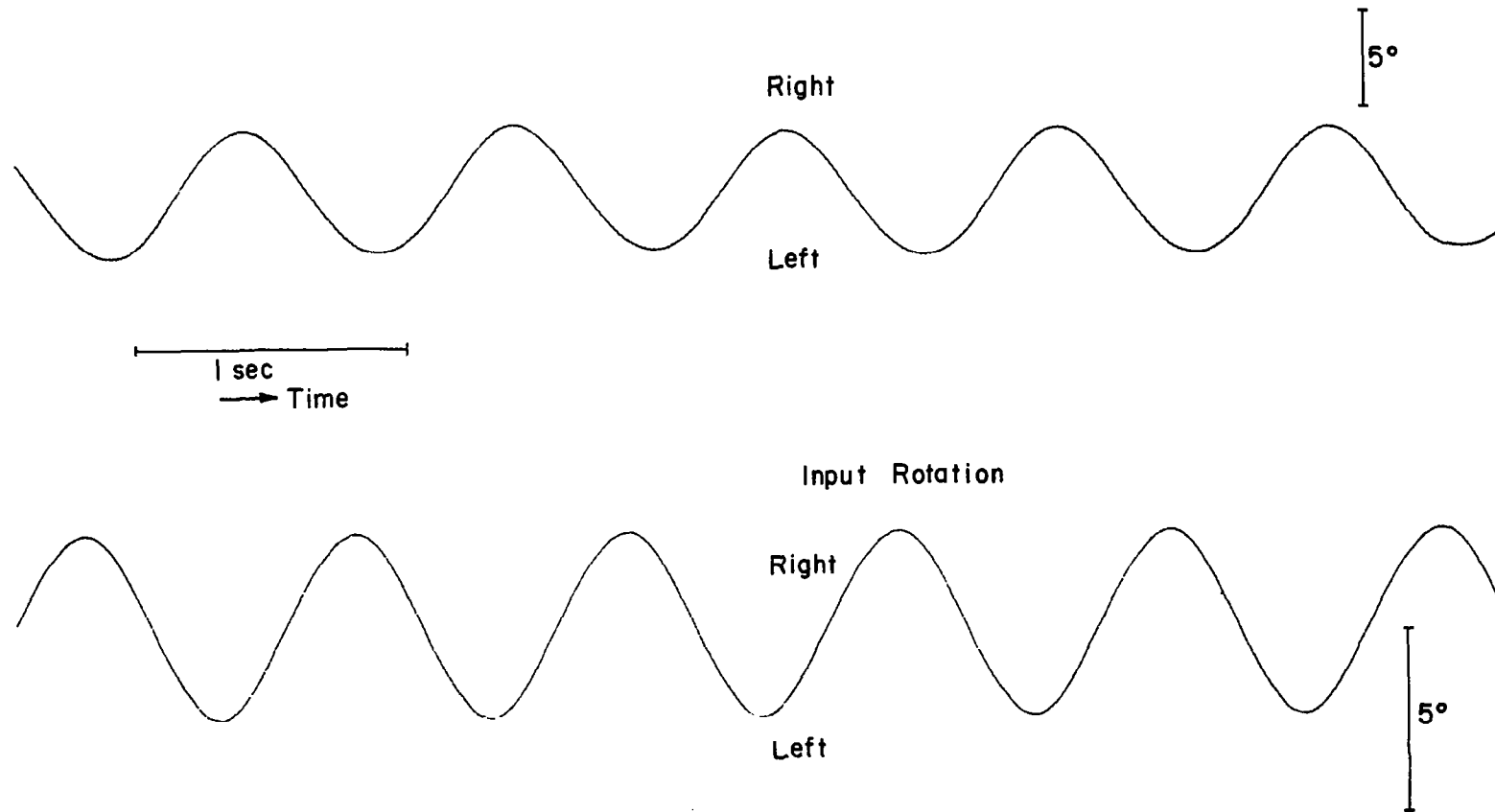


Fig. 5.6 Vestibular Compensatory Eye Movements With Earth-fixed Fixation Point, $f=1.0$ cps

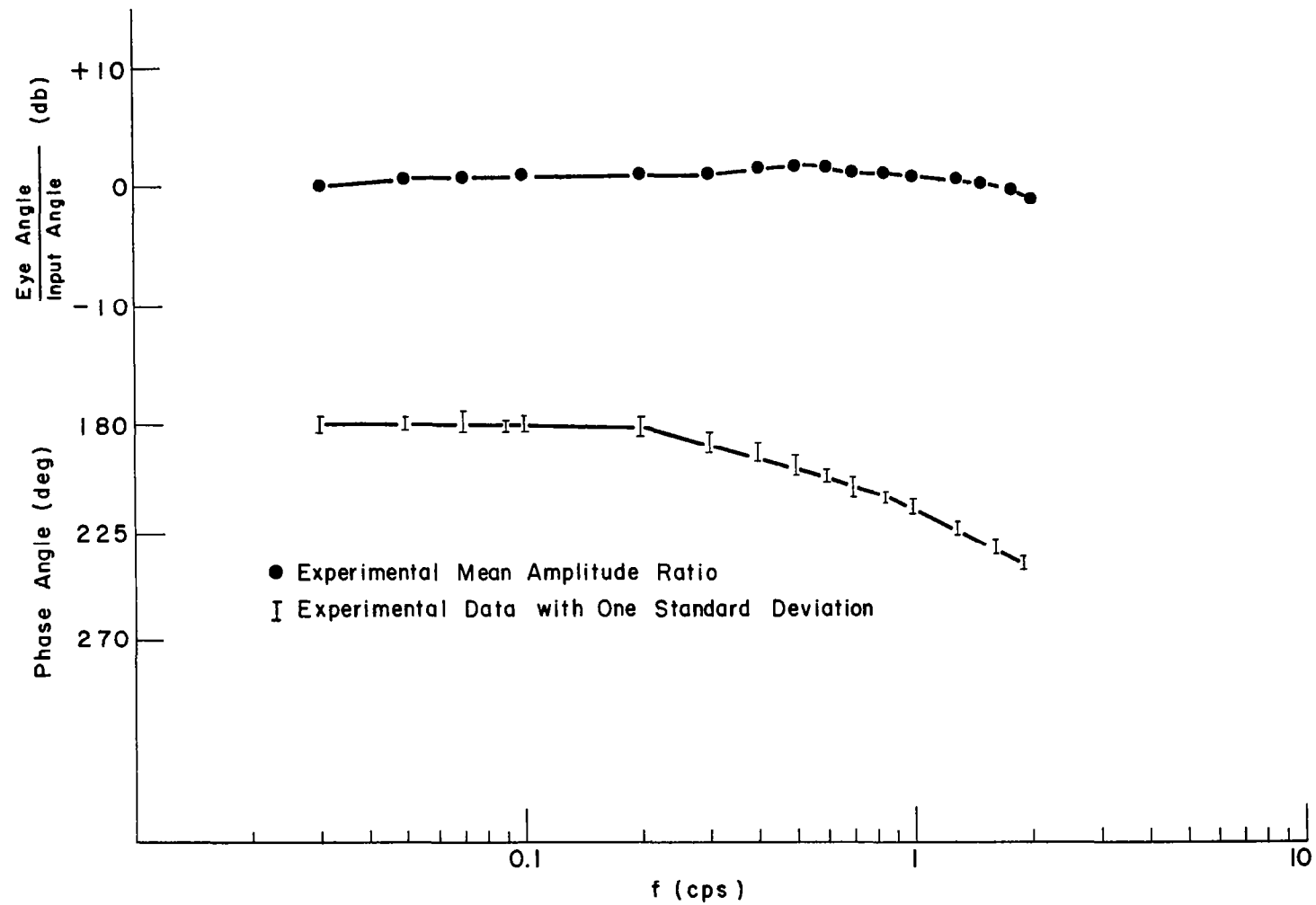


Fig. 5.7 Bode Plot of Compensatory Eye Movements (Vestibular Stimulation with Earth Fixation Point)

early literature.⁵⁴ In the rabbit, eye movements were recorded while the neck was bent, but the validity of the observation is questionable since the vestibular system of the animal was also stimulated in the process. For man, the only experiment intended to isolate the effect of neck receptors upon eye movements is reported in the literature back in 1928. The conclusion the author reached there maintains that for the experimental condition of fixed head and moving trunk, the corresponding eye movements were small.⁵⁴

If compensatory eye movements are produced, the atlanto-axial joints of the neck and the muscles participating in the relative head-trunk rotation (see Appendix C) have to contain the nerve endings which control the oculomotor muscles. Unlike the nerves of the vestibular system, no direct pathway from the nerves of the neck joints and muscles to the motor nuclei of the eye has been identified yet.⁴³ Nevertheless, through central processing or a feedback path to the vestibular nerves, a tie pathway of innervation from the neck receptors to the eye muscles is, in all probability, established.

The experimental setup for the vestibular stimulation (Sec. 5.2.1) was rearranged to allow rotation of the trunk while the head is kept still. The subject was seated in the cab of the simulator with the vertical axis of it running along the neck. His eye was illuminated with a stationary infrared light source. With the skull fixed to the

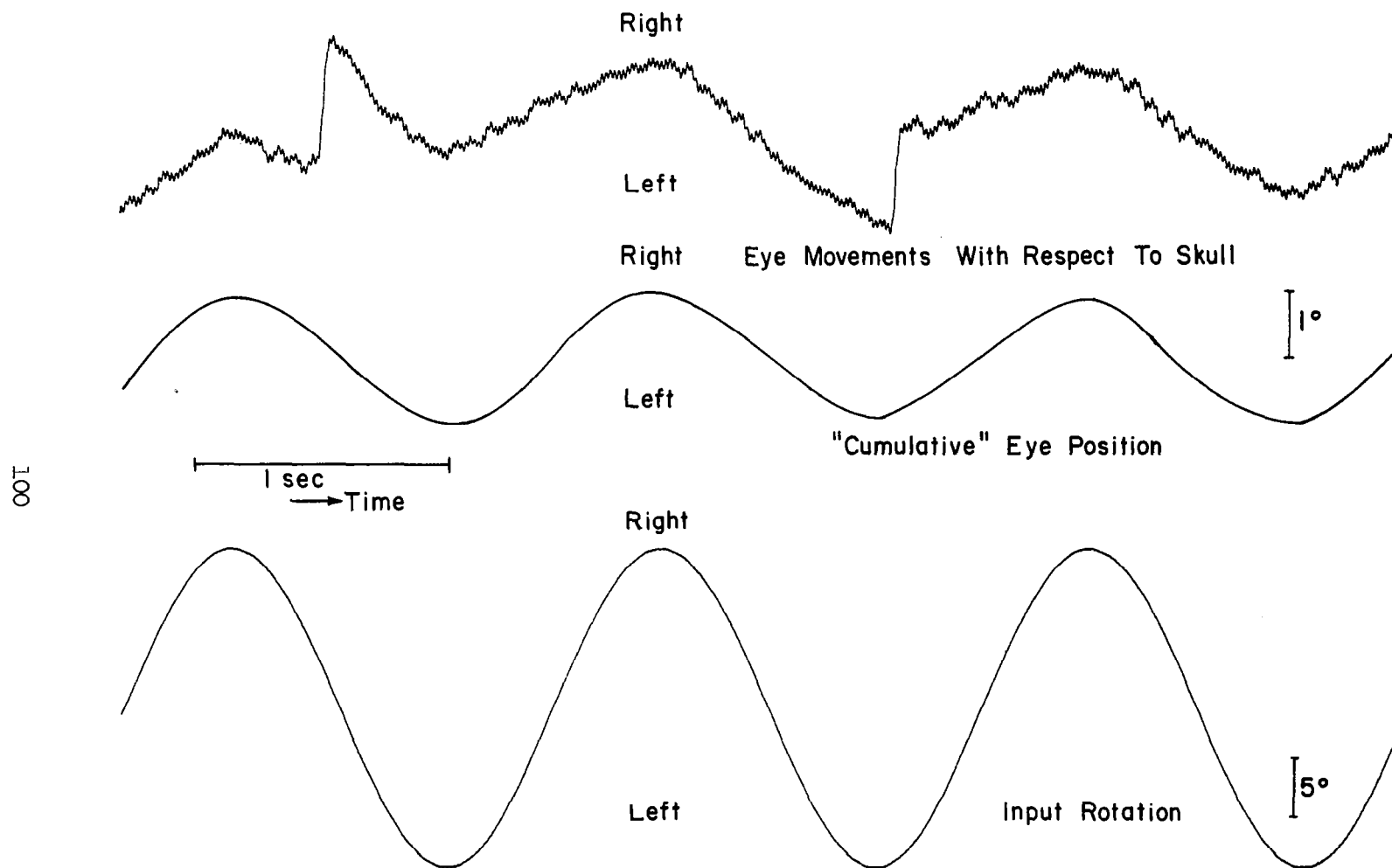


Fig. 5.8 Compensatory Eye Movements By Neck Receptors, $f = 0.6$ cps

stationary gimbal of the simulator by a bite board, care was exercised to provide rotation of the trunk that is free of bending.

As seen in Fig. 5.8, distinct compensatory eye movements are recorded for sinusoidal rotation of the trunk. The experimental record is for input frequency of 0.6 cps and the input amplitude is ± 13.5 degrees. The "cumulative" eye position shows an angular travel of the eyeball of ± 1.0 degrees.

Examination of the recording emphasizes two characteristic features of the eye motion: 1) eye movements resemble vestibular nystagmus with slow and fast phases; 2) the eyeball is driven in phase with the motion of the trunk. The latter observation is indeed in agreement with expected compensation for normal head on body rotations. Rotation of the trunk to the left with head fixed corresponds to rotation of the head to the right, while the trunk is stationary. For these relative angular rotations, the compensatory motion of the slow phase should be to the left as is the case at hand.

The frequency response of the experimental data from input angular velocity to compensatory eye velocity is shown in Fig. 5.9. Examination of it finds the eye movements recorded to be extremely small for frequencies above 2.5 rad/sec. However, the amount of compensation rises approximately to the vestibular level (in the range 0.02 cps - 4.0 cps) at frequencies below 0.6 rad/sec. A theoretical fit to

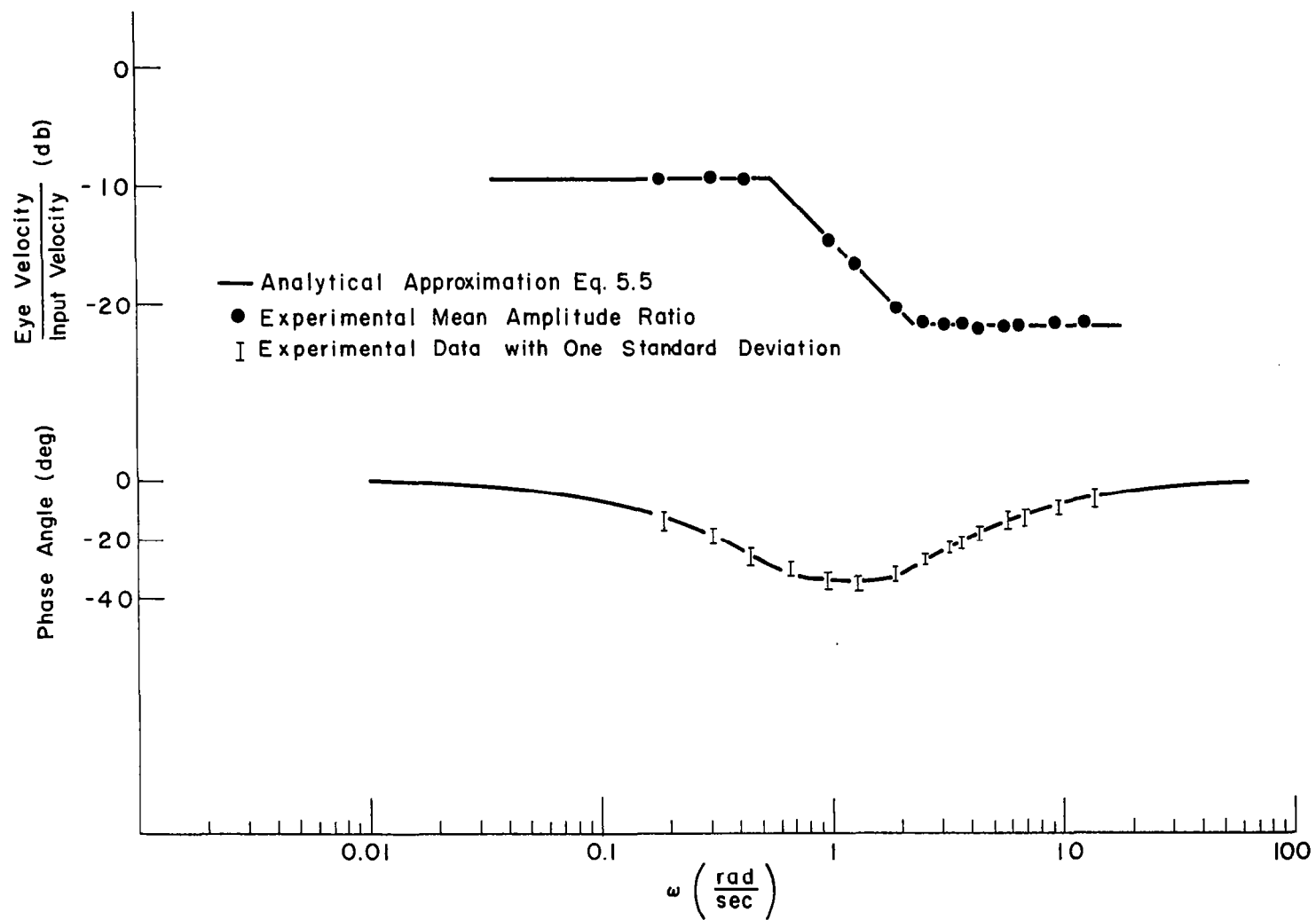


Fig. 5.9 Bode Plot of Compensatory Eye Movements by Neck Proprioception

the data, in the form of a lag-lead network is given by:

$$\frac{\text{eye velocity (s)}}{\text{input angular velocity}} = \frac{.325 (1+0.43s)}{(1 + 1.74s)} \quad (5.5)$$

This series of experiments established the relation of compensatory eye movements to stimulation of the neck proprioceptors. Their transfer function, approximated by Eq. (5.5) indicates eye velocities from D.C. to about 1 rad/sec comparable in amplitude to the velocities measured in response to stimulation of the semicircular canals (0.02 cps to 4 cps). However, the phase relations attributed to the two branches of the control system differ rather radically. While eye velocity due to the vestibular branch leads the input velocity for the spectrum of frequencies under consideration, the compensatory motion by proprioception lags the input rotation.

5.3.1 Environmental and Earth-fixed Fixation Points

The study of the simultaneous stimulation to the neck proprioceptors and the tracking branch of the eye movement control system is of a distinct academic interest, since these conditions are not encountered in real life. However, the experimental evaluation of eye movements in the presence of an environmental or earth-fixed fixation point can provide data for further validation of the model of the control system. Experimentally, the environmental fixation is achieved by illuminating the interior of the rotating cab

of the simulator, while still maintaining the head fixed to the stationary gimbal of it. The response of the control system calls for sinusoidal eye movements, with the main contribution being that of visual tracking. Since proprioceptive drive of the eye is negligible for frequencies above 0.4 cps, the regularity in tracking movements should deteriorate with increase in frequency in a manner similar to the movements recorded for tracking only.¹⁷⁷ The record shown in Fig. 5.10 is for eye movements with environmental fixation at $f = 0.8$ cps. When the input frequency is raised further, the Fourier series of the response contain sizable terms besides the fundamental.

With earth-fixed fixation point during stimulation of the neck receptors, the eye is driven to maintain its mean position constant relative to the skull. Therefore, at low frequencies, the visual tracking loop should correct for compensatory movements driven by the proprioceptors, and at high frequencies the tracking loop prevents eye drift. Examination of Fig. 5.11, which presents movements with earth-fixed fixation point at $f = 0.2$ cps, supports this notion of response of the eye movement control system. The total travel of the eye from its center position is ± 0.5 degrees, while the "cumulative" eye position for the same conditions without a fixation should have been ± 2.0 degrees.

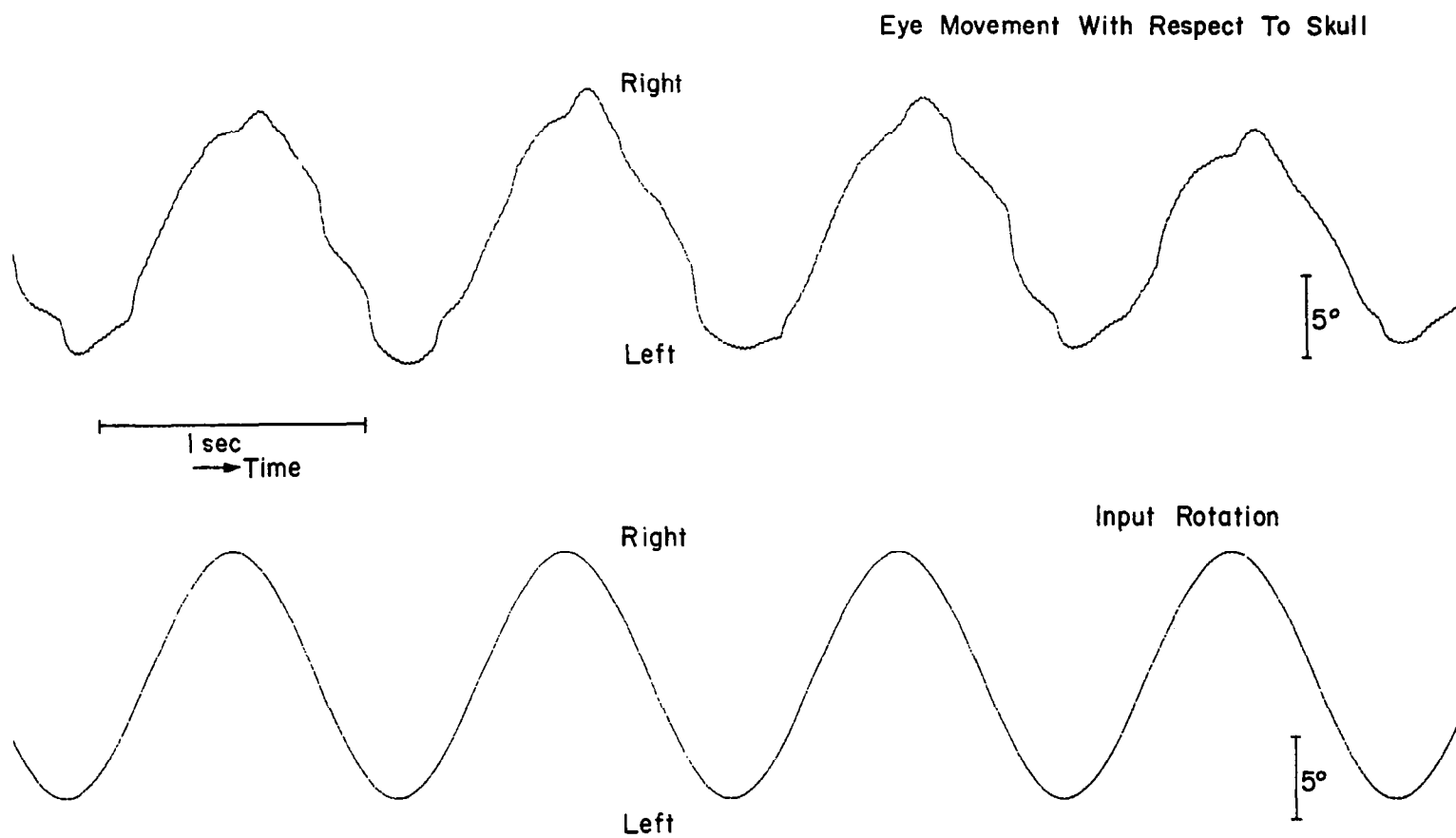
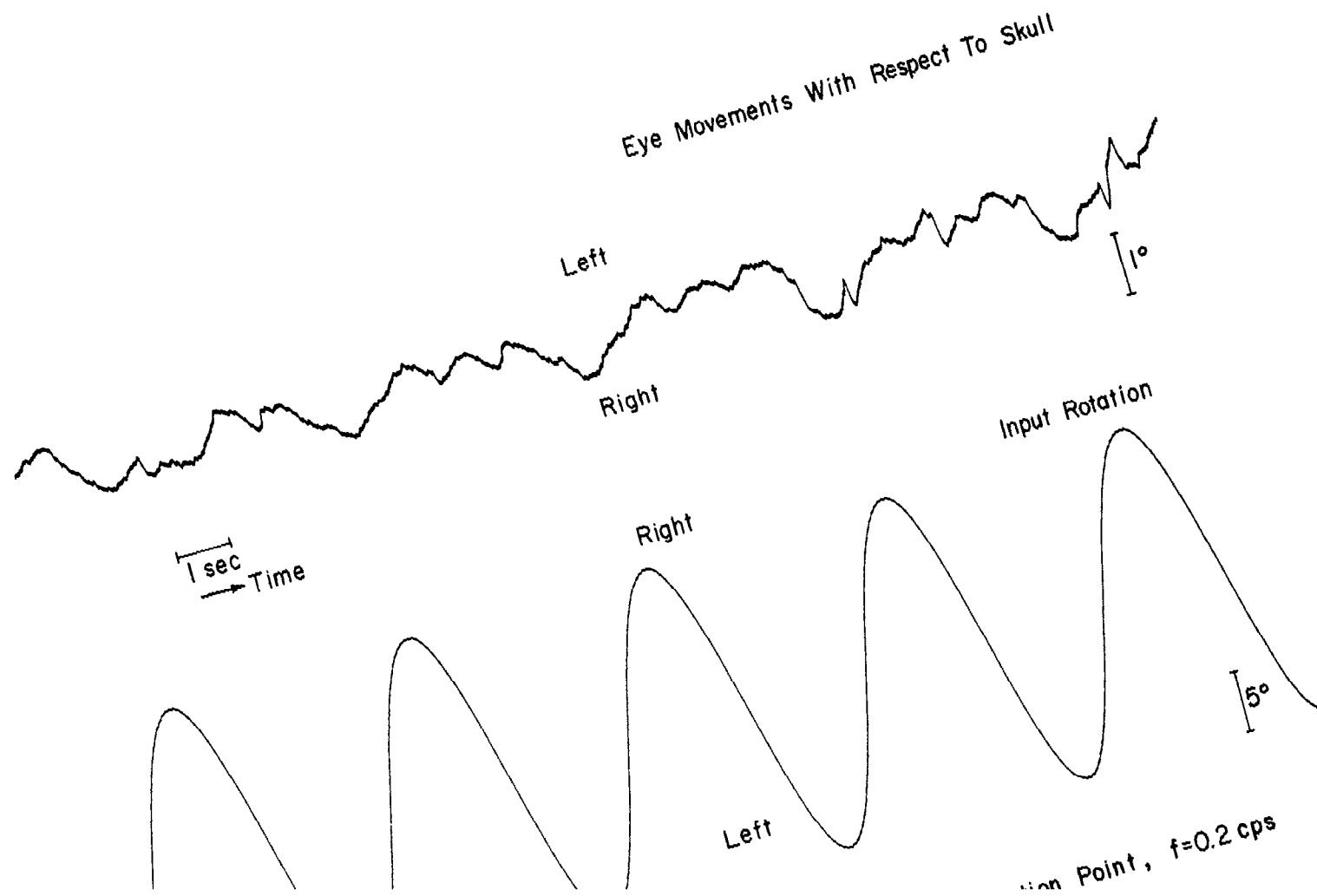


Fig. 5.10 Eye Movements, Neck Proprioception And Environmental Fixation Point, $f=0.8\text{cps}$



5.4 COMPENSATORY EYE MOVEMENTS - VESTIBULAR AND NECK PROPRIOCEPTORS STIMULATION

Frequent movements of the human involve rotation of the head while the eye is fixated upon a given object in the visual field. During these rotating motions, the vestibular system and the neck proprioceptors are stimulated. Therefore, the accompanying eye movements are due to all three of the motion sensors, the eye, the semicircular canals and the neck proprioceptors. The compensation achieved for these circumstances is a measure of the maximum capability of the eye movement control system to preserve a stationary reference on the eye.

One should raise the question whether the control system is linear over the spectrum of frequencies measured in these series of experiments. If affirmative, the compensatory eye movements for combined stimulation of the three motion sensors will be the vectorial sum of the individual contributions by the semicircular canals, the neck proprioceptors, and visual tracking. The importance of the concept of linearity of the control system is far reaching. By virtue of it, compensatory eye movements are predictable just on the basis of the data on the environmental conditions and a mathematical model of the control system. Evidently, the crucial experiment testing the linearity of the system is for combined stimulation of the semicircular canals and the neck proprioceptors in the absence of visual fixation.

a) Method: The subject was accommodated in a chair with his back supported in upright position. His head was fitted with an adjustable head band which carried a small infrared light. A potentiometer with its case stationary and its slider in the head band was used to measure head position. The experimenter, by counting throughout the experiment, provided the beat according to which the subject rotated his head, simulating sinusoidal rotation. The experimental series was carried through in a dark room.

b) Results and Discussion: The recorded data was analyzed by reconstructing the cumulative eye position relative to the head and measuring the respective amplitude ratio and phase lag at any given frequency. A Bode plot of the results with one standard deviation around the mean is presented in Fig. 5.12. The sum of the eye-semicircular canals transfer function (Eq. (5.4)) and the eye-neck proprioceptors transfer function (Eq. (5.5)) is also shown in Fig. 5.12 represented by its straight line approximation. The sum of Eq. (5.4) and Eq. (5.5) is given by:

$$\frac{\text{eye velocity (s)}}{\text{input angular velocity (s)}} = \frac{-0.325 (19.2s + 1)(1.12s + 1)(0.0067s + 1)}{(8s + 1)(1.74s + 1)(0.04s + 1)}$$

Examination of Fig. 5. shows complete agreement between the experimental data and the predicted response

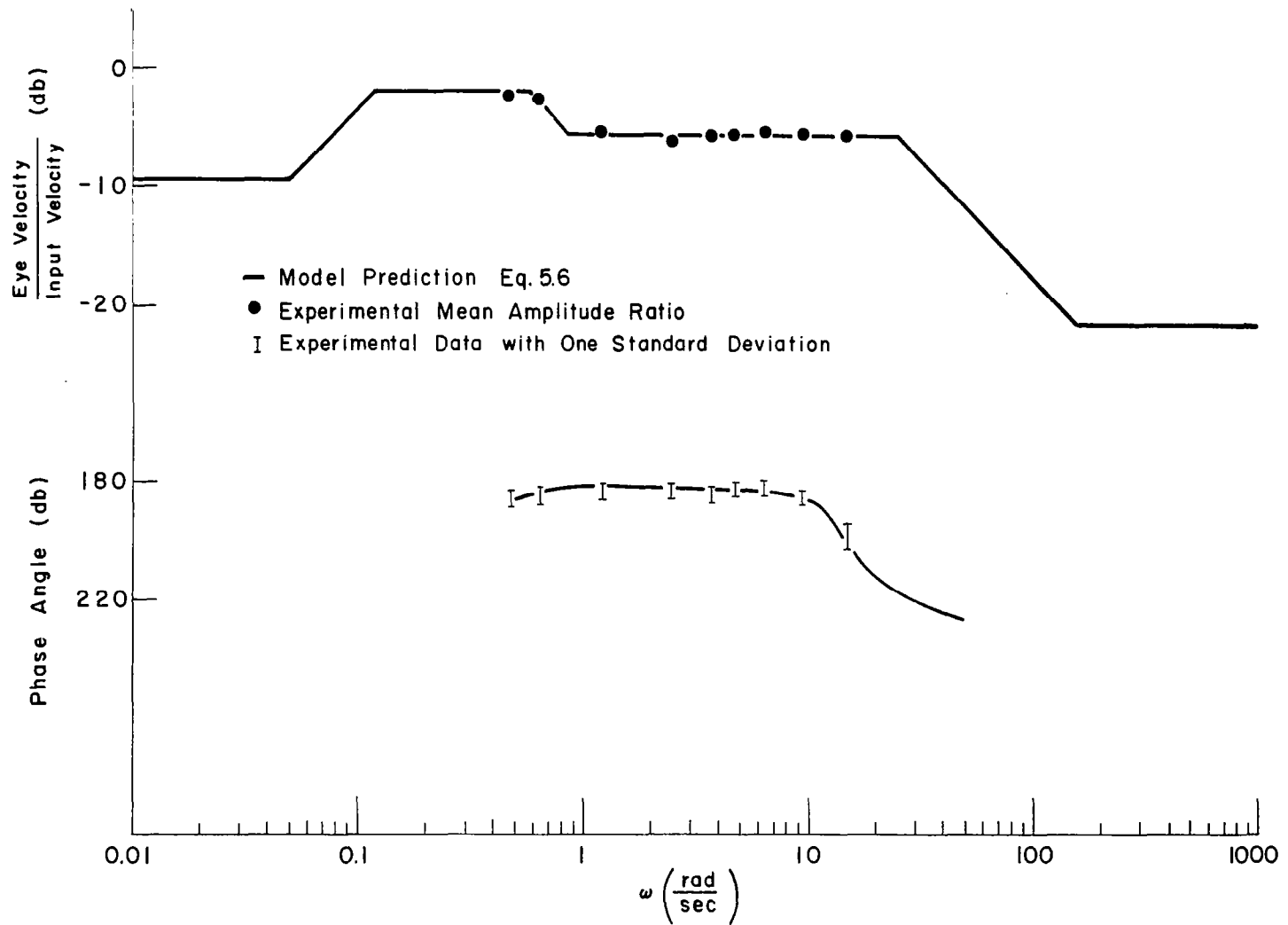


Fig. 5.12 Bode Plot of Compensatory Eye Movements (Vestibular and Neck Proprioception)

from the separate transfer functions for the vestibular system and the neck proprioceptors. Therefore, the eye movement control system is a linear system at least over the range of frequencies tested here (0.03 cps to 2.0 cps). Since the amplitude ratio is between 0.35 and 0.55 for the frequency range from 0.02 cps to 2 cps, the compensation is only partial and the preservation of a stationary image on the retina without the participation of visual tracking is impossible. The relative contribution of the vestibular system in the resultant compensatory eye movement is larger compared to that of the neck proprioceptors at frequencies above 0.2 cps while below it, the effect of both systems is approximately equal.

5.4.1 Environmental and Earth-fixed Fixation Points

Rotations of the skull in the presence of a fixation point is the most common pattern of maneuvers, during which the eye movement control system is called upon to stabilize the eyeball on a given object. For such rotations, all the loops of the control system are activated, thus the response of the system is the ultimate of stabilization the eye can achieve.

Experiments done here show the total travel of the eye in the presence of an environmental fixation point to be at the maximum of ± 0.5 degrees. And for earth-fixed fixation, the frequency response of the control system shown in Fig. 5.13 exhibits good compensation capabilities over the

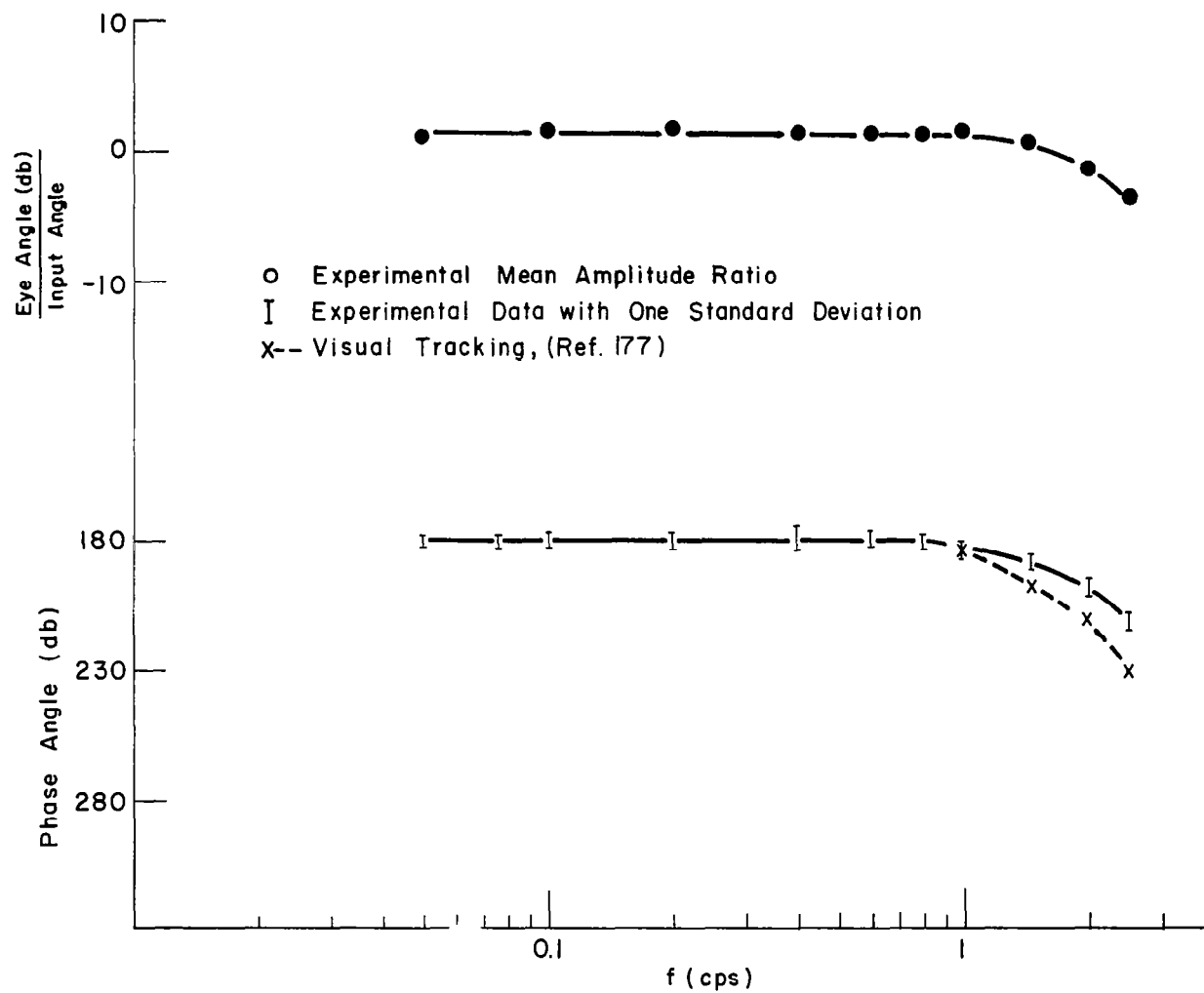


Fig. 5.13 Bode Plot of Eye Movements (Vestibular, Proprioception and Earth-fixed Fixation Point)

whole spectrum of frequencies up to 2.0 cps. The phase angle for visual tracking of predictable sinusoids¹⁷⁷ is also shown on Fig. 5.13. Note the distinct contribution of the vestibular system and the neck proprioceptors in reducing the phase lag of the eye at high frequencies.

5.5 STABILIZATION OF EYE POSITION IN SPACE

The eye movement control system as presented in the block diagram of Fig. 5.1 consists of three branches, each of which contributes to the control of the eyeball position relative to the skull and the environment. The compensatory eye movements attributed to the vestibular system and the neck proprioceptors are of the nature of reflex responses with no voluntary control upon them. Tracking movements, on the other hand, depend upon the wish to maintain a certain object, in the immediate vicinity, under observation. Regardless of their origin, eye movements during periods of motion disturbances are controlled to keep the eye position stationary with respect to an environment which is judged as stationary too.

Table 5.1 summarizes qualitatively the experimental results obtained in the series of experiments performed here. In the presence of fixation points, rotation of the skull with respect to the body or rotations of the body as a whole, tend to displace the stationary picture observed by the eye. The experiments show that the eye is stabilized in space within ± 0.5 degrees when the fixation is on the

Table 5.1
Space Stabilization Of Eye

	No Fixation Point	Environmental Fixation	Earth-fixed Fixation
Vestibular	Partial Compensation Of Rotational Rate over Frequencies from 0.02 cps to 4.0 cps	Maintain Eye Angle within $\pm 0.5^\circ$ up to 2 cps	Full Compensation up to 2 cps
Neck Proprieceptors	Partial Compensation of Rotational Rate Below 0.15 cps	Poor Compensation above 1 cps	Maintain Eye Angle within $\pm 0.5^\circ$ up to 2 cps
Vestibular and Neck Proprieceptors	Partial Compensation of Rotational Rate up to 4.0 cps	Maintain Eye Angle within $\pm 0.5^\circ$ up to 2 cps	Full Compensation up to 2 cps

moving surrounding. And for an earth-fixed fixation point, the eye compensates with essentially a constant amplitude ratio and minimal phase lag in response to input frequencies of rotations up to 2 cps. Fig. 5.14 is the mathematical model for the horizontal eye movement control mechanism. It incorporates the visual tracking model proposed by Young¹⁷⁷, and the dynamic characteristics of the semicircular canals and the neck proprioceptors, when related to compensatory eye movements as measured here. The linearity of the summing point prior to the motor mechanism of the eyeball was established experimentally for addition of vestibular and proprioceptor signals. Therefore, the assumption of additive property for the visual tracking branch too is plausible and experiments show quantitatively such behavior.

The eye movement model was simulated on an EAI TR48 computer and the response of the simulated system was compared with the experimental results. The model reproduced very well the measured eye movements in the presence of visual fixation. Without this fixation, the "cumulative" eye position only ("fast" phase was not simulated) was obtained.

The performance capabilities of the eye as an orientation sensor can be derived from the model presented here for any maneuver involving rotation around a vertical axis. Comparison of eye movements with an earth fixation point, with and without the participation of the vestibular system,

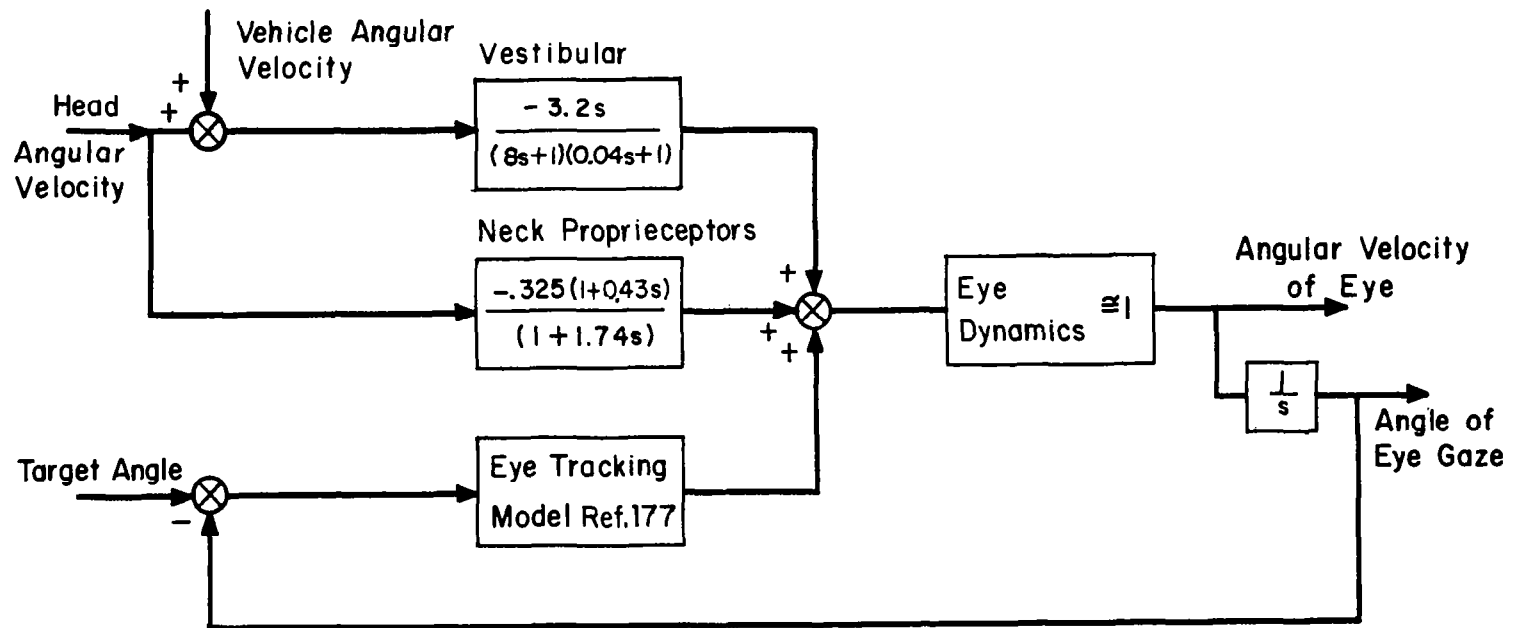


Fig. 5.14 Model for Multi-input Horizontal Eye Movement Control System

in the control loop outlines the contribution of this system toward stabilization of the eye. With the vestibular system stimulated, eye movements are smooth and regular, free of harmonics. When the vestibular system is unstimulated, eye movements' wave shape loses similarity to the input sinusoid for frequencies above 0.8 cps. The visual tracking loop alone, which is a position control system, shows similar distortion of the wave shape of eye movements for high input frequencies.¹⁷⁷ However, with the vestibular system stimulated and with visual fixation, the wave shape regularity of eye movements is preserved for input frequencies close to 2.5 cps. In view of these findings and considering the semicircular canals as angular velocity meters, one can conclude that the vestibular system provides the rate information for the eye movement control system, while the visual tracking monitors mainly the deviation of the eye from a given fixation point.

CHAPTER VI

SIMPLE MANUAL CONTROL SYSTEMS WITH MOTION INPUTS

A manual control system is a closed loop system in which the human operator attempts to reduce the system error. In a single axis, compensatory tracking loop, the operator perceives the system error only and affects the system output by manipulating a control stick (Fig. 6.1). The mathematical representation of the operator's response for a given task is generally assumed to fit a quasi-linear description.^{129,50} Thus, the model of the human operator contains a "describing function" linearly correlated with the system error, and an additive remnant uncorrelated with it. The ability of the human operator to adapt his response to the system inputs and to the controlled elements provides the manual control systems with a desirable flexibility. However, this feature also prevents a unique presentation of the transfer characteristic of the operator since his dynamic response is a function of the control system parameters. Nevertheless, a tabulation of describing functions for various system conditions, is of great importance to the preliminary design of manual control systems.

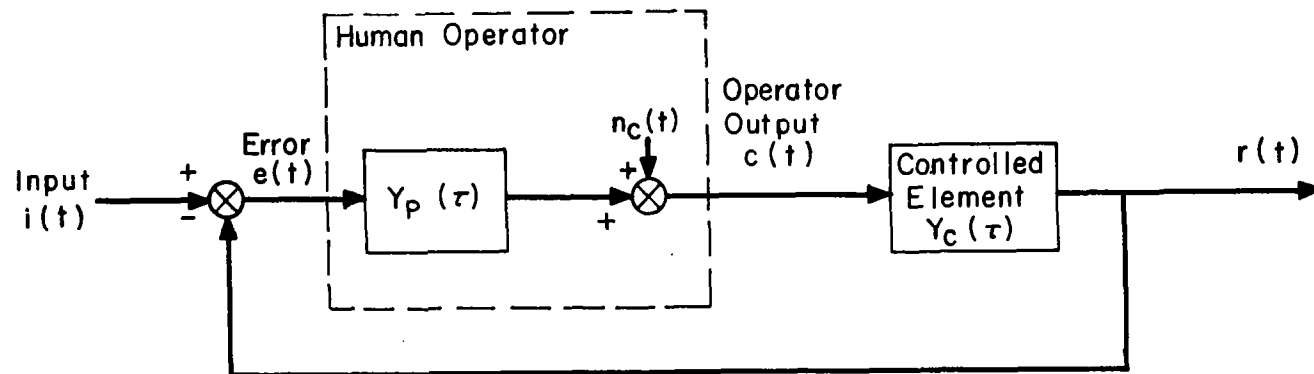


Fig.6.1 Block Diagram of Simple Compensatory Manual Control System (Ref. 129)

6.1 THE VESTIBULAR SYSTEM AS AN INPUT CHANNEL IN MANUAL CONTROL SYSTEMS

The human operator in a vehicle orientation control loop receives the necessary information for his control decisions through a visual display, by motion sensing, or by means of audio communication. Describing functions have been obtained by others for manual control systems in a single axis compensatory task with visual input and manual output covering a wide class of controlled elements.¹²⁹

In a vehicle control loop, the operator always receives motion inputs when seated in the vehicle. The effect of these motion cues on the operator's characteristics is, in general, acknowledged.^{150,53} However, their contribution to the operator's ability to generate lead compensation and to satisfactorily control a closed loop system have not been assessed prior to this investigation.

Consider the restricted case of control of vehicle orientation to a stationary reference frame. Nonvisual perception of motion in the human is provided by the vestibular sensors, supplemented by tactile and kinesthetic sensations. The vestibular sensors perceive the resultant angular accelerations and specific forces acting on the man in the vehicle. The motion inputs the operator senses are, therefore, compatible with the definitions of a compensatory tracking task for a stationary reference.

Vehicle motions combine rotations and translations stimulating both the semicircular canals and the otoliths.

However, an experimental situation can be simulated where motions are classified according to three categories:

1) pure rotational motion in the horizontal plane; 2) pure translation; and 3) rotational motion with respect to the gravity vector. Under these simulated conditions, angular, linear, or combined accelerations are perceived by the human. They provide the desired separation between the orientation information of the semicircular canals and the otoliths.

In a typical manual control system, the human operator will attempt to maintain some reference orientation in the presence of a disturbance. The block diagram in Fig. 6.2 represents the manual control system simulated for this study of the vestibular system in simple, compensatory tasks. The dynamics of the vehicle in the system were a single integration, presumably the optimum one for the operator to control. In this system, operator stick displacement is proportional to vehicle velocity. The human operator may have three modes: visual, motion, or combined. He attempts to control his vehicle to a preset reference in the presence of orientation disturbances.

The characteristics of the human operator in these manual control systems were analyzed in terms of quasi-linear describing functions. The identification technique outlined in Appendix D defines the transfer function of the human operator as:

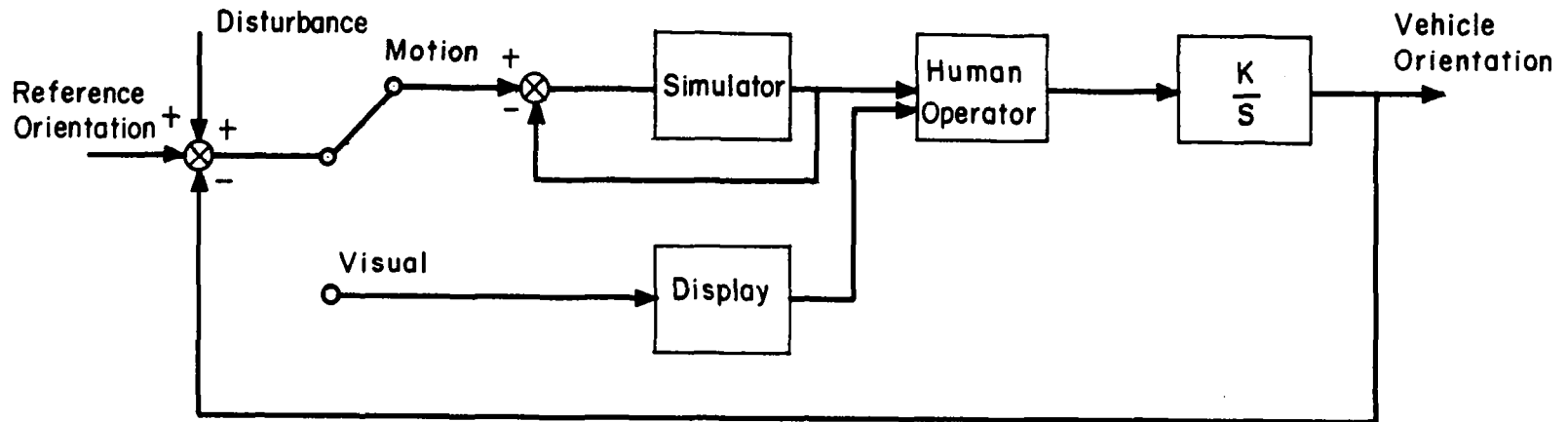


Fig. 6.2 Velocity Control with Visual or Motion Mode

$$y_p = \frac{\bar{\Phi}_{ic}(\omega)}{\bar{\Phi}_{ie}(\omega)} \quad (6.1)$$

where $\bar{\Phi}_{ic}(\omega)$ = cross power spectral density of input and operator's output and

$\bar{\Phi}_{ie}(\omega)$ = cross power spectral density of input and system error.

For the experimental manual control system, the input is the noise disturbance, and the system error is the deviation of the vehicle orientation from the reference. A measure of the similarity of the human operator's transfer characteristics to a linear element is provided by the square of the linear correlation, ρ , given by:

$$\rho^2 = \frac{|\bar{\Phi}_{ic}|^2}{\bar{\Phi}_{ii} \bar{\Phi}_{cc}} = 1 - \frac{\bar{\Phi}_{nn}}{\bar{\Phi}_{cc}} \quad (6.2)$$

where $\bar{\Phi}_{nn}(\omega)$ = the remnant power spectral density,

$\bar{\Phi}_{ii}(\omega)$ = the input (disturbance) power spectral density, and

$\bar{\Phi}_{cc}(\omega)$ = the human operator's response power spectral density.

A value of ρ^2 near unity implies that the operator's remnant is small compared with his output, which is correlated with the system input. In a manual control system with a stochastic disturbance, to avoid prediction, the measured operator's characteristics are closely approximated by the calculated transfer functions.

The disturbance input in this experimental series was filtered Gaussian noise, generated by a noise generator, with a constant power spectral density from D.C. to 50 cps. This noise was shaped with two cascaded first order filters, with corner frequencies at 0.15 cps, while its rms amplitude was adjusted for each experimental condition.

6.2 A MANUAL CONTROL SYSTEM WITH PURE HORIZONTAL ROTATION

Rotation of a vehicle about the gravity vector (Yaw) is a control situation where the otoliths can be maintained unstimulated by linear accelerations, except for the ever present gravity field. If the head of the subject is placed in the axis of rotation of the simulator, and maintained fixed with respect to the moving cab, the centrifugal and the tangential accelerations arising from the rotational motion can be minimized.

The block diagram of Fig. 6.2 points to three modes for the human operator, all of which were investigated here:

1) visual display with no motion, corresponding to a fixed base control system; 2) vestibular information with no visual display; and 3) combined visual display and vestibular sensation of motion.

a) Method: Manual control of attitude was performed driving a moving base simulator about its vertical axis. In the rotating cab of the simulator, an oscilloscope displaying a vertical line provided the visual, compensatory input. The operator, strapped to his chair, had his head

supported with a headrest. He exercised control on the system with a lightweight, spring restrained, linear stick, mounted beside his seat for right hand manipulation. The experimental parameters were:

white noise disturbance - 15° rms

visual display - 2/15 inch/degree of rotation

control gain - $K = 0.5$ deg/sec/degree of stick

stick - linear, with maximum travel of $\pm 45^{\circ}$, corresponding to velocity command of ± 22.5 deg/sec.

In visual and combined modes the operator was instructed to maintain his initial orientation. Two different operator tasks were experimented with, for motion tracking only: 1) to keep the vehicle on course; and 2) to keep the vehicle stationary. The difference between these instructions is whether or not a correction for accumulated drift, off course, should be introduced by the operator.

Three subjects were used for this experimental series. They had previous experience in operating manual control systems and were trained for the experimental tasks. Each subject was scored on 10 runs of 90 seconds duration for each experimental condition.

b) Results: For each run of the visual and visual-motion tracking, the noise disturbance, system error, operator's output, and integrated stick output were recorded on magnetic tape, converted to digital form, and processed by an IBM 7094 digital computer. The describing functions for the human operator were determined by the identification

procedure outlined in Appendix D. These results were averaged for each subject yielding the mean amplitude ratio and the phase angle versus frequency. Standard deviation of these were also evaluated. The correlation coefficient at any given frequency was determined. Results with $\rho^2 < 0.75$ were dropped because the assumption of quasi-linearity becomes poor. This procedure provided experimental describing functions in terms of amplitude ratio and phase angle over the frequencies from 0.056 cps to 0.8 cps for each subject.

The describing functions were tested for inter-subject differences which were not found to be significant ($P > 0.100$). Following this observation, a theoretical fit to the averaged experimental data was obtained with the results summarized below:

$$\text{visual input } Y_p(s) = \frac{7e^{-0.2s}(2.4s+1)}{(3.15s+1)}, \frac{\overline{e^2(t)}}{i^2(t)} = 0.075 \quad (6.3)$$

$$\begin{array}{l} \text{visual and} \\ \text{motion} \\ \text{input} \end{array} Y_p(s) = \frac{7e^{-0.1s}(2.4s+1)}{(3.15s+1)}, \frac{\overline{e^2(t)}}{i^2(t)} = 0.050 \quad (6.4)$$

The describing function obtained for visual input is in good agreement with results published previously.^{89,148} At frequencies up to 0.2 cps, the data agree with that of Russell.¹⁴⁸ For larger frequencies, the operator's phase

lag follows closely the results of Hall.⁸⁹ Note that Hall used input noise comparable to the disturbance input here.

The experimental compensatory task, with motion sensing only, did not yield any meaningful results in terms of describing functions for the human operator. Subjects were unable to keep the simulator within its travel limits (about $\pm 35^\circ$) for periods longer than 25 to 30 seconds. During this time, the deviation of the cab off course increased at a steady rate between 1 and 3 degrees per second, with superimposed oscillations representing the control activity of the operator in response to the input disturbance.

c) Discussion: The experimental describing functions and their corresponding analytical approximations point out the significant contribution of motion cues to satisfactory performance in a manual control system. A considerable reduction of operator phase lag is noticed for the moving base simulation relative to the fixed base one (Fig. 6.3). In the analytic transfer function this reduction is expressed as a decrease in dead time delay from 0.2 seconds to 0.1 seconds. The describing functions are otherwise equal. The conclusion is that the operator is able to reduce his delay time in a manual control system where his semicircular canals provide information on the vehicle motion, compared to the delay in a system with visual display only.

Since the semicircular canals are angular accelerometers, they cannot detect a constant angular velocity. This was demonstrated experimentally in the motion compensatory

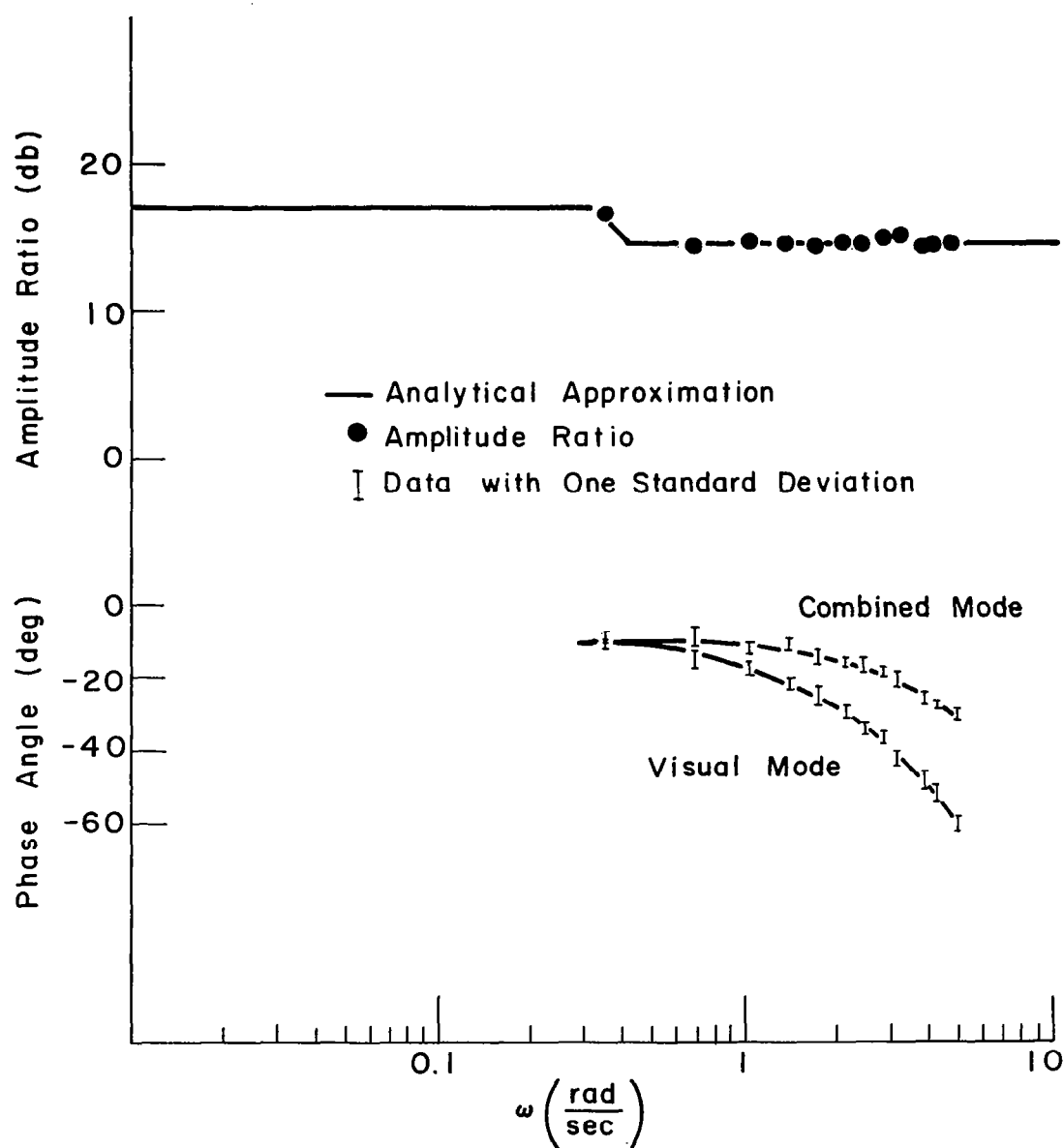


Fig. 6.3 Describing Function of The Human Operator in Visual and Combined Mode. Horizontal Rotation

task where the simulator drifted away from the reference with approximately constant angular velocity. Therefore, complete control of vehicle attitude, including low frequency drift, is impossible by only vestibular sensing of motion. However, when a visual reference is provided, the information originating in the semicircular canals is utilized by the human operator. It was previously shown that over the frequency range from 0.1 rad/sec to 10 rad/sec the canals are essentially angular velocity meters. Thus, they are a source of rate information for the operator, which he apparently uses to generate lead compensation.

6.3 MANUAL CONTROL SYSTEM WITH LINEAR MOTION

In Section 6.2, the observation was made that the semicircular canals alone cannot be used as sensors in a manual control system. A similar statement is true for the otoliths, the human specific force sensors. The difficulty arises from the fact that the compensatory task assigned to the operator in pure linear or rotational motion does not fit the sensing capabilities of the vestibular sensors. The otoliths are insensitive to constant linear velocity. Consequently, a vehicle can drift away with constant linear velocity, and the operator is unable to perceive this motion.

Experimentally, the operator was given velocity control on a linear motion simulator (see Appendix B). The control system was as shown in Fig. 6.2 with input noise

disturbance of 10 feet, rms, and $K = 1.0 \text{ ft/sec/degree}$ of stick. With motion inputs only, the operator could not maintain the simulator within its travel limits for more than 40 sec.

6.4 CONTROL OF MOTION WITH RESPECT TO THE GRAVITY VECTOR

The control of vehicle motion in roll stimulates both the semicircular canals and the otoliths. In this single axis task, the vehicle motion provides sufficient input information for control by the human operator. The otoliths are sensitive to any angular deviations from the vertical gravity vector, and the semicircular canals sense angular rates. The manual control system permits comparison of the effects of various combinations of inputs on the operator's performance.

a) Method: A single axis compensatory task was simulated on the moving base simulator driven about its roll axis. The visual input was an oscilloscope, displaying a line whose angle with the vertical corresponded to the roll angle of the simulator. The operator was seated in the simulator as described in Sec. 6.2.

The experimental parameters were:

white noise disturbance - 20°rms

visual display - angle of display corresponds to
error angle

control gain - $K = 1.0 \text{ deg/sec/degree}$ of stick

stick - linear with maximum travel of $\pm 45^{\circ}$

corresponding to velocity command of ± 45 deg/sec
dead time delay of visual display - 1 sec

The operator was instructed to maintain the simulator vertical throughout the experimental series. His performance was measured in the following control situations:

- 1) Rotation with respect to gravity - motion input with hard seat
- 2) Rotation with respect to gravity - motion input with soft seat
- 3) Rotation with respect to gravity - motion input and visual indicator
- 4) Rotation with respect to gravity - motion input and delayed visual indicator

In comparing two control situations differing only in the seat on which the operator sat, an attempt was made to indicate the effect of tactile sensation on the operator's performance. Similarly the study of the control loop with visual indicator, in phase with the motion and delayed, was intended to separate the effect of the visual input from the contribution of the motion cues.

b) Results: The describing functions of the human operator in these control situations were measured and analyzed as described in Sec. 6.1. These results are summarized below:

$$\text{motion input and hard seat } Y_p(s) = 5 \frac{\overline{e^2(t)}}{\overline{i^2(t)}} = 0.045 \quad (6.5)$$

$$\text{motion input and soft seat } Y_p(s) = 5 \frac{\overline{e^2(t)}}{\overline{i^2(t)}} = 0.046 \quad (6.6)$$

$$\text{motion and visual inputs } Y_p(s) = 5 \frac{\overline{e^2(t)}}{\overline{i^2(t)}} = 0.044 \quad (6.7)$$

In the control system with motion input and delayed visual indicator, the visual information was delayed with a dead time delay of one second. All the three subjects reported that they discarded this information since it impaired their performance. The describing function of the human operator for this condition, as well as others, was similar to this measured for motion input with hard seat. Note the extent of compensation the operator achieves in this control system. His transfer function is a pure gain, indicating a capability to compensate his phase lag for frequencies up to 0.8 cps.

c) Discussion: As described before, motion information, in absence of visual input, is perceived by the vestibular sensors and the tactile receptors. Here, in an attempt to demonstrate the effect of the tactile sensation on the operator response, his performance was measured in two control tasks differing only in the seat on which the operator sat. In one case, it was a very hard plastic seat, in the other an extremely soft, foam rubber cushion. The hardness of the seat was believed to vary

the extent of the perceived tactile sensation. The measured describing functions do not indicate any variation of performance between the two control situations. Similarly, the variation of the ratio of mean square error to mean square input is not significant statistically. The conclusion is that for this experimental situation, the tactile sensation does not have noticeable influence on the operator's ability to perform his task.

A comparison of the operator's characteristics in a system with visual and motion inputs, to those with no visual input, does not show a significant influence of the visual input. Similarly, the fact that the operator was able to distinguish discrepancies between his motion inputs and the visual display, indicates probably that he monitors the display, rather than using it as an input.

The experimental results presented here demonstrate the dominant role of the vestibular sensor in the performance of the operator. In the simulated, manual control system, without specific instructions to the subjects, the visual input is either disregarded, or used as a secondary source of information with small influence on the control decisions of the operator. Note that the describing function of the operator in this control system simulated on a fixed base with visual input would have been approximately:

$$Y_p = \frac{3.5 e^{-0.2s}(2.4s + 1)}{(3.15s + 1)}$$

based on the measurements described in Section 6.2.

The performance of the human operator in this vehicle control system is approximately a pure gain (see Fig. 6.4). This approximation indicates that the human operator is able to compensate for his dead time delay and other lags by virtue of sensing motion away from vertical. The motion inputs substantially improve the performance of the human operator compared to his characteristics obtained in a fixed base simulation.

6.5 SUMMARY

The characteristics of the human operator were measured in a simple manual control of vehicle orientation. It was verified that the operator cannot use motion inputs alone for satisfactory control when his sensors do not receive a constant reference stimulus. The vertical is the only reference with respect to which the human can establish his orientation. Therefore, the conclusion follows that control of vehicle orientation to the vertical is the only orientation task the human can perform with the vestibular system as sole input sensor. The presence of motion cues in a simple compensatory control task provides the operator with information which greatly improves his control characteristics.

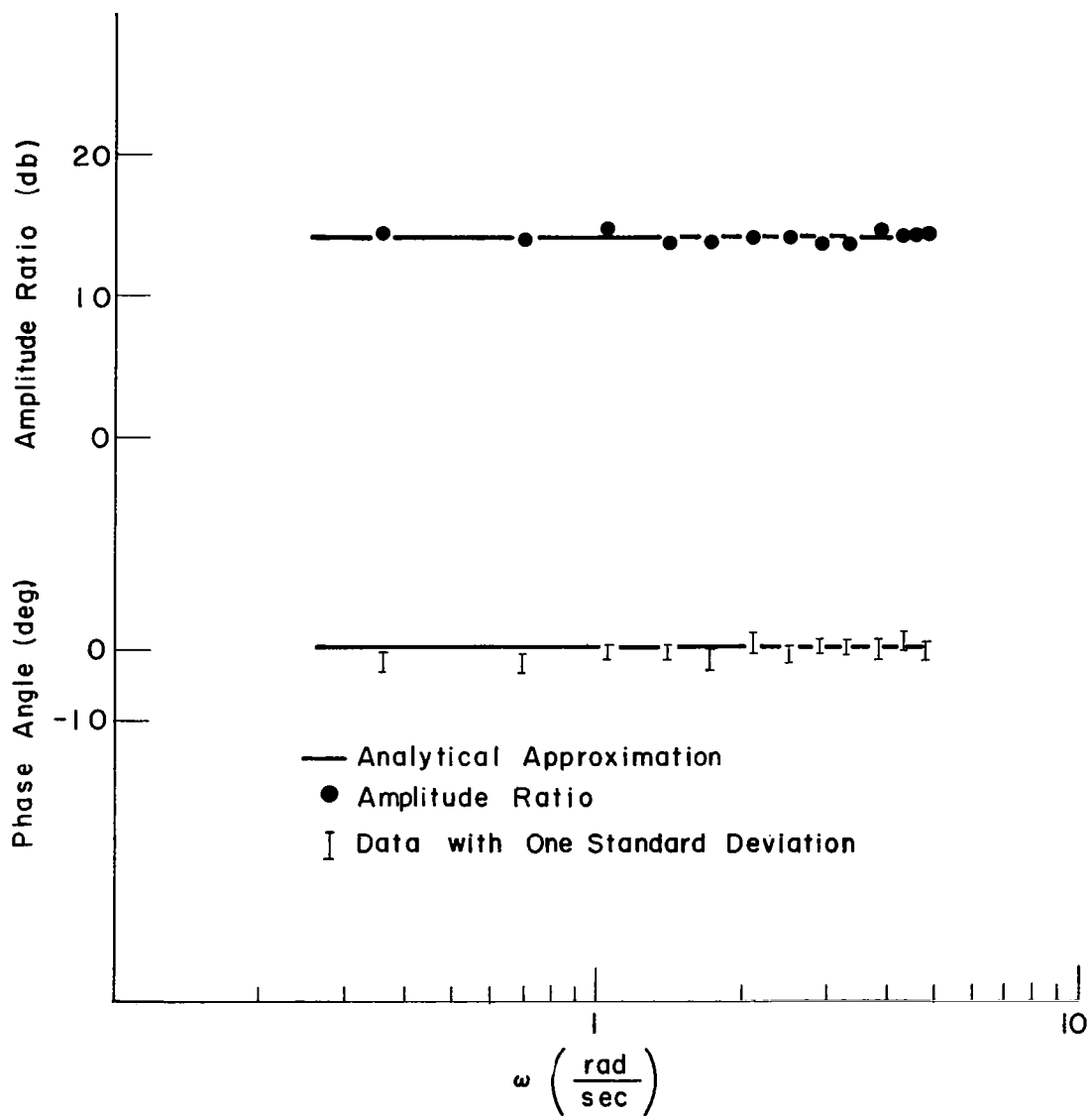


Fig. 6.4 Describing Function of the Human Operator in Motion Mode. Rotation with Respect to the Gravity Vector

CHAPTER VII

VISUAL AND VESTIBULAR CONTROL OF AN UNSTABLE SYSTEM

In Chapter VI, simple manual control systems were investigated and "describing functions" for the human operator were presented. There, a substantial difference in performance of the operator was found when systems with visual input only were compared with systems with motion inputs or visual and motion inputs. For identical system parameters, the describing function of the operator measured with motion inputs exhibits large reduction of phase lag relative to the characteristics obtained with a fixed base simulation. This observation, which is an indication of the compensation capabilities of the human, was attributed mainly to the rate information the operator receives from his vestibular sensors. The results, although convincing, did not establish quantitative comparison of the lead compensation abilities of the operator related to the nature of inputs he perceives.

By experimenting with control situations involving unstable systems, in which the operator had visual or motion inputs or both, it was hoped to isolate and identify his compensation characteristics.

7.1 CONTROL OF AN UNSTABLE SYSTEM

7.1.1 Method

The control of the deviation from the vertical of a moving base flight simulator (see Appendix A) driven about its roll axis, simulated a single-axis compensatory tracking task for the human operator.

Three control situations, 1) visual, 2) motion, or 3) combined visual and motion, were studied for identical external loop characteristics as illustrated in Fig. 7.1. For the visual experiments the subject was outside the simulator, seated 10 feet away from it. A reference marker, mounted horizontally on the moving cab, aided the operator in judging any tilt of it with respect to the laboratory background. For the motion experiments, the operator was forced to utilize the sensing capabilities of the vestibular system and the pressure sensing tactile sensors to control orientation to the vertical. The subject was seated in the moving cab, strapped to his chair, with head supported and fixed in order to control inputs to the vestibular mechanism. The simulator cab was covered with a light proof hood, no instruments were used inside the cab and the interior was not lighted. The subject was seated and supported in a similar manner for the combined visual and motion cues study except that the cab hood was removed. Crossed horizontal and vertical reference lines were taped to the laboratory wall facing the simulator, at subject's eye level and at a distance of 10 feet.

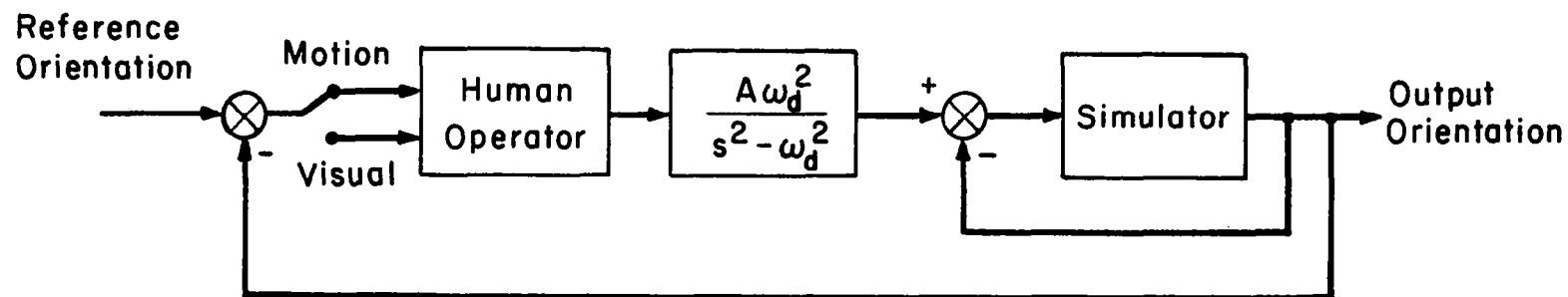


Fig. 7I Control of Inverted Pendulum with Visual or Motion Feedback

The reference orientation was the vertical, and the operator was instructed to maintain this orientation for all the experiments. No external input signal (disturbance) was fed into the control loop. Control of self-induced errors with unstable controlled elements imposes sufficient difficulty and challenge for the operator.

The simulated controlled element was of the form

$$\frac{A\omega_d^2}{s^2 - \omega_d^2}$$

representing an undamped inverted pendulum. ω_d^2 took the discrete values of 0.5, 1, 2, 3, 4, and 5, where higher ω_d represents a more difficult element to control because of faster divergence of the system. The gain A was set at the constant value $A = 2$, for all experiments. The operator exercised acceleration control on the system with a light, spring-restrained stick. The control stick was linear with maximum travel of $\pm 45^\circ/\text{sec}^2$, thus having maximum specific torque capability $(A\omega_d^2)$ in the range of $\pm 45^\circ/\text{sec}^2$ up to $\pm 450^\circ/\text{sec}^2$ depending upon the system characteristics; greater control power associated with more divergent systems.

The flight simulator was driven as a position servo about its roll axis. Its dynamics up to one cycle per second can be described as a time delay ($e^{-0.1s}$) and are neglected for the purpose of this investigation.

Three subjects with previous tracking experience were used in these experimental series. They were trained in control of the simulator in the visual and motion mode for one half hour during which their performance was monitored. After reaching a relative plateau of proficiency, five scoring runs for each value of ω_d^2 in ascending order, were recorded. The runs were 90 seconds long, taken after a 30-second "warm-up" period. Resting periods of at least 90 seconds were allowed between consecutive runs.

7.1.2 Results

The simulator roll angle (deviation from the vertical) and control stick output (human operator response) for each run were recorded on magnetic tape and paper recorder. Inspection of this data reveals some obvious characteristics of the control loop.

The tracking record shown in Fig. 7.2 was taken for visual control tracking conditions at $\omega_d^2 = 2$. Changes in the divergence frequency or tracking conditions primarily affect the error amplitude.

The deviation from the vertical, shown as the upper trace of the recording, points to the fact that the operator maintains good control of the system. No uncontrollable divergence is found, and when excess deviation develops, the system can be brought under control by the operator. The low frequency oscillations observed are characteristic for the loop. This system behavior is sufficient evidence that

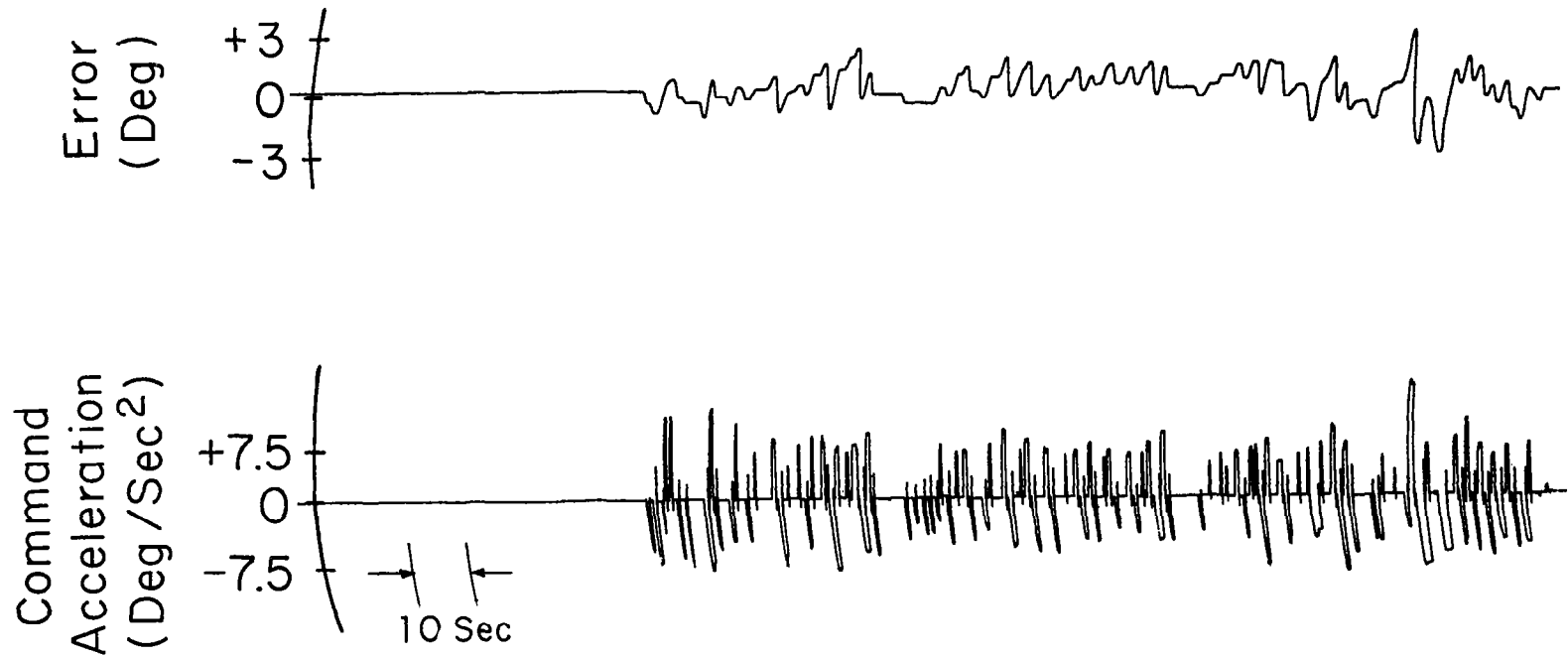


Fig.7.2 Time-Record -Control of Inverted Pendulum Showing Bang-Bang Use of Linear Controller

the human operator develops compensation needed to stabilize the loop.

The operator's control movements represented by the command accelerations shown in the lower tracing of the record are of the bang-bang type, with no indication of fine corrections around the zero level, despite his exercise of control through a linear stick. This response of the operator is of distinct non-linear nature resembling the output of a relay or 3-mode switch. The total stick travel is kept approximately constant with controlled element variations, indicating a linearly increasing specific torque related to ω_d^2 .

Examination of the tracking records is rather revealing. The lead compensation capability of the operator is well demonstrated by the stability of the closed loop. It is also noted that the human operator is adapting to the difficult control task by resorting to a fairly non-linear output. The on-off or bang-bang response of the operator under these conditions can be considered an independent feature of his, rather than being forced to use it by design of the controller.

7.2 AN ON-OFF MODEL FOR THE HUMAN OPERATOR

The analog description of the human operator should preserve the nature of his control mode (linear, bang-bang) along with a presentation of equivalent electro-mechanical networks. By virtue of this method, engineering analysis

of loop behavior will resemble the actual control situation in overall performance and in addition will allow simulation of expected human response.

In view of the control loop characteristics just discussed, an on-off model for the human operator might be considered. Since the major contribution of the operator is the provision of lead equalization, a model such as given in Fig. 7.3 may be a sufficient description of the human operator. Here he is assigned a reaction delay, and permitted to generate lead, but is restricted to three output levels. A remnant term $N(s)$ accounts for uncertainty in triggering of the switch. With no disturbance, the on-off control model and second order controlled element are amenable to analysis in the phase plane.^{144,68} The representation is one of a controller whose nature is known, but its associated characteristics (rate compensation and delay time) have to be determined. This information is provided by the switching lines, the locus of roll angle and roll angular velocity (error and error rate) at which the operator would switch polarity of his command.

To use phase plane for data analysis, the recorded data for each run was converted to digital form and processed in an IBM 7094 computer where smoothed error (e) and error rate (\dot{e}) were computed. An experimental trajectory on the $e-\dot{e}$ plane, picking up at the point $(-3.8, 0)$ and lasting for approximately 10 seconds, is shown in Fig. 7.4 Notice the general shape of the trajectories centered about

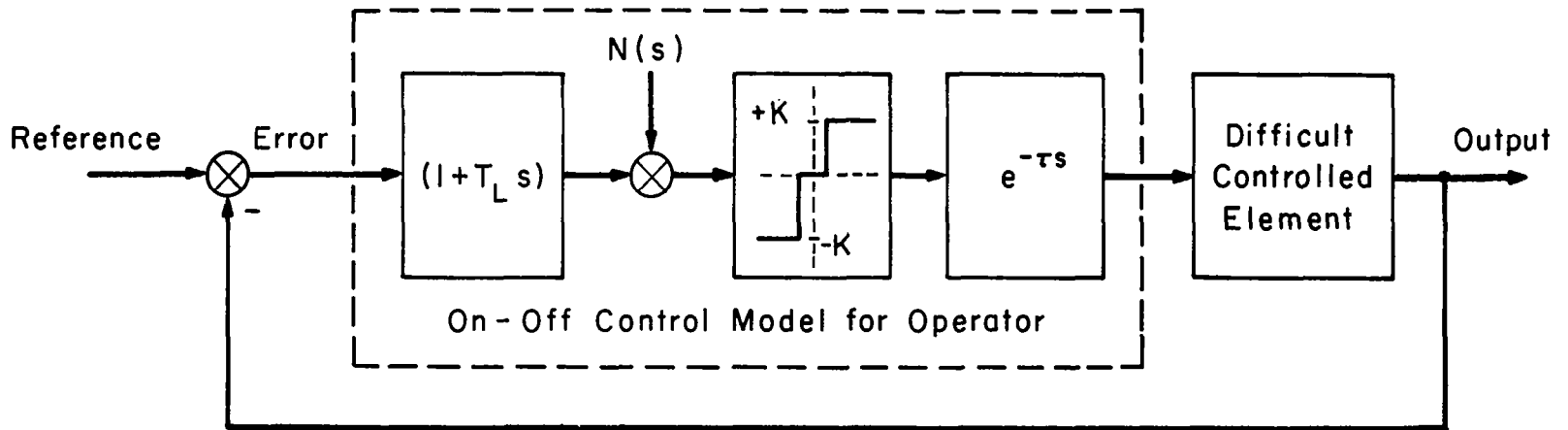


Fig. 7.3 Proposed On-Off Control Model for Human Operator in "Difficult" Control Task

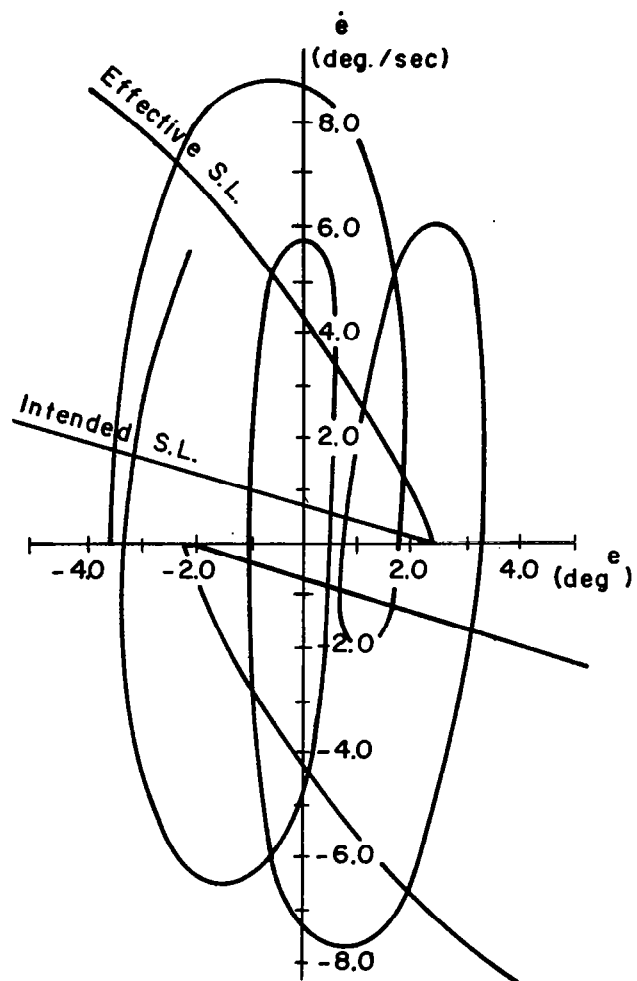


Fig.74 Experimental Trajectory and
Switching Lines

regions near the origin and leading to a limit cycle type of behavior.

After computing the error and error rate, the computer searched the record of the stick position for sign changes and defined those as switching points. It was found that only a small percentage of transitions were to the zero level (6 per cent); also the average time for completion of a transition is of the order of 0.4 sec. On the basis of these findings, two assumptions were made for future analysis: 1) the human operator behaves like an ideal relay, and 2) his characteristics are described by a set of intended switching lines.

An intended switching line is a locus representing switching points where the operator intended to switch (about 0.4 sec before the actual torque reversal). If his control activation were that of an ideal relay, the control torques would have reversed along this locus. The intended switching lines together with the specific torque levels completely define the model for the human operator in this control loop.

A least squares curve fit was used to approximate regression lines in the second and fourth quadrant for the intended switching line coordinates.¹⁴¹ First order and second order polynomials of e and \dot{e} were fitted, with the criteria for acceptance based on the value of χ^2 (chi square) distribution. With significance of one per cent or better, the straight line regression was found to be sufficient repre-

sentation of the intended switching lines. The parameters of the intended switching line, its slope and intercept with the \dot{e} axis, are significant in terms of the proposed on-off model for the human operator. For controlled element dynamics of pure inertia, the switching lines equation is:⁶⁸

$$\dot{e} = - \frac{e}{T_L - \tau} + AK\omega_d^2 \frac{\tau(2T_L - \tau)}{2(T_L - \tau)} \quad (7.1)$$

where T_L is the lead equalization time constant and τ is the dead time delay. The use of this equation is a justified approximation since the dynamics of the loop for this series of experiments resemble those of a pure inertia when small roll angles are considered. The intended switching lines are the straight lines shown in Fig. 7.4. From these intended switching lines one observes that the operator was indeed using lead compensation and that a dead time delay breaks the switching line into two segments which do not pass through the origin. However, calculation of theoretical trajectories based on a switching model for the operator requires the use of the effective switching lines rather than the intended switching just discussed. The effective switching lines are shown in Fig. 7.5 and are computed from the intended switching lines by advancing the switching points along the phase portrait by 0.4 sec from the intended switching lines previously calculated. This

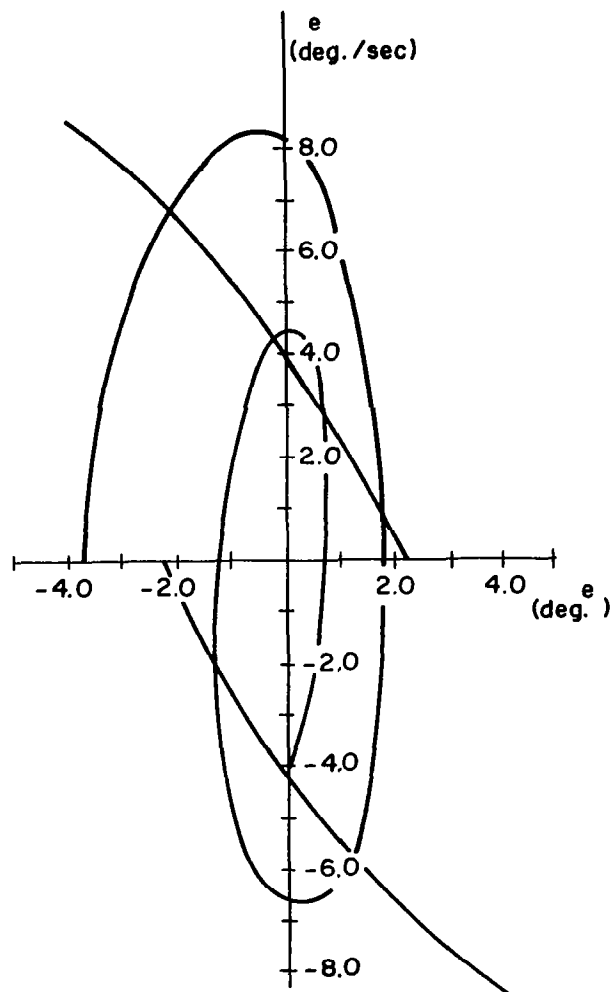


Fig. 7.5 Calculated Phase Portrait and Switching Lines

advance represents the average distance the system has progressed along its trajectory from the time of the beginning of a control transition until this reversal was completed. A theoretical trajectory starting at the point $(-3.8, 0)$ as in the experimental trajectory of Fig. 7.4, and calculated on the basis of the effective switching lines, is shown, superimposed on these switching lines in the phase plane, of Fig. 7.5. The resemblance of the two trajectories, both in size of the approximate limit cycle and general shape, provides encouraging support for the use of an on-off model for the human operator in this control situation.

Note the conceptual difference between the switching lines. The intended switching line is characteristic of the human operator and his model representation. It specifies the lead equalization time constant the pilot will utilize in a given control situation. On the other hand, the effective switching line is a curve dependent upon the controlled element and the operator's control actions. Due to an average lag in executing his decision to reverse polarity of control, the pilot will allow the system to travel up to the effective switching line before a complete torque reversal is achieved. It is obvious then that the locus of effective switching points will vary with the dynamics of the controlled system.

The statistically fitted lines can be compared to the theoretical equation (Eq. (7.1)) and values of lead time constant and dead time delay are evaluated.

The mean slope and the mean intercept for each ω_d and each experimental condition were computed and tested for one per cent significance by the difference of matched pairs test.^{140,141} These statistical tests were evaluated for different values of ω_d under the same tracking conditions (visual, motion, or combined) and for similar values of ω_d among the three classes of control. The slope of the intended switching line, $-\frac{1}{T_L - \tau}$, is an indication of the amount of lead equalization introduced by the human operator; the smaller the slope, the larger the phase lead. The results of this computation are given in Fig. 7.6. The value of τ computed from Eq. (7.1) was

$$0.095 \leq \tau \leq 0.11$$

for all the conditions tested in this series.

The intended lead equalization provided by the human operator under various sensing combinations is important in its absolute magnitude as well as its relative values. For visual control, the trend is for less lead compensation with increasing ω_d (difficulty of control). On the contrary, the vestibular-tactile control produces more and more lead, as needed by the system for an increase in ω_d . For relatively easy controlled elements ($\omega_d < 1$) the vestibular-tactile lead term is less than that found with pure visual control. It might be expected, then, that combined visual-motion control will be the best combination of sensing capabilities both for low and high values of ω_d as is generally found in Fig. 7.6

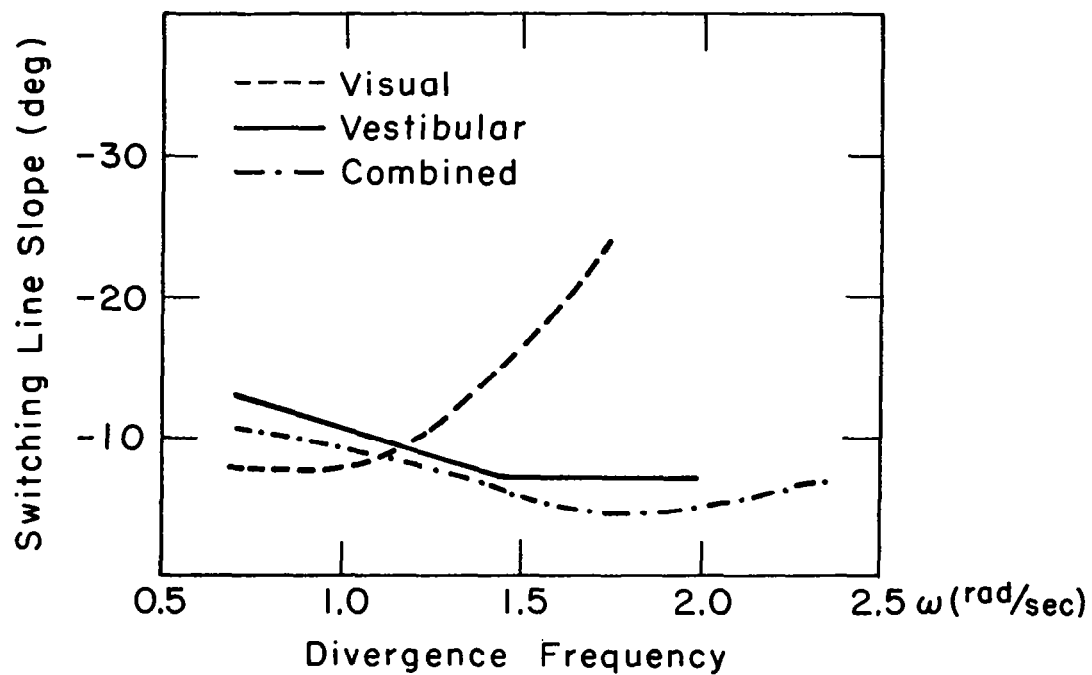


Fig. 7.6 Switching Line Slope for Control of Inverted Pendulum

The lead equalization, aside from its requirement for stabilization, is also an indication of the expected performance of the overall loop. If rms error is chosen as the performance criterion, the control with motion sensing should be superior to the visual one for difficult control situations and the combined control would be the best for the whole range of divergence frequencies. The results presented in Fig. 7.7 closely support the lead equalization data. It is found that for every control situation, the rms error increases with divergence frequency due to the increasing difficulty of the control task. The rms errors recorded with visual control exceed by far those taken for motion tracking, when the divergence frequency is increased beyond $\omega_d = 1$. With combined sensing, the human operator maintains somewhat lower rms error than that scored with the vestibular sensors only, and is able to extend the controllable range of divergence frequency to $\omega_d = 2.25$.

The information on the human operator provided by the on-off model is useful in determining the overall loop stability and behavior. In Fig. 7.2 a limit cycle of $1/4$ to $1/3$ cps with rather constant amplitude of about 1° is observed. The theoretical trajectory in Fig. 7.5, computed for the same experimental conditions (visual tracking, $\omega_d=2$) points to a limit cycle with parameters similar to the measured ones. The limits of control reached by the operator at high ω_d are predictable too on the phase plane. For this unstable region, large portions of the effective

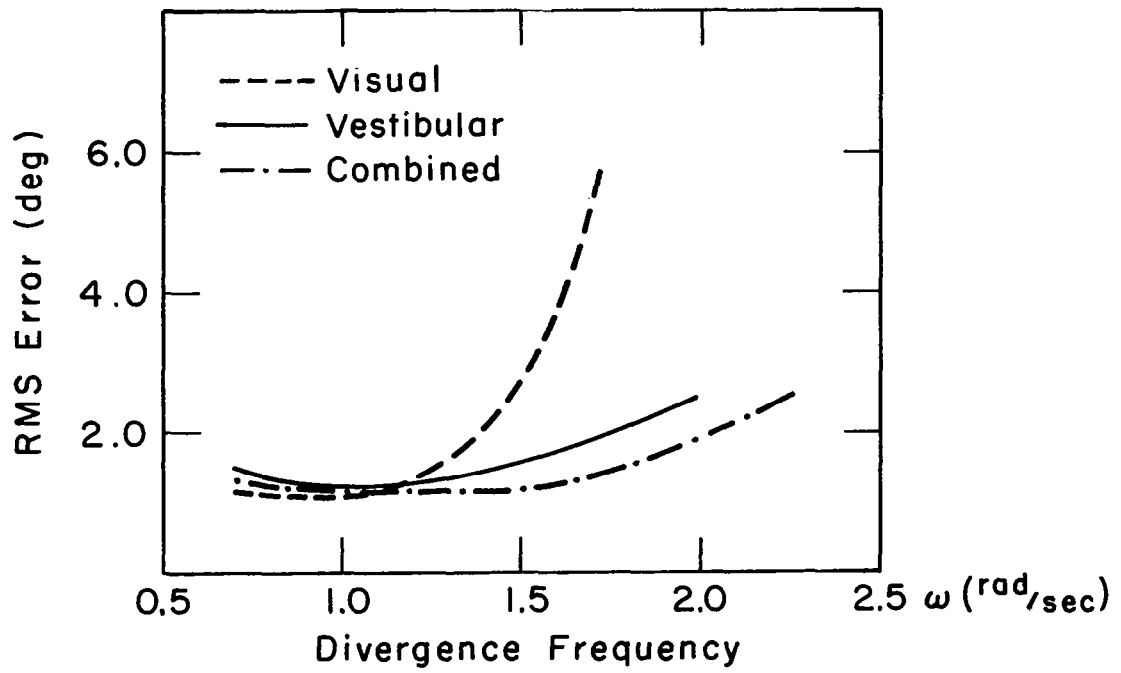


Fig. 7.7 RMS Error for Control of Inverted Pendulum

switching lines lie in the first and third quadrant; thus the operator is adding energy to the system contrary to the requirements.

7.3 DISCUSSION

The series of experiments just described were initiated with the specific intention of demonstrating the contribution of man's motion sensing abilities in control of vehicle motion. The acceleration sensors of the vestibular system have been shown previously to be a channel of information with a resolution depending upon the thresholds of perception. Therefore, the lead compensation capabilities with vestibular sensing should be superior to those of the visual system in which direct sensing of velocity is a secondary function.

The experimental results support the observation about the role of the vestibular sensors in control situations where the lead compensation is essential for stable closed loop performance. The rms error, as a single scoring indicator, is also a significant description of the control utilization of the vestibular sensors by the operator. For a system with low divergence, the response is sluggish and errors often do not exceed the threshold of the human sensors. The system error for these conditions will be large for motion sensing, compared with the fine resolution capabilities of visual control. With difficult control tasks, where adequate rate information is required, the system

response falls well within the frequency range of the vestibular sensors and the operator's control is improved as reflected by the values of the rms errors.

The experimental results merit some comments on fixed base versus moving base simulation. It was shown here that the visual system is inadequate for vehicle control in orientation tasks with high lead compensation requirements. These systems are highly oscillatory, they diverge fast and in general are controlled, within a region of marginal stability, to a limit cycle. Stability cannot be achieved under those conditions without adequate rate information. Consequently, control quality deteriorates rapidly whenever the human operator is deprived of his natural sensation of motion. According to the experimental results presented here, it can be stated that for missions where lead compensation is a needed control characteristic of the operator, moving base simulation will prove to be an easier task and closer to reality than fixed base simulation.

The proposed on-off model for the human operator and its analysis in the phase plane demonstrate the potential of this approach for a wide class of control situations usually referred to as limits of control of the operator. The controlled elements in these situations are generally ones for which fine minor control about the reference is either not possible or not necessary. Such systems will typically exhibit a steady state limit cycle and the performance of the closed loop is often determined by the

amplitude and frequency of the terminal limit cycle. When a human operator is called upon to control such an element, his task will correspond to that of establishing a limit cycle which keeps the error within allowable bounds. It is not surprising therefore to find that the human uses a bang-bang mode in order to achieve tight control of the system while permitting some inevitable limit cycle. For the type of system discussed in these experiments, the limit cycle can result from the subject's inability to sense the true reference orientation accurately, as well as from his inability to make control corrections without any delay. The analytic approach described here indicates how the system performance may be predicted on the basis of an on-off model for the operator and its associated switching lines on the phase plane.

CHAPTER VIII

CONCLUSIONS

The object of this thesis was to investigate the control engineering characteristics of the vestibular system and the use of motion information by the human operator. This was an effort to extend the mathematical models of the operator to include the description of the role of the vestibular sensors in dynamic space orientation.

A general model of the human operator distinguished among sensors, control and compensation, and output. The thesis concentrated both on some "components" of the human and some of his system characteristics. At the sensory end, mathematical models were presented for the characteristics of the vestibular system and the eye movement control system. In control and compensation, the man's non-linear performance and his control abilities with compatible and incompatible multiple inputs were examined. Finally, in closing the loop through the dynamics of the controlled vehicle, the transfer functions of the operator with and without motion inputs were measured.

8.1 THE VESTIBULAR SYSTEM

The investigation of the vestibular system was an effort to establish control descriptions of its sensors. The dynamic characteristics of the vestibular sensors, the semicircular canals and the otoliths were represented by simple mathematical models. Spatial orientation, as sensed by the vestibular system, was analyzed with respect to objective motions of the vehicle.

The semicircular canals are known to be heavily damped, angular accelerometers. Consequently, they respond as angular velocity meters over the frequency range from 0.02 cps to about 1.5 cps. The thresholds of perception of angular acceleration are $0.14^\circ/\text{sec}^2$ for rotation about the Y_h (Yaw) axis and $0.5^\circ/\text{sec}^2$ about the X_h (Roll) axis. A similar value of threshold ($0.5^\circ/\text{sec}^2$) is presumably valid for rotation about the Z_h (Pitch) axis.

The otoliths are planar linear accelerometers sensitive to the specific force applied to the skull. Statically, they measure head orientation with respect to the apparent vertical quite accurately. This sense of orientation to the vertical is modified by habituation during prolonged stay in tilted positions. Dynamically, the otoliths function as linear velocity meters for motions with frequencies within the range 0.016 cps to 0.25 cps. The threshold of perception of linear accelerations is about 0.005g in the plane of the otoliths.

The mathematical models for the semicircular canals and the otoliths are summarized in Fig. 8.1. Each sensor model consists of a linear second order portion followed by a non-linearity corresponding to the threshold of perception. This overall model of the vestibular system is an engineering description of the motion information perceived by the human. A "specification" summary for the vestibular sensors is given in Table 8-1.

8.2 THE EYE MOVEMENT CONTROL SYSTEM

Eye movements are controlled with respect to a target or reference by a multi-input control system. A program of experiments showed that the horizontal eye movement control system stabilized the eye in the presence of body and head rotations. This stabilization is within $\pm 0.5^\circ$ for frequencies up to 2 cps. Three sensory systems, the vestibular system, the neck proprioceptors and the eye itself (by visual tracking), were considered to participate in the control system. Compensatory eye movements were identified in response to stimulation of the neck proprioceptors and described by a lag-lead transfer function. The compensatory eye movements resulting from neck proprioception and those attributed to the vestibular system were found to obey superposition, indicating linearity of the control system. The control system is shown to receive rate information from the neck proprioceptors at low frequencies (up to 0.1 cps) and from the vestibular system in an overlapping intermediate range of frequencies (0.02 cps to 4.0 cps).

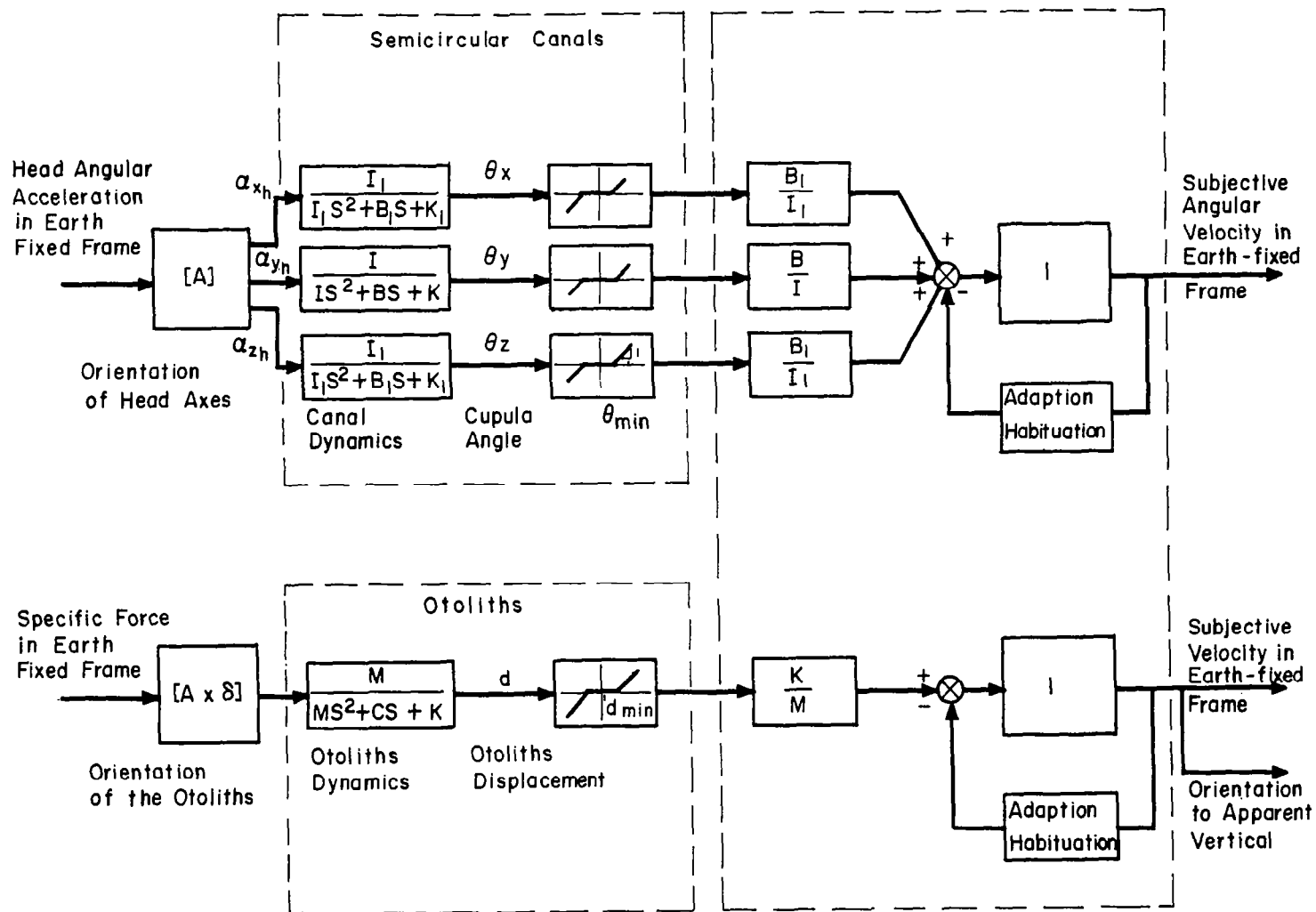


Fig. 8.1 Block Diagram of the Vestibular System

Table 8-I
The Vestibular System

Sensor	Semicircular Canals	Utricle
Input Variable	Angular Acceleration	Specific force in the Plane of the Otolith
Sensitive Axis	Sensitive to Angular Accelerations about an Axis Perpendicular to the Plane of the Canals	Sensitive to Accelerations in the Plane of the Otolith
Output Variable	Subjective Sensation of Angular Velocity; Vestibular Nystagmus	Subjective Sensation of Tilt and Linear Velocity; Counterrolling Eye Movements
Sensor Transfer Function	$H(s) = \frac{\text{subjective angular velocity}}{\text{input angular velocity}}$ <p>Rotation about the Sagittal Head Axis X_h (Roll)</p> $H_{x_h}(s) = \frac{7s}{(7s+1)(0.1s+1)}$ <p>Rotation about the Vertical Head Axis Y_h (Yaw)</p> $H_{z_h}(s) = \frac{10s}{(10s+1)(0.1s+1)}$ <p>Rotation about the Lateral Head Axis Z_h (Pitch)</p> $H_{z_h}(s) = \frac{7s}{(7s+1)(0.1s+1)}$	$\frac{\text{subjective velocity}}{\text{input velocity}} = \frac{Ks}{(10s+1)(0.66s+1)}$
Threshold of Perception	<p>Angular Acceleration</p> $\alpha_{X_h} = 0.5^\circ / \text{sec}^2$ $\alpha_{Y_h} = 0.14^\circ / \text{sec}^2$ $\alpha_{Z_h} = 0.5^\circ / \text{sec}^2$	<p>Acceleration in the Plane of the Otolith</p> $a_0 = 0.005g$

8.3 CONTROL OF VEHICLE ORIENTATION

The role of motion inputs to the human operator was investigated in simple vehicle orientation control systems. The control characteristics of the human in stable and unstable systems were compared under three modes of operation: visual, motion, and combined. The task was single axis compensatory orientation of a vehicle simulated by a single integration, reportedly the optimum dynamics for the human operator to control. Vehicle control to a reference orientation, by motion cues only, was found impossible with the sole exception of control of orientation to the vertical. In general, the phase lag attributed to the operator was significantly reduced when controlling with motion cues or combined visual-motion inputs, compared to control with visual input only.

The lead compensation the human can generate was also measured in a difficult compensatory task controlling an unstable system. The operator's control characteristics in this loop were distinctly non-linear. A bang-bang model of the operator was proposed and analyzed in the phase plane and used to predict experimentally determined limit cycles.

Performance of the operator with motion cues shows significant improvement over control situations with visual input only. Motion cues extend his ability to stabilize unstable systems near the limit of controllability.

In summary, the vestibular sensors play a very significant part in providing rate information to the human operator in a closed loop system of vehicle orientation.

APPENDIX A

ANY-TWO-DEGREES OF ANGULAR FREEDOM MOTION SIMULATOR

The NE-2 motion simulator, shown in Fig. A.1, was built by Ames Research Center, NASA. The moving cab of the simulator is mounted on two gimbals. The orientation of the gimbals and the mounting of the cab inside the gimbals may be varied to allow simultaneous rotation of the cab about any two perpendicular axes. When operated as a single axis motion simulator, the inactive gimbal is locked. Each gimbal of the simulator is driven as a D.C. position servomechanism by an electric amplidyne-motor set. The motion simulator was modified at the Man-Vehicle Control Laboratory to adapt it to the required angular acceleration levels for studies of the vestibular system.

The motion characteristics of the simulator in the Roll-Yaw mode are:

Maximum rotation - Yaw - $\pm 35^{\circ}$

Roll - $\pm 360^{\circ}$

Maximum angular velocity - Yaw - 2 rad/sec

Roll - 8 rad/sec

Maximum angular acceleration - Yaw - 10 rad/sec²

Roll - 15 rad/sec²

Maximum angular acceleration noise -

Yaw - $0.1^{\circ}/\text{sec}^2$

Roll - $0.05^{\circ}/\text{sec}^2$

The dynamics of the simulator can be approximated to a pure dead time delay, $e^{-0.1s}$ in Roll and $e^{-0.15s}$ in Yaw. The bandwidth of both servo loops is flat to 2 cps.

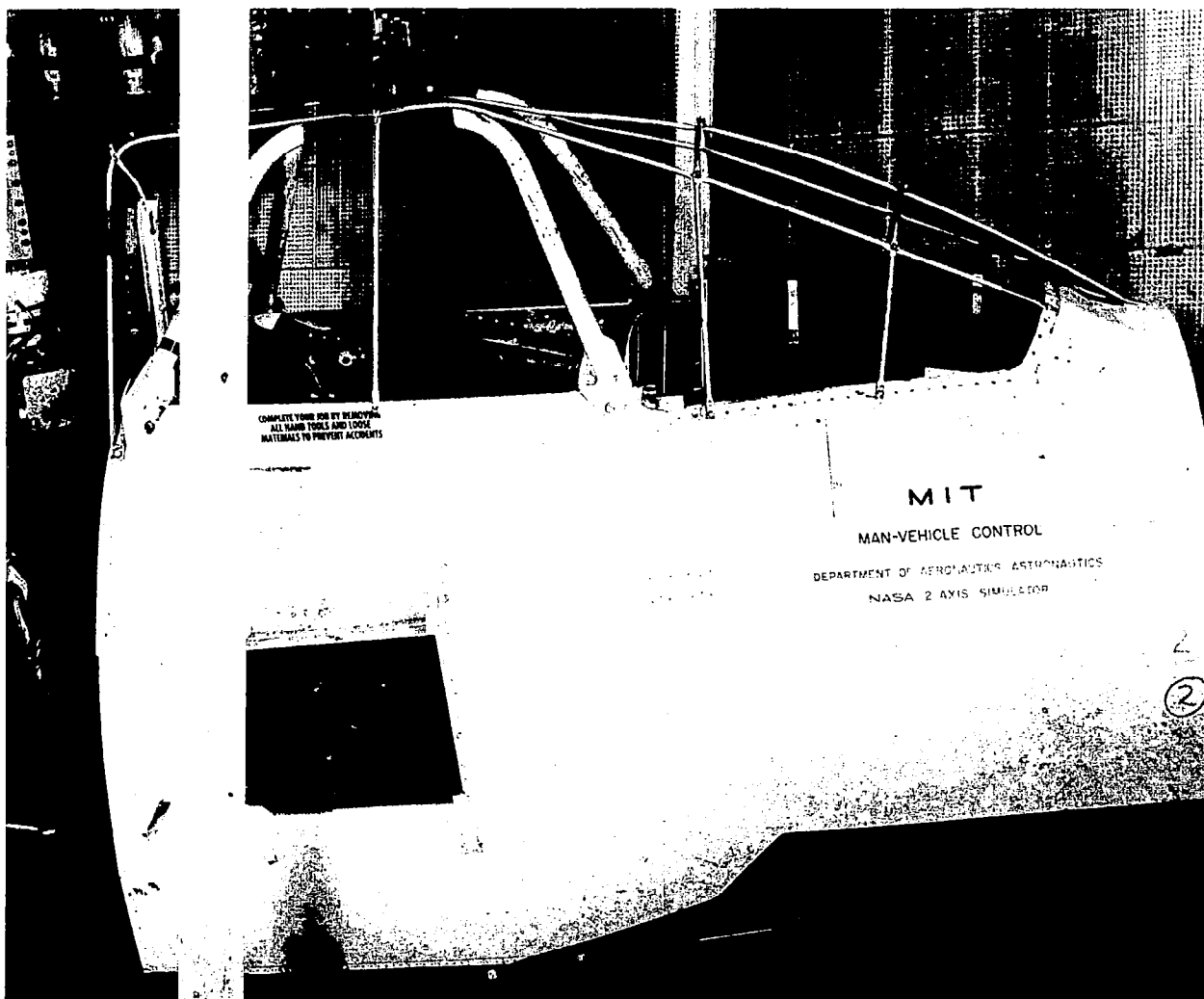


Fig. A.1 The NE-2 Motion Simulator in the Yaw-Roll Mode.

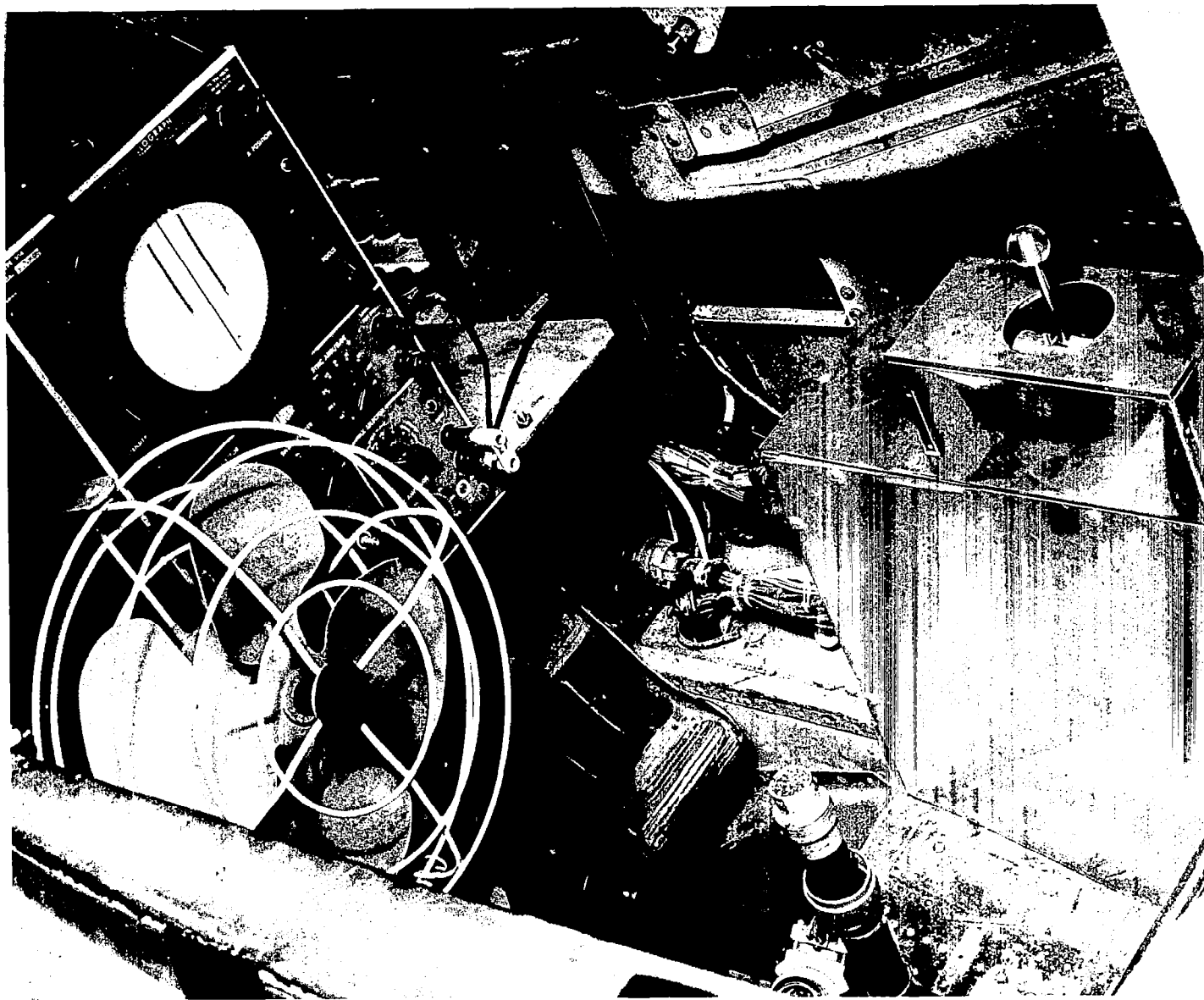


Fig. A.2 The Display Scope and the Control Stick Used with the NE-2 Motion Simulator.

APPENDIX B

LINEAR MOTION SIMULATOR

The linear motion simulator, built at M.I.T.,¹⁵² is a carriage which can be driven along a 32 foot horizontal track. The carriage has four rubber wheels running on the concrete laboratory floor. Its lateral movement is reduced by two teflon runners, which straddle a guide rail. The carriage is driven along the track with a spring-loaded continuous steel cable. The linear motion simulator is driven as a position servomechanism by a hydraulic valve energizing a hydraulic motor.

The performance parameters of the simulator are:

Maximum travel - 32 feet

Maximum constant acceleration - 0.3g

Minimum constant acceleration - 0.003g to 0.005g

Bandwidth - D.C. flat to 0.9 cps

Dynamics - approximately $e^{-0.15s}$

Lateral and vertical vibrations of the carriage along the track do not exceed 0.01g.

The carriage is covered with a light-proof cardboard structure. The subject is seated on a chair which can be adjusted from 90° sitting to supine.

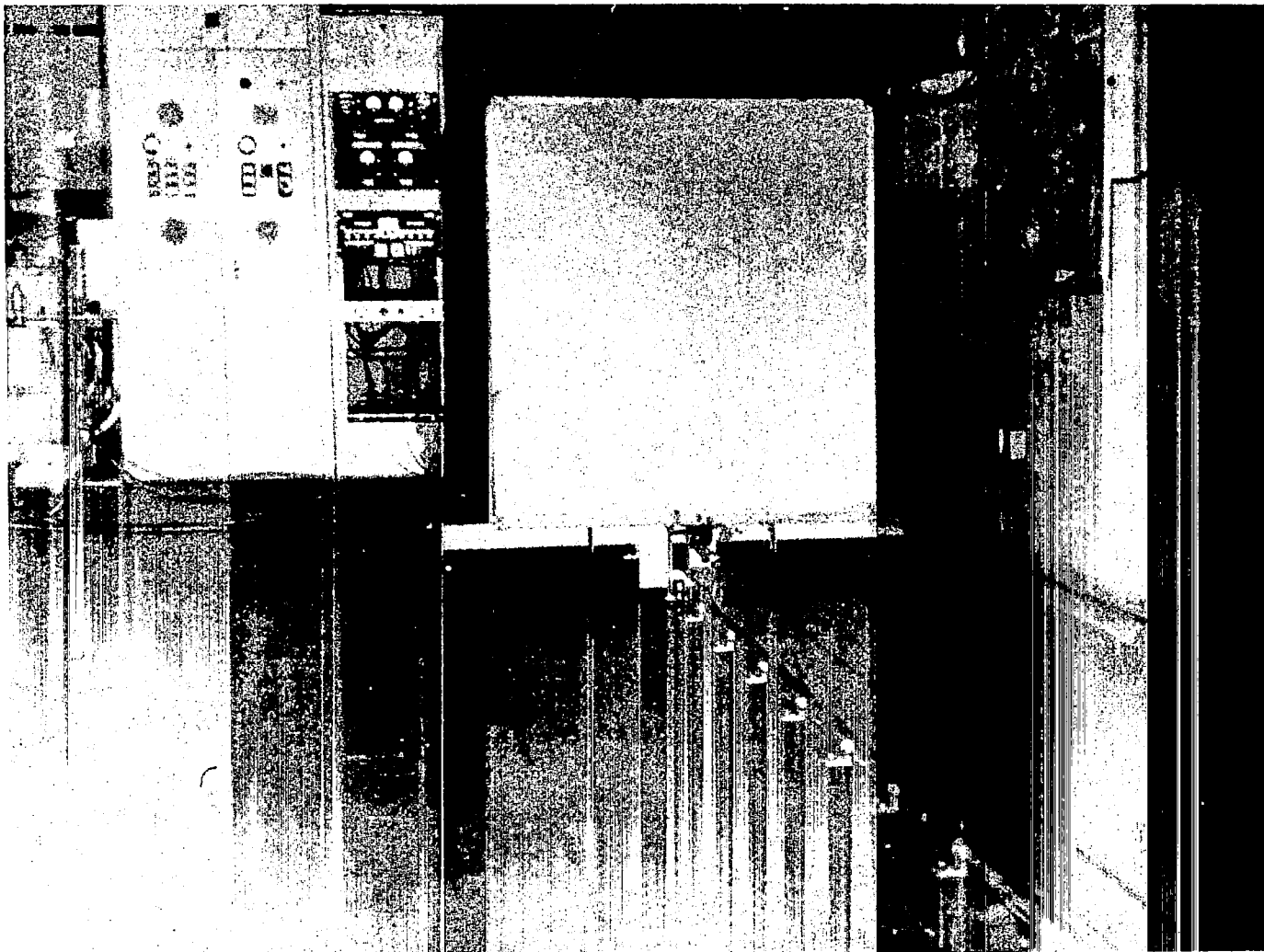


Fig. B.1 The Linear Motion Simulator on Its Track.

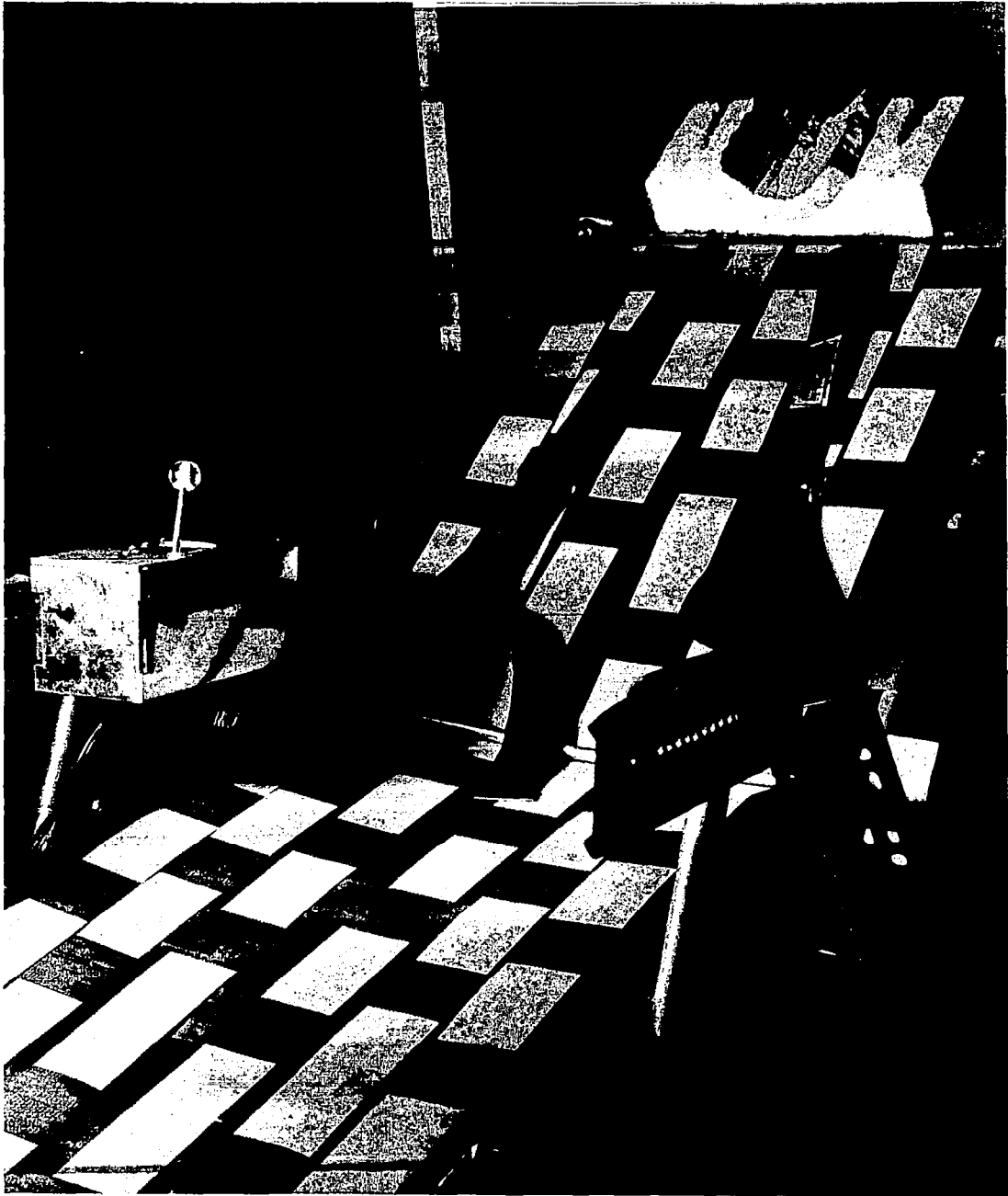


Fig. B.2 The Interior of the Linear Motion Simulator.

APPENDIX C

ANATOMY OF THE NECK - ROTATION⁷⁶

Rotation of the head with respect to the trunk is a coordinated effort of a number of joints and muscles. The head rotates about a vertical axis on a pivot joint. The dens of the axis vertebrae are a pivot around which the atlas rotates. These are the atlanto-axial joints which form a sealed capsule containing a viscous fluid called synovia. The atlanto-axial joints are three: 1) the two lateral atlanto-axial joints together with the ligamentum florum in back and part of the longitudinal ligament in front, form the joint cavity which encloses the space between the atlas and the axis vertebrae; 2) the median atlanto-axial joint is the pivot joint between the dens of the axis and the ring in the atlas.

Simultaneous movement of all the three atlanto-axial joints must occur to allow the rotation of the atlas and the skull with it upon the axis. The angular travel of the head is limited to about 150° . The muscles which produce these movements are the Obliquus capitis inferior, the Rectus capitis posterior major and the Splenius capitis of one side, acting with the Sternocleidomastoid of the

other side. Note that rotational motion of the head is induced by three muscles running along the back of the neck, counterbalanced by the Sternocleidomastoid muscle which contours the side of the neck. The nerves activating the muscles involved in rotation of the head branch from the cervical plexus, and are believed to be for proprioception.

APPENDIX D

MEASUREMENT OF DESCRIBING FUNCTIONS FOR THE HUMAN OPERATOR

The characteristics of the human operator in simple compensatory manual control systems can be described by a quasi linear describing function.¹²⁸ This approach is based on the notion that the operator's performance reaches stationary after learning the control task. Since the inputs to the system are in general random of "random appearing functions", the human cannot predict their time pattern. Consequently his characteristics in these manual control systems are assumed to be stationary, when measured over a limited period of operation.

The quasi-linear control characteristics of the human operator consist of: (1) a describing function, linearly correlated with the system input; and (2) a remnant which is uncorrelated with the system input. This description of the operator's performance in compensatory control systems is one generally used and is analyzed extensively by McRuer and Krendel.

The most common techniques of describing and analyzing stationary signals are by correlation functions and power spectral densities. The power spectral densities which are

measurable in a compensatory manual control system are the following:

$\Phi_{11}(\omega)$ = input power spectral density

$\Phi_{cc}(\omega)$ = operator's response power spectral density

$\Phi_{1e}(\omega)$ = cross power spectral density of input and system error

$\Phi_{1c}(\omega)$ = cross power spectral density of input and operator's response

Since by definition the remnant is uncorrelated with the system input, one obtains the following equations:

$$\Phi_{1e}(\omega) = \frac{1}{1 + Y_p(j\omega)Y_c(j\omega)} \Phi_{11}(\omega) \quad (D.1)$$

$$\Phi_{1c}(\omega) = \frac{Y_p(j\omega)}{1 + Y_p(j\omega)Y_c(j\omega)} \Phi_{11}(\omega) \quad (D.2)$$

where $Y_p(j\omega)$ = the describing function of the human operator, and

$Y_c(j\omega)$ = controlled element transfer function.

A division of Eq. (D.2) by Eq. (D.1) will yield the describing function of the human operator as:

$$Y_p(j\omega) = \frac{\Phi_{1c}(\omega)}{\Phi_{1e}(\omega)} \quad (D.3)$$

Note the difference between the method of measuring the operator's describing function here and the standard

evaluation of transfer functions in linear systems. If the human did not inject a remnant term $N_o(j\omega)$, his transfer function could be measured as:

$$Y_p(j\omega) = \frac{\Phi_{ec}(\omega)}{\Phi_{ee}(\omega)} \quad (D.4)$$

where Φ_{ee} = system error spectral density and

Φ_{ec} = cross spectral density of system error and operator's response.

However, both these spectral densities contain the effect of the remnant output. Thus, they are not valid estimates of the describing function. This difficulty is overcome by cross-correlating the signals in the system with the input, a process which eliminates the effect of the uncorrelated remnant.

From the block diagram of Fig. 6.1 one obtains the following relations:

$$C(j\omega) = \frac{Y_p(j\omega)}{1+Y_p(j\omega)Y_c(j\omega)} I(j\omega) + \frac{N_c(j\omega)}{1+Y_p(j\omega)Y_c(j\omega)} \quad (D.5)$$

$$\Phi_{cc}(\omega) = \left| \frac{Y_p}{1+Y_p Y_c} \right|^2 \Phi_{11}(\omega) + \left| \frac{1}{1+Y_p Y_c} \right|^2 \Phi_{nn_c} \quad (D.6)$$

$$\Phi_{nn}(\omega) = \left| \frac{1}{1+Y_p Y_c} \right|^2 \Phi_{nn_c}(\omega) \quad (D.7)$$

$$\Phi_{cc}(\omega) = \left| \frac{Y_p}{1 + Y_p Y_c} \right|^2 \Phi_{11}(\omega) + \Phi_{nn}(\omega) \quad (D.8)$$

where $\Phi_{nn_c}(\omega)$ = remnant power spectral density at the operator's output

$\Phi_{nn}(\omega)$ = remnant power spectral density expressed as a closed loop quantity.

The relation $H = \frac{Y_p}{1 + Y_p Y_c}$ is the closed loop describing function of the operator measured from system input to operator's output. Consequently,

$$\Phi_{cc}(\omega) = |H|^2 \Phi_{11} + \Phi_{nn} \quad (D.9)$$

Eq. (D.9) indicates that the total operator power spectra contains two portions: (1) a part correlated with the system input, and (2) a closed loop noise power injected in the system. The ratio of the spectral density correlated with the system input to the total operator spectra is the square of the linear correlation, .

$$\rho^2 = \frac{|H|^2 \Phi_{11}(\omega)}{\Phi_{cc}(\omega)} = 1 - \frac{\Phi_{nn}(\omega)}{\Phi_{cc}(\omega)} \quad (D.10)$$

Since

$$H = \frac{\Phi_{1c}(\omega)}{\Phi_{11}(\omega)} \quad (D.11)$$

$$\rho^2 = \frac{|\Phi_{ic}(\omega)|^2}{\Phi_{ii}(\omega) \Phi_{cc}(\omega)} \quad (D.12)$$

The describing function of the human operator can be determined from Eq. (D.3). The correlation coefficient ρ^2 is evaluated from Eq. (D.12). A value of ρ^2 near unity implies that the operator's performance is well accounted for by his describing function.

The most frequently used method of measuring describing functions is by digital computation. In this method, an analog record T seconds long is sampled every ΔT seconds. The correlation function and the power spectral density are determined from the total $M = \frac{T}{\Delta T}$ points. The correlation function is evaluated for m lags of ΔT . Several considerations are involved in the use of this method.

1. The sampled data can have no spectral power at frequencies above ω_{high} where:

$$\omega_{\text{high}} = \frac{\pi}{\Delta T} \quad (D.13)$$

Consequently ω_{high} has to be a frequency above which the continuous signal does not have appreciable power.

2. Since the spectral density is evaluated at m points equally spaced in the range of frequencies $0 - \omega_{\text{high}}$, the frequency resolution of the digitally computed, power spectral density is:

$$\Delta \omega = \frac{\pi}{m \Delta T} \quad (D.14)$$

3. The probable error of the computed spectral density is:²⁰

$$\epsilon = \frac{\sqrt{|\Phi(\omega)_{\text{measured}} - \Phi(\omega)|^2}}{\Phi(\omega)} = \sqrt{\frac{m}{M}} \quad (\text{D.15})$$

This error is reduced when the spectral densities are averaged for N independent computations:

$$\epsilon = \sqrt{\frac{m}{NM}} \quad (\text{D.16})$$

Eq. (D.15) indicates that m should be a small fraction of M; in general, use $m = 0.1M$.

A program, written by the staff of Health Sciences Computing Facility, UCLA and made available to the author by Ames Research Center, NASA, was used for the experimental series reported in Chapter VI. This program for autocovariance and power spectral analysis was modified to compute the describing function of the human operator according to Eq. (D.3). The following parameters were used for the computation procedure:

$T = 90$ seconds

$T = 0.2$ seconds

$M = 450$ points , $\epsilon = \sqrt{\frac{m}{NM}} = 0.1$

$m = 45$ lags

$N = 10$

BIBLIOGRAPHY

1. Adrian, E.D., "Discharges from Vestibular Receptors in the Cat," J. Physiol., London, 101:389-407, 1943.
2. Agin, L.J., Marcum, S.G., Daugherty, F.J., Ferrell, M.B., and Trager, F.N., "Airsickness and Related Psychosomatic Complaints," Air Surgeon's Bulletin, 2:235, 1945.
3. Armstrong, C.R., "Space Physiology," J. British Interplanetary Society, 12:172-175, 1953.
4. Asch, S.E., and Witkin, H.A., "Studies in Space Orientation: I. Perception of the Upright with Displaced Visual Fields," J. Exper. Psych., 38:325-337, 1948.
5. Asch, S.E. and Witkin, H.A., "Studies in Space Orientation: II. Perception of the Upright with Displaced Visual Fields and with Body Tilted," J. Exper. Psych., 38:455-477, 1948.
6. Aschan, G., "Response to Rotary Stimuli in Fighter Pilots," Acta Oto-laryngologica, Supp. 116, 1954.
7. Barnhill, J.H., Surgical Anatomy of the Head and Neck, The Williams and Wilkins Co., Baltimore, 1940.
8. Biosystems, Inc., "Vestibular Control System," Progress Report No. 2 on NaS 2-1372, Cambridge, Mass., November 1963.
9. Bourbon, B., "Sur le Role de la Tête dans la Perception de L'espace," Rev. Philos., 61:526-529, 1936.
10. Brandt, V., "Reorientation and Vestibular Function," Acta Oto-laryng., 50:163-170, 1959.
11. Brandt, V., "Cause and Practical Importance of the Oculogravic Illusions," Acta Oto-laryng., 54:127-135, 1962.

12. Brandt., V., "Gravitational Stress and Equilibrium," *AeroSpace Med.*, 35:657-661, 1964.
13. Breuer, J., "Über die Funktion der Otolithenapparate," *Pflüg. Arch. ges. Physiol.*, 48:195, 1891.
14. Bridges, C.C. and Bitterman, M.E., "The Measurement of Autokinetic Movement," *Amer. J. Psych.*, 67:525-529, 1954.
15. Brodal, A., "Fiber Connections of the Vestibular Nuclei, in Neural Mechanisms of the Auditory and Vestibular Systems," Charles C. Thomas, Springfield, Ill., 224-246, 1960.
16. Brodal, A., Pompeiano, O., and Walberg, F., *The Vestibular Nuclei and their Connections, Anatomy and Functional Correlations*, Charles C. Thomas, Springfield, Ill., 1962.
17. Brown, J.L. and Lechner, M., "Acceleration and Human Performance," *J. Aviation Med.*, 27:32-49, 1956.
18. Cawthorne, T., et al., "The Investigation of Vestibular Function," *Brit. Med. Bull.*, 12:131-142, 1956.
19. Cawthorne, T.E., Fitzgerald, G. and Hallpike, S.C., "Studies in Human Vestibular Function. II. Observations on the Directional Preponderance of Caloric Nystagmus ("Nystagmusbereitschaft") Resulting from Unilateral Labyrinthectomy," *Brain*, 65:138-160, 1942.
20. Chang, S.S.L., Synthesis of Optimum Control Systems, McGraw-Hill Book Company, Inc., 1961.
21. Chinn, H. and Smith, P.K., "Motion Sickness," *Pharmacol. Rev.*, 7:33-82, 1955.
22. Clark, B. and Braybiel, A., "Antecedent Visual Frame of Reference as a Contributing Factor in the Perception of the Oculogravic Illusion," *Bur. of Med. and Surg.*, Project MR005.13-6001, Subtask 1, Report No. 56.
23. Clark, B. and Graybiel, A., "The Breakoff Phenomenon," *J. Aviation Med.*, 28:121-126, 1957.
24. Clark, B. and Graybiel, A., "Contributing Factors in the Perception of the Oculogravic Illusion," *Am. J. Psychol.*, 76:18-27, 1963.
25. Clark, B. and Graybiel, A., "Human Performance during Adaptation to Stress in the Pensacola Slow Rotation Room," *J. Aerospace Med.*, No. 32, February 1961.

26. Clark, B., and Graybiel, A., "The Lag Effect Associated with Stimulation of the Semicircular Canals as Indicated by the Oculogyral Illusion," U.S. Naval Sch. of Aviation Medicine, Project Report No. NM 001 059.01.25, Nov. 1950.
27. Clark, B. and Graybiel, A., "Perception of the Postural Vertical as a Function of Practice in Normal Persons and Subjects with Labyrinthine Defects," Bur. Med. and Surg., Project MR005.13-6001, Subtask 1, Report No. 63, 1961.
28. Clark, B. and Graybiel, A., "Vertigo as a Cause of Pilot Error in Jet Aircraft," J. Aviation Med., 28:469-478, 1957.
29. Clark, B. and Graybiel, A., "Visual Perception of the Horizontal following Exposure to Radial Acceleration on a Centrifuge," J. Comp. and Physiol. Psychol., 44:525-534, 1951.
30. Clark, B., Graybiel, A., and MacCorquodale, "The Illusory Perception of Movement Caused by Angular Acceleration and by Centrifugal Force during Flight. II. Visually Perceived Motion and Displacement of a Fixed Target during Turns," J. Exp. Psychol., 38:298-309, 1948.
31. Clark, B. and Nicholson, M.A., "Aviator's Vertigo: A Cause of Pilot Error in Naval Aviation Students," J. Aviation Med., 25:171-179, 1954.
32. Clark, B. and Stewart, J.D., "Perception of Angular Acceleration about the Yaw Axis of a Flight Simulator," Aerospace Med., 33, December 1962.
33. Clegg, W.C. and Dunfield, N.M., "Non-Visual Perception of the Postural Vertical: II. Lateral Plane," Canad. J. Psychol., 8:80-86, 1954.
34. Cogan, D.G., Neurology of the Ocular Muscles, Charles C. Thomas Company, Springfield, Ill., 1948.
35. Cohen, L.A., "Human Spatial Orientation and its Critical Role in Space Travel," Aerospace Med., 35, Nov. 1964.
36. Collins, W.E., "Further Studies of the Effects of Mental Set upon Vestibular Nystagmus," US Army Med. Res. Lab., Fort Knox, Ky., Report No. 443, 1960.
37. Collins, W.E., Crampton, C.H., and Posner, J.B., "The Effect of Mental Set upon Vestibular Nystagmus and the Electroencephalogram," US Army Med. Res. Lab., Fort Knox, Ky., Report No. 439, 1960.

38. Collins, W.E. and Guedry, F.E., Jr., "Arousal Effects and Nystagmus during Prolonged Constant Angular Acceleration," US Army Med. Res. Lab., Fort Knox, Ky., Report No. 500, 1961.
39. Collins, W.E., Guedry, F.E., Jr., and Posner, J.B., "Control of Caloric Nystagmus by Manipulating Arousal and Visual Fixation Distance," US Army Med. Res. Lab., Fort Knox, Ky., Report No. 485, 1961.
40. Cramer, R.L., "Response of Mammalian Gravity Receptors to Sustained Tilt," J. Aero. Med., 33:663-666, 1962.
41. Cramer, R.L., Dowd, P.J., and Helms, D.B., "Vestibular Responses to Oscillation about the Yaw Axis," Aerospace Med., 34:1031-1034, 1963.
42. Crampton, G.H. and Schwam, W.J., "Effects of the Arousal Reaction on Nystagmus Habituation in Cat," US Army Med. Res. Lab., Fort Knox, Ky., Report No. 434, 1960.
43. Crosby, E.C., personal communication to Dr. Carl Kupfer.
44. Dearnaley, E.J., et al., "Nature and Duration of After-Sensations following the Cessation of Turning in a Chipmunk Aircraft," J. Aero. Med., October 1962.
45. De Kleyn, A., "Tonische Labyrinth-und Halsreflexe auf die Augen," Arch. ges. Physiol., 186:82, 1921.
46. De Witt, G., "Seasickness (Motion Sickness), A Labyrinthological Study," Acta Oto-laryng., Supp. 108:1-56, 1953.
47. Diringshofen, H. von, Kissel, G. and Osypka, P., "Thresholds for the Perception of Linearly Increasing Angular Accelerations," 35:775-778, 1964.
48. Dix, M.R. and Hallpike, C.S., "Lesions of the Cerebral Hemispheres and their Effects upon Optokinetic and Caloric Nystagmus," J. Physiol., 114:55, 1951.
49. Dodge, R., "Thresholds of Rotation," J. Exp. Psychol., 6:107-137, 1923.
50. Elkind, J.I., "Characteristics of Simple Manual Control Systems," Technical Report No. 111, M.I.T. Lincoln Laboratory, April 6, 1956.
51. Engstrom, H., "On the Double Innervation of the Sensory Epithelia of the Inner Ear," Acta Oto-laryng., Stockholm, 49:109-118, 1958.

52. Fernandez, C. and Schmidt, R.S., "Studies in Habituation of Vestibular Reflexes, a Revision," *Aerospace Med.*, 34:311-315, 1963.
53. Final Report, Bu Aer Report AE-61-6 and Goodyear Aircraft Corp., Report GER 5452, "Investigation of Vestibular and Body Reactions to the Dynamic Response of the Human Operator," Nov. 25, 1953.
54. Fisher, M.H., "Die Regulationsfunktionen des Menschlichen Labyrinthes und die Zusammenhänge mit Verwandten Funktionen," *Ergenbn. Physiol.*, 27:14-379, 1928.
55. Fitzgerald, G. and Hallpike, C.S., "Studies in Human Vestibular Functions: I. Observations on Directional Preponderance ("Nystagmusbereitschaft") of Caloric Nystagmus Resulting from Cerebral Lesions," *Brain*, 65:115-137, 1942.
56. Fleishman, E.A., "The Influence of Fixed Versus Free Head Position on the Perception of Body Position," Human Resources Res. Center, Lackland Air Force Base, Tex., Res. Bull. 53-37, Oct. 1953.
57. Fleishman, E.A., "The Perception of Body Position -- Effect of Speed, Magnitude, and Direction of Displacement on Accuracy of Adjustment to an Upright Position," Human Resources Res. Center, Lackland Air Force Base, Tex., Res. Bull. 53-1, Jan. 1953.
58. Fleishman, E.A., "Perception of Body Position in the Absence of Visual Cues," *J. Exp. Psychol.*, 24:176-187, 1953.
59. Fluor, E., "The Mechanism of Nystagmus," *Acta Otolaryng.*, 54:181-188, 1962.
60. Furey, J.A. and Kraus, R.N., "A Clinical Classification of Vertigo," *Aeromed. Reviews*, Rev. 7-61, April 1962.
61. Gerathewohl, S.J. and Stallings, H.D., "Experiments during Weightlessness: A Study of the Oculo-gravic Illusion," *J. Av. Med.*, 29:504-516, 1958.
62. Gerathewohl, S.J. and Stallings, H.D., "The Labyrinthine Postural Reflex (righting reflex) in the Cat during Weightlessness," *J. Av. Med.*, 28:345, 1957.
63. Gerebtzoff, M.A., "Recherches sur la Projection Corticale de Labyrinthe, I. Des Effects de la Stimulation Labyrinthique sur l'activite Electrique de l'ecorce Cerebrale," *Arch. Int. Physiol.*, 50:59-99, 1940.

64. Gernandt, B., "Midbrain Activity in Response to Vestibular Stimulation," *Acta Physiol. Scand.*, 21:73-81, 1950.
65. Gernandt, B.E. and Gilman, S., Generation of Labyrinthine Impulses, Descending Vestibular Pathways, and Modulation of Vestibular Activity by Proprioceptive, Cerebellar, and Reticular Influences, *Neural Mechanisms of the Auditory and Vestibular Systems*, Ed. by G.L. Rasmussen and W.F. Windle, Charles C. Thomas Company, Springfield, Ill., pp. 324-348, 1960.
66. Gooddy, W. and Reinhold, M., "Some Aspects of Human Orientation in Space, (i) Sensation and Movement," *Brain*, 75:472-509, 1952.
67. Gooddy, W. and Reinhold, M., "Some Aspects of Human Orientation in Space, (ii) The Dynamic Nature of Nervous Activity. (a) "Motion Sense" (b) Sense of Direction," *Brain*, 76:337-363, 1953.
68. Graham, D. and McRuer, D., Analysis of Nonlinear Control Systems, John Wiley and Sons, Inc., 1961.
69. Graybiel, A. and Clark, B., "Perception of the Horizontal or Vertical with Head Upright, On the Side, and Inverted under Static Conditions, and during Exposure to Centripetal Force," *J. Aero. Med.*, 33:147-155, 1962.
70. Graybiel, A., Clark, B., and Zarriello, J.J., "Observations on Human Subjects Living in a 'Slow Rotation Room' for Periods of Two Days," *AMA Arch. Neurol.*, 3, July 1960.
71. Graybiel, A., Guedry, F.E., Johnson, W. and Kennedy, R., "Adaptation to Bizarre Stimulation of the Semicircular Canals as Indicated by the Oculogyral Illusion," *J. Aero. Med.*, 32:321-327, 1961.
72. Graybiel, A. and Hupp, D., "The Oculogyral Illusion: A Form of Apparent Motion Which May be Observed following Stimulation of the Semicircular Canals," *J. Avia. Med.*, 17:3, 1946.
73. Graybiel, A. and Johnson, W.H., "A Comparison of the Symptomatology Experienced by Healthy Persons and Subjects with Loss of Labyrinthine Function When Exposed to Unusual Patterns of Centripetal Force in a Counter-Rotating Room," *Ann. Otol. Rhinol. and Laryngol.*, 72:357, 1963.

74. Graybiel, A., Kerr, W.A., and Bartley, S.H., "Stimulus Thresholds of the Semicircular Canals as a Function of Angular Acceleration," *Am. J. Psychol.*, 61:21-36, 1948.
75. Graybiel, A., Niven, J.I., and Walsh, T.E., "The Differentiation between Symptoms Referable to the Otolith Organs and Semicircular Canals in Patients with Non-suppurative Labyrinthitis," *The Laryngoscope*, 62:924-933, 1952.
76. Gray's Anatomy, Thirty-third Edition, Longmans, Green and Company, 1962.
77. Groen, J.J., "The Semicircular Canal System of the Organs of Equilibrium - I and II," *Physics in Medicine and Biology*, 1, 1956-57.
78. Groen, J.J., Lowenstein, O., and Vendrik, A.J.M., "The Mechanical Analysis of the Responses from the End Organs of the Horizontal Semicircular Canal in the Isolated Elasmobranch Labyrinth," *J. Physiol.*, London, 117:329-346, 1952.
79. Guedry, F.E., Jr., and Beberman, N., "Apparent Adaptation Effects in Vestibular Reactions," *US Army Med. Res. Lab.*, Fort Knox, Ky., Report No. 293, Aug. 1957.
80. Guedry, F.E., Jr. and Ceran, S.J., "Derivation of 'Subjective Velocity' from Angular Displacement Estimates Made during Prolonged Angular Accelerations: Adaptation Effects," *US Army Med. Res. Lab.*, Fort Knox, Ky., Report No. 376, 1959.
81. Guedry, F.E., Jr., Collins, W.E., and Sheffey, P.L., "Perceptual and Oculomotor Reactions to Interacting Visual and Vestibular Stimulation," *US Army Med. Res. Lab.*, Fort Knox, Ky., Report No. 463, March 1961.
82. Guedry, F.E., Jr., Cramer, R.L., and Koella, W.P., "Experiments on the Rate of Development and Rate of Recovery of Apparent Adaptation Effects in the Vestibular System," *US Army Med. Res. Lab.*, Fort Knox, Ky., Report No. 336, June 1958.
83. Guedry, F.E., Jr. and Graybiel, A., "The Appearance of Compensatory Nystagmus in Human Subjects as a Conditioned Response during Adaptation to a Continuously Rotating Environment," *Bur. of Med. and Surg.*, Project MRO05.13-6001, Subtask 1, Report No. 61.
84. Guedry, F.E., Jr., and Graybiel, A., "Compensatory Nystagmus Conditioned during Adaptation to Living in a Rotating Room," *J. App. Physiol.*, 17, May 1962.

85. Guedry, F.E., Jr. and Kalter, H., "Description of Human Rotation Device," US Army Med. Res. Lab., Fort Knox, Ky., Report No. 242, May 1956.
86. Guedry, F.E., Jr., and Lauver, L.S., "The Oculomotor and Subjective Aspect of the Vestibular Reaction during Prolonged Constant Angular Acceleration," US Army Med. Res. Lab., Fort Knox, Ky., Report No. 438, September 1960.
87. Guedry, F.E., Jr., and Montague, E.K., "Relationship between Magnitudes of Vestibular Reactions and Effective Coriolis Couples in the Semicircular Canal System," US Army Med. Res. Lab., Fort Knox, Ky., Report No. 456, Dec. 1960.
88. Guedry, F.E., Jr., Peacock, L.J., and Cramer, R.L., "Nystagmic Eye Movements during Interacting Vestibular Stimuli," US Army Med. Res. Lab., Fort Knox, Ky., Report No. 275, March 1957.
89. Hall, I.A.M., "Effect of Controlled Element on the Human Pilot," WADC TR57-509, October 1957.
90. Hammer, L.R., "Perception of the Visual Vertical under Reduced Gravity," Technical Documentary Report No. MRL-TRL-62-55, Wright Patterson Air Force Base, Ohio, May 1962.
91. Hartinger, H., "Motion and Perception of Space," USAF Sch. Av. Med., Special Report, 1951.
92. Hartman, B.O., "The Effect of Target Frequency on Compensatory Tracking," US Army Med. Res. Lab., Fort Knox, Ky., Report No. 272, April 1957.
93. Hawkes, G.R., Bailey, R.W., and Warm, J.S., "Method and Modality in Judgments of Brief Stimulus Duration," US Army Med. Res. Lab., Fort Knox, Ky., Report No. 442, Sept. 1960.
94. Hemingway, A., "Results of 500 Swing Tests for Investigating Motion Sickness," AAF Sch. Av. Med., Randolph AFB, Res. Project 31, Report No. 2, Nov. 1942.
95. Henry, J.P., et al., "Effects of Weightlessness in Ballistic and Orbital Flight," J. Aero. Med., Sept. 1962.
96. Hixson, W.C. and Niven, J.I., "Application of the System Transfer Function Concept to a Mathematical Description of the Labyrinth: I. Steady-State Nystagmus Response to Semicircular Canal Stimulation by Angular Acceleration," Bureau of Med. and Surg., Project MR005.13-6001, Subtask 1, Report No. 57, 1961.

97. Johnson, W.H., "Head Movement Measurements in Relation to Spatial Disorientation and Vestibular Stimulation," J. Av. Med., 27:148-152, 1956.
98. Johnson, W.H., "The Importance of Head Movements in the Production of Motion Sickness," J. Def. Res. Bd., Canada, Library of Congress, Tech. Info. Div. No. U22185, April 1952.
99. Johnson, W.H. and Mayne, J.W., "Stimulus Required to Produce Motion Sickness: Restriction of Head Movements as a Preventive of Airsickness - Field Studies on Airborne Troops," J. Av. Med., 24:400-411, 1953.
100. Johnson, W.H. and Smith, B., "Functions of the Utricular Macula. A Preliminary Report," Can. J. Biochem. Physiol., 37:605-606, 1959.
101. Jones, G.M., "Predominance of Anti-compensatory Oculomotor Response during Rapid Head Rotation," Aerospace Med., 35:965-968, 1964.
102. Jones, G.M., Barry, W., and Kowalsky, N., "Dynamics of the Semicircular Canals Compared in Yaw, Pitch and Roll," Aerospace Med., 35:984-989, 1964.
103. Jones, G.M. and Spells, K.E., "A Theoretical and Comparative Study of the Functional Dependence of the Semicircular Canal upon its Physical Dimensions," Proc. Roy. Soc. B, 1957.
104. Jongkees, L.B.W., "On the Function of the Sacculle," Acta Oto-laryng, 38, 18, 1950.
105. Kennedy, R.S. and Graybiel, A., "Symptomatology during Prolonged Exposure in a Constantly Rotating Environment at a Velocity of One Revolution per Minute," Bureau of Med. and Surg., Project MR005.13-6001, Subtask 1, Report No. 62.
106. Kennedy, R.S. and Graybiel, A., "Symptomatology during Prolonged Exposure in a Constantly Rotating Environment at a Velocity of One Revolution per Minute," J. Aero. Med., 33:817-825, 1962.
107. Kraus, R.N., "Disorientation in Flight: An Evaluation of the Etiological Factors," Aero. Med., 30:664-673, 1959.
108. Ledoux, A., "Les Canaux Semi-circulaires: Etude Electrophysiologique; Contribution a L'effort D'uniformisation des Epreuves Vestibulaires, Essai D'interpretation de la Semiologie Vestibulaire," Acta Otolinolar. belg., 12:111-346, 1958.

109. Loftus, J.P., ed., Symposium on Motion Sickness with Special Reference to Weightlessness. Technical Documentary Report No. AMRL-TDR-63-25, June 1963.
110. Lowenback, H. and W.H. Gantt, "Conditional Vestibular Reactions," J. Neuro. Physiol., J. 4348, 1940.
111. Lowenstein, O., "The Equilibrium Function of the Vertebrate Labyrinth," Biol. Rev., 11:113-145, 1936.
112. Lowenstein, F.R.S., Osborne, M.P., and Wersal, Jan, "Structure and Innervation of the Sensory Epithelia of the Labyrinth in the Thornback Ray (Raja Clavata)," Pro. Roy. Soc. B, 160:1-12, April 14, 1964.
113. Lowenstein, O. and Sand, A., "The Activity of the Horizontal Semicircular Canal of the Dogfish, Scyllium canicula," J. Exp. Biol., 13:416-428, 1936.
114. Lowry, R.H. and Johnson, W.H., "'Pseudo Motion Sickness' due to Sudden Negative 'G': Its Relation to 'Airsickness'," J. Av. Med., April 1954.
115. MacCorquodale, K., "Effects of Angular Acceleration and Centrifugal Force on Nonvisual Space Orientation During Flight," J. Av. Med., 19:146-157, 1948.
116. Magnus, R., Animal Posture (The Croonian Lecture), Proc. R. Soc. (B.), 98:339-353, 1925.
117. Magnus, R., "Some Results of Studies on the Physiology of Posture," Lancet, pp. 531-536 and 585-588, 1926.
118. Mann, C.W., "Visual Factors in the Perception of Verticality," J. Exp. Psychol., 44:460-464, 1952.
119. Mann, C.W., "Which Way is Up?," Research Reviews, ONR, Dept. Navy, October 1951.
120. Mann, C.W., Berthelot-Berry, N.H. and Dauterive, H.J., Jr., "The Perception of the Vertical: I. Visual and Non-Labyrinthine Cues," J. Exp. Psychol., 39:700-707, 1949.
121. Mann, C.W., Canella, C.J. and Graybiel, A., "An Examination of the Technique of Cupulometry," Joint Project Report No. 42, US Naval Sch. Av. Med., Pensacola, Fla., May 1956.
122. Mann, C.W., and Passey, G.E., "The Perception of the Vertical: V. Adjustment to the Postural Vertical as a Function of Postural Tilt and Duration of Exposure," J. Exp. Psychol., 41:108-113, 1951.

123. Mann, C.W. and Ray, J.T., "The Perception of the Vertical: XIV. The Effect of the Rate of Movement on the Judgment of the Vertical," Naval Sch. Av. Med. and Tulane U., Joint Project Report No. 40, 1956.
124. Mayne, R., "Some Engineering Aspects of the Mechanism of Body Control," Electrical Engineering, 70:207-212, 1951.
125. McCabe, B.F., "Vestibular Suppression in Figure Skaters," Trans. Amer. Acad. Opth. and Otol., 64:1960.
126. McNally, W.J., "The Otoliths and the Part They Play in Man," Laryngoscope, 54:304-323, 1944.
127. McNally, W.J. and Stuart, E.A., "Physiology of the Labyrinth Reviewed in Relation to Seasickness and Other Forms of Motion Sickness," War Medicine, 2:683-771, 1942.
128. McRuer, D.T. and Krendel, E.S., "Dynamic Response of Human Operators," WADC TR56-524, August 1957.
129. McRuer, D.T. and Krendel, E.S., "The Human Operator as a Servo Element," J. of the Franklin Institute, 267: No.5 and No.6, June 1959.
130. Miller, E.F., "Counterrolling of the Human Eyes Produced by Head Tilt with Respect to Gravity," Acta Oto-laryng., 54:479-501, 1962.
131. Miller, E.F. and Graybiel, A., "A Comparison of Ocular Counterrolling Movements between Normal Persons and Deaf Subjects with Bilateral Labyrinthine Defects," Joint Report, Bureau of Med. and Surg., Project MR005.13-6001, Subtask 1, Report No. 68, 1962.
132. Miller, E.F. and Graybiel, A., "Role of the Otolith Organs in the Perception of Horizontality," Joint Report, Bureau Med. and Surg., Project MR005.13-6001, Subtask 1, Report No. 80, 1963.
133. Milsum, J.H. and Jones, G.M., "On the Physiological Control System for Ocular Stabilisation," Paper No. 2, Digest of 15th Ann. Conf. on Eng. in Med. and Biol., Chicago, Ill., p. 51, Nov. 5-7, 1962.
134. Moore, E.W. and Cramer, R.L., "Perception of Postural Verticality," USAF Sch. Av. Med., TDR-62-72, June 1962.
135. Niven, J.L. and Hixson, W.C., "Frequency Response of the Human Semicircular Canals: Steady-State Ocular Nystagmus Response to High-Level Sinusoidal Angular

- Rotations," Bureau Med. and Surg., Project MR005.13-6001, Subtask 1, Report No. 58.
136. Noble, C.E., "The Visual Vertical as a Function of Centrifugal and Gravitational Forces," J. Exp. Psychol., 39, 1949.
 137. North, J.D., Lomnicki, Z.A., and Zaremba, S.K., "The Design and Interpretation of Human Control Experiments," Ergonomics, 1:314-327, 1957-58.
 138. Nuttall, J.B., "The Problem of Spatial Disorientation," J. AMA, 166:431-438, 1958.
 139. Nuttall, J.B. and Sanford, W.G., "Spatial Disorientation in Operational Flying," USAF Norton AFB, San Bernardino, Calif., Report No. M-27-56, May 1956.
 140. Ordnance Engineering Design Handbook, Experimental Statistics, June 1962.
 141. Ostle, B., Statistics in Research, The Iowa State College Press, Ames, Iowa, 1954.
 142. Passey, G.E., "The Perception of the Vertical, IV. Adjustment to the Vertical with Normal and Tilted Visual Frames of Reference," J. Exp. Psychol., 40:738-745, 1950.
 143. Passey, G.E. and Guedry, F.E., Jr., "The Perception of the Vertical: II. Adaption Effects in Four Planes," J. Exp. Psychol., 39:700-707, 1949.
 144. Pew, R.W., "Temporal Organization in Skilled Performance," Doctoral Dissertation, University of Michigan, 1963.
 145. Quix, F.H., "Epreuves Vestibulaires," L-Oto-Rhino-Laryng. Internat., 6:484, 1922.
 146. Roman, J.A., Warren B.H., and Graybiel, A., "Observation of the Elevator Illusion during Subgravity Preceded by Negative Accelerations," Joint Report, Bureau Med. and Surg., Project MR005.13-6001, Subtask 1, Report No. 83, 1963.
 147. Roman, J.A., Warren, B.H. and Graybiel, A., "The Sensitivity to Stimulation of the Semicircular Canals during Weightlessness," Joint Report, Bureau Med. and Surg., Project MR005.13-6001, Subtask No. 1, Report No. 84, 1963.
 148. Russell, L., "Characteristics of the Human as a Linear Servo-Element," M.S. Thesis, M.I.T., May 18, 1951.

149. Sadoff, M., "A Study of a Pilot's Ability to Control During Simulated Stability Augmentation System Failures," NASA TN D-1552, 1962.
150. Sadoff, M., McFadden, N.M. and Heinle, D.R., "A Study of Longitudinal Control Problems at Low and Negative Damping and Stability with Emphasis on the Effects of Motion Cues," NASA TN D-348, 1961.
151. Schöne, H., "On the Role of Gravity in Human Spatial Orientation," Aerospace Med., 35:764-772, 1964.
152. Schulte, R.J. and Vreeland, R.E., "The Design and Construction of an Acceleration Cart," M.Sc. Thesis, M.I.T., June 1964.
153. Second Semi-Annual Status Report on NASA Grant Nsg-577, Man-Vehicle Control Laboratory, Center for Space Research, M.I.T., Cambridge, Mass., December 1964.
154. Steinhausen, W., "Über den Nachweis der Bewegung der Cupula in der Intakten Bogengangsampeulle des Labyrinthes bei der Natürlichen Rotatorischen und Calorischen Reizung," Pflugers Arch. ges. Physiol., 228:322-328, 1931.
155. Stone, R.W. and Letko, W., "Some Observations during Weightlessness Simulation with Subject Immersed in a Rotating Water Tank," NASA Tn D-2195.
156. Useller, J.W. and Algranti, J.S., "Pilot Reaction to High-Speed Rotation," IAF Meeting, Stockholm, 1960.
157. Van Egmond, A.A.J., Groen, J.J., and Jongkees, L.B.W., "The Mechanics of the Semicircular Canal," J. Physiol., 110:1-17, 1949.
158. Vinacke, W.E., "Aviator's Vertigo," J. Av. Med., 19:158-170, 1948.
159. Walsh, E.G., "The Perception of Rhythmically Repeated Linear Motion in the Horizontal Plane," Brit. J. Psychol., 53:439-445, 1962.
160. Walton, W.G., "Compensatory Cyclo-torsion Accompanying Head Tilt," Amer. J. Optom. of Arch. Amer. Acad. Optom., 25:525, 1948.
161. Wapner, S. and Witkin, H.A., "The Role of Visual Factors in the Maintenance of Body-Balance," Am. J. Psychol., 385-408, 1950.

162. Webb Associates, NASA Life Sciences Data Book, Director of Aerospace Medicine, Contract R-89, NASA, 1962.
163. Wersäll, J. and Flock, Å., "Physiological Aspects on the Structure of Vestibular End Organs," *Acta Otolaryng.*, Suppl. 192.
164. White, W.J., "Acceleration and Vision," USAFWADC TR 58-333, Aero Medical Laboratory, November 1958.
165. Whitsett, C.E., Jr., "Some Dynamic Response Characteristics of Weightless Man," Technical Documentary Report No. AMRL-TDR-63-18, Wright-Patterson Air Force Base, Ohio, April 1963.
166. Whitteridge, D., "Central Control of Eye Movements," *Handbook of Physiology*, Chapter XLII, American Physiological Society, Washington, D.C., 1960.
167. Witkin, H.A., "Further Studies of Perception of the Upright When the Direction of the Force Acting on the Body is Changed," *J. Exp. Psychol.*, 43:9-20, 1952.
168. Witkin, H.A., "The Nature and Importance of Individual Differences in Perception," *J. Personality*, 18:145-170, 1949.
169. Witkin, H.A. and Asch, S.E., "Studies in Space Orientation. III. Perception of the Upright in the Absence of a Visual Field," *J. Exp. Psychol.*, 38:603-614, 1948.
170. Witkin, H.A. and Asch, "Studies in Space Orientation. IV. Further Experiments on Perception of the Upright with Displaced Visual Fields," *J. Exp. Psychol.*, 38:762-782, 1948.
171. Witkin, H.A. and Wapner, S., "Visual Factors in the Maintenance of Upright Posture," *Am. J. Psychol.*, 63:31-50, 1950.
172. Woellner, R.C., "The Perception of Vertical in the Presence of Increased Accelerative Forces," Bureau of Med. and Surg., Research Project NM 17 01 11, Subtask 1, Report No. 45, 1957.
173. Woellner, R.C. and Graybiel, A., "Counterrolling of the Eyes and its Dependence on the Magnitude of Gravitational or Inertial Force Acting Laterally on the Body," *J. App. Physiol.*, 14:632-634, 1959.

174. Woellner, R.C. and Graybiel, A., "The Loss of Counter-rolling of the Eyes in Three Persons Presumably without Functional Otolith Organs," Ann. Otol., Rhin. and Laryng., 69:1006-1012, 1960.
175. Worchel, P., "The Role of the Vestibular Organs in Space Orientation," J. Exp. Psychol., 44:4-10, 1952.
176. Worchel, P., "The Vestibular Organs in Space Orientation," Perceptual and Motor Skills, 5:164, 1955.
177. Young, L.R., "A Sampled Data Model for Eye Tracking Movements," Doctoral Thesis, Massachusetts Institute of Technology, June 1962.